Thermodynamics and Signatures of Bose-Condensation of Excitons and Polaritons.

Thermodynamics and Signatures of Bose-Condensation of Excitons and Polaritons

Jonathan Mark James Keeling

Jesus College

University of Cambridge

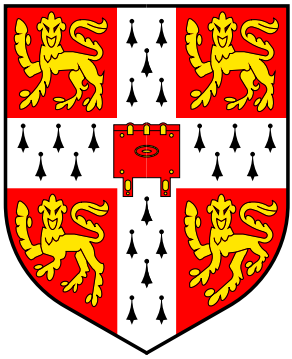

This Dissertation is submitted

for the Degree of

Doctor of Philosophy

Summary

This dissertation studies Bose-Einstein condensation (BEC) of excitons and microcavity polaritons. BEC is a phase transition, whereby at low temperatures a system spontaneously develops coherence, allowing quantum mechanical effects to be visible on macroscopic scales. Excitons are the bound states of an electron and a hole in a semiconductor. Microcavity polaritons are the result of strongly coupling excitons to radiation modes confined in a microcavity — a cavity on the scale of the wavelength of light.

The first part of the dissertation considers signatures of exciton BEC in bilayer quantum well systems. In such systems, excitons are formed from electrons and holes confined to parallel two dimensional layers. This leads to a repulsive dipole interaction between excitons. There has been experimental work on systems with the excitons further confined in shallow in-plane traps. Because of the interaction between particles, it is shown that BEC does not lead to any dramatic change of the spatial profile of radiation. However, phase coherence between the excitons does lead to a change in the angular profile of emitted radiation — coherence leads to interference between emission from opposite sides of the exciton cloud. By considering the thermal population of phase fluctuations, which reduce long-range phase correlations, it is shown how this angular profile is modified at non-zero temperatures.

The second part considers the condensation temperature for a model of microcavity polaritons, constructed from localised excitons and propagating photons. This condensation may be described in

two different ways. At low densities, it may be considered as BEC of weakly interacting bosons, with a transition temperature $T_c \propto \rho$. At high densities a mean-field theory of self-consistent polarisation and optical fields is more appropriate. The crossover between these regimes is found by considering fluctuations on top of the mean-field theory. Due to the photon component of polaritons this crossover occurs at densities much lower than those at which excitons overlap, and becomes relevant for current experiments aimed at polariton BEC.

From the excitation spectrum, which differs between the condensed and uncondensed state, one can also predict a number of experimentally accessible signatures which could indicate the presence of a condensate. The excitation spectrum is directly related to experimentally accessible luminescence and absorption spectra.

Declaration of originality

This dissertation is my own work and contains nothing which is the outcome of work done in collaboration with others, except as specified in the text and Acknowledgements.

Parts of this dissertation have been published, or submitted for publication as follows:

Chapter 4. J. Keeling, L. S. Levitov, P. B. Littlewood, *Angular distribution of photoluminescence as a probe of Bose condensation of trapped excitons.* Phys. Rev. Lett. **92** 176402 (2004).

Chapters 5 and 6. J. Keeling, P. R. Eastham, M. H. Szymanska, P. B. Littlewood, *Polariton condensation with localised excitons and propagating photons.* Phys. Rev. Lett. **93** 226403 (2004).

J. Keeling, P. R. Eastham, M. H. Szymanska, P. B. Littlewood, *BCS-BEC crossover in a system of microcavity polaritons.* Submitted to Phys. Rev. B.

Chapter 7. J. Keeling, *A note on the Hepp and Lieb transition for the Dicke model.* Submitted to Phys. Rev. A.

Statement of length

This dissertation does not exceed 60,000 words in length.

Acknowledgements

It has been a great privilege to have been supervised by Peter Littlewood, and to have worked with Leonid Levitov. I have found my time working with them both enjoyable and educational, and have appreciated the opportunity to visit MIT and work with Leonid Levitov provided by funding from the Cambridge-MIT institute.

I would like to thank those with whom I have worked particularly closely, and from whom I have learnt much, Paul Eastham, Francesca Marchetti and Marzena Szymańska; and also the members of staff in TCM who have taught me much, both through lectures and private discussions, Nigel Cooper, David Khmelnitskii, Ben Simons. Many thanks are also due to thank Michael Rutter and Mike Rose for providing computing facilities that always work, and Tracey Ingham and Pam Hadder for all their help. Finally in TCM I would like to thank the other PhD students and postdocs who have variously managed to keep me entertained for three years, including James Acton, James Adams, Sebastian Ahnert, James Burridge, Lucy Heady, Siân Joyce, Malcom Kennet, Mat Tunney.

I have appreciated the opportunities I have had to talk with experimental groups, which have clarified my thinking on many points, and provided continuing motivation for this and future work. In particular I am very grateful for discussions with Leonid Butov, Hui Deng, Le Si Dang, Jacek Kasprzak, and Yoshisha Yamamoto.

Finally, I should like to thank the physics and mathematics staff at Beaumont school for my first introduction to physics, and my parents for their continued support over many years of education.

Contents

List of Figures

Part I

Introduction and Theoretical Background

Chapter 1

General Introduction

One of the more remarkable features of quantum mechanics is that at low temperatures, many systems undergo a phase transition, leading to a spontaneously phase coherent state. Such phase coherence allows quantum mechanical effects to be visible with large numbers of particles despite interactions with the environment that cause decoherence. As a result, coherent quantum systems show classically surprising behaviour such as flow without resistance, quantised rotation, and interference fringes for macroscopic objects.

There are now many examples of systems showing spontaneous phase coherence. The earliest to be discovered, but one of the latest to be theoretically described is the superconductor [1]. Another early example of the effects of phase coherence is superfluid Helium [2, 3, 4]. In both these examples, it is clear that interactions play an important role. More recently, Bose condensation of atomic gases [5, 6] has provided an opportunity to study experimentally spontaneous coherence of weakly interacting bosons. Condensation of weakly interacting bosons has been widely studied (see *e.g.* [7, 8, 9] and refs. therein), and provides a connection to the textbook picture of the statistical transition for a non-interacting gas.

Somewhere in the above list should also appear the laser, however this differs from the above examples, in being strongly pumped

and far from thermal equilibrium. Further, in the laser, phase coherence only exists for the light, while the pumped gain medium does not attain coherence. Nevertheless, a laser shows spontaneous phase coherence when pumped strongly, and provides an alternative paradigm for spontaneous coherence.

Excitons and polaritons have both been studied as possible candidates for spontaneous coherence. Despite the almost routine realisation of condensation in atomic gas systems, they continue to remain of interest for several reasons. Their low mass (of the order of the free electron mass for excitons, and 10^4 times less for polaritons) means such effects may be seen at much higher temperatures. Exciton and polariton condensates can decay into free photons, which provides the possibility for generation of, and measurement and experiments on coherent light. Such decay however also proves an obstacle to exciton and polariton condensation; they must cool and thermalise before they decay. The "problem" of slow thermalisation compared to particle life time also provides an opportunity to study spontaneous coherence of systems out of equilibrium.

This dissertation contains two distinct projects relating to condensation of excitons and polaritons. The first studies signatures of condensation of coupled quantum well excitons in traps, and shows that the angular dependence of radiation provides such a signature. The second project considers the thermodynamics of the phase transition for microcavity polaritons. The internal structure of the polariton leads to a crossover from a phase boundary given by a theory of weakly interacting bosons at low densities to a phase boundary governed by the internal structure at higher, yet experimentally relevant, densities.

1.1 Overview

The remainder of this introduction provides a brief introduction to topics of spontaneous coherence and condensation, and a brief summary of experiments in this area. An important topic in understanding condensation is the relation between spontaneous phase

coherence and superfluidity. This becomes particularly important in understanding the phase transition that occurs in two dimensions. Therefore, chapter 2 collects important theoretical results about superfluidity that will be used later, and chapter 3 provides an explicit calculation illustrating those results.

Signatures of condensation for a system of trapped excitons, in coupled quantum well systems are considered in chapter 4. It is shown that, due to strong repulsion between the excitons, the spatial profile of excitons changes little at the phase transition. However, phase coherence between the excitons does lead to a change in the angular profile of emitted radiation. This can be simply understood as interference between emission from phase coherent sources at opposite sides of the exciton cloud. At non-zero temperatures, it is necessary to consider the thermal population of phase fluctuations, which reduce long-range phase correlations to power law correlations, and thus modify the angular profile.

Chapters 5 and 6 study the phase boundary and signatures of polariton condensation, including internal structure of the polariton. This is in contrast to much recent work where polaritons are described as structureless bosons with a given dispersion and interaction [10, 11, 12]. In order to describe the effects of internal polariton structure on the phase transition, the model used starts from a continuum of radiation modes interacting with two-level systems (*i.e.* localised excitons). Such a model is an extension of that introduced by Dicke [13]. By considering the spectrum of fluctuations on top of the mean-field theory, and thermally populating this spectrum [14, 15], it is possible to describe a crossover from a low densities — where the phase boundary may be described by structureless bosons, to high densities where internal structure matters.

The mean-field phase transition of the Dicke model introduced in chapter 5 is closely related to the phase transition studied by Hepp and Lieb [16, 17]. Hepp and Lieb considered two-level molecules coupled to a radiation field, and a transition to a superradiant state. It was later shown by Rzążewski *et al.* that this transition is an artefact of approximations involved in using the Dicke model to describe such a system. However, in chapter 7, an extended Dicke model, including

dipole-dipole interactions between two-level systems is considered, in which the Hepp and Lieb transition is restored.

There are two appendices, discussing technical issues. The first discusses the calculation of phase correlations in a harmonic density profile. The second discusses terms proportional to δ_ω in the thermal Green's function for a broken symmetry system.

1.2 Condensation and spontaneous coherence

It is customary to introduce Bose-Einstein condensation by considering non-interacting bosons in three dimensions. Such an approach predicts the phase transition, but fails to describe many of the interesting properties of the condensed phase. An alternate approach is to start from a Landau-Ginzburg free energy, for a complex superfluid order parameter, Ψ:

$$F_{\text{G.L.}} = \int d^d r \left(|\nabla \Psi|^2 + a|\Psi|^2 + b|\Psi|^4 \right). \tag{1.1}$$

Considering mean-field solutions, $\Psi(r) = \Psi_0$, which minimise $F_{\text{G.L.}}$, a transition occurs at $a = 0$ to a state with a macroscopic expectation of Ψ_0.

Although the free energy is symmetric under global rotations of the order parameter phase, a solution with non-zero expectation of Ψ_0 breaks this symmetry. This broken symmetry leads to the appearance of a Goldstone mode, with linear dispersion, in the condensed state. In dimensions less than 4, because of this low energy mode, spatially varying configurations of the order parameter make an important contribution to the macroscopic free energy:

$$\mathcal{Z} = \exp(-\beta F_{\text{macro}}) = \int \mathcal{D}\Psi \exp(-F_{\text{G.L.}}[\Psi]). \tag{1.2}$$

Normally it is understood that one should write $a = \alpha(T - T_c)/T_c$, so the phase transition occurs with a changing sign when $T = T_c$.

This is the case for superconductivity, and also applies to the polariton condensation transition discussed in this dissertation. However, if rather than starting from a phenomenological mesoscopic theory, one instead considers a microscopic model, a different analysis follows. Consider a weakly interacting Bose gas in equilibrium with a particle reservoir:

$$H - \mu N = \sum_k (\epsilon_k - \mu) a_k^\dagger a_k + \frac{g}{2} \sum_{k,k',q} a_{k+q}^\dagger a_{k'-q}^\dagger a_k a_{k'}. \tag{1.3}$$

Written in real space, such a model leads to a Ginzburg-Landau theory where $a = -\mu$. Therefore, for such a model, the mean-field theory does not predict a transition temperature.

In order to find the transition temperature of such a model, it is necessary to include fluctuations about the mean field solution. This weakly interacting Bose gas model, and the fluctuation corrections to the mean-field theory are discussed in detail in section 6.1. At the phase transition, it is shown that the total density, including fluctuation corrections, is given by populating the uncondensed modes with an effective chemical potential $\mu = 0$:

$$\rho = \int_0^\infty g \frac{4\pi k^2 dk}{(2\pi)^3} \frac{1}{e^{\beta \epsilon_k} - 1}, \tag{1.4}$$

where g is the spin degeneracy.

Therefore, the mean-field theory and fluctuation corrections in three dimensions recover the textbook result for a non-interacting gas. For the non-interacting gas, the critical temperature is found when the chemical potential required to accommodate a given density reaches 0. This gives the same form as eq. (1.4), leading to:

$$k_B T_{BEC}^{3D} = \frac{2\pi\hbar^2}{m} \left(\frac{\rho}{2.612 g} \right)^{2/3}. \tag{1.5}$$

In two dimensions, fluctuations destroy the condensed phase at any non-zero temperature. Equivalently, there is no statistical transition in a non-interacting gas in two dimensions — any density

can be accommodated with a negative chemical potential. However, a phase transition to a power-law correlated state is possible in two dimensions as described by Kosterlitz and Thouless [18]. The Kosterlitz-Thouless transition involves the unbinding of vortex-antivortex pairs. By mapping the dilute Bose gas to a gas of interacting vortices [19], it is possible to describe this transition for a 2D Bose gas [20, 21].

By starting with an interacting theory, the more interesting properties of the condensed state are immediately apparent. For example, the broken symmetry leads to the existence of a low energy Goldstone mode, changing the excitation spectrum of the system. The change to the excitation spectra is also responsible for superfluidity, as is discussed in some detail in chapter 2. Another important aspect of interactions, discussed next, is the idea of phase locking, which leads to an unfragmented condensate, and the use of coherent states.

As argued by Nozières [22], interactions between particles lead to an extensive energy difference between populating a single mode, or two almost degenerate modes. Considering again the weakly interacting Bose gas model of eq. (1.3), a trial wavefunction can be constructed:

$$|\psi_0\rangle = (a_0^\dagger)^N (a_{k_1}^\dagger)^M |0\rangle \,. \tag{1.6}$$

If k_1 is chosen to be the lowest non-zero momentum state (considering quantisation in a box), then the quadratic terms in the Hamiltonian, eq. (1.3), lead only to an energy M/V where V is the box volume, which is non-extensive. However, the quartic interaction term in eq. (1.3),

$$\hat{V} = \frac{g}{2} \sum_{k,k',q} a_{k+q}^\dagger a_{k'-q}^\dagger a_k a_{k'}, \tag{1.7}$$

gives the following energy;

$$\begin{aligned} \left\langle \psi_0 \middle| \hat{V} \middle| \psi_0 \right\rangle &= \frac{g}{2} \left(N(N-1) + M(M-1) + 4NM \right) \\ &\approx \frac{g}{2}(N+M)^2 + gNM. \end{aligned} \tag{1.8}$$

The terms linear in number of particles have been neglected in the second line as they do not give an extensive energy. The remaining terms show that, for a repulsive interaction, there is an exchange term, gNM which disfavours a fragmented state, *i.e.* favour a state with $N = 0$ or $M = 0$.

The state given by eq. (1.6) with $M = 0$ is however not the lowest energy state for Hamiltonian eq. (1.3). A better approximation to the ground state, which also better shows the coherence associated with Bose condensation comes from considering the coherent state,

$$|\psi_{\text{coh.}}\rangle = \exp\left(\alpha a_0^\dagger\right)|0\rangle\,. \tag{1.9}$$

Although this state itself does not have an extensively smaller energy than the state in eq. (1.6), by considering a population of non-zero k particles as well, one can construct a lower energy state. This can be understood in two ways. The first way is to construct the trial wavefunction:

$$|\psi\rangle = \exp\left(\alpha a_0^\dagger + \sum_k \lambda_k a_k^\dagger a_{-k}^\dagger\right)|0\rangle\,. \tag{1.10}$$

As discussed by Nozières and Saint James [23], the energy of this state can be minimised to find λ_k, and this minimum energy is less than that of either of the states in eq. (1.6) or eq. (1.9). The physical origin of this reduction in energy is the contribution from interaction terms such as $a_0^\dagger a_0^\dagger a_k a_{-k}$. Such terms only give an expectation if the wavefunction is a coherent sum of states with different numbers of particles in the condensate. It is important to note that even projected onto a state with fixed total number of particles:

$$|\psi_N\rangle = \left[(a_0^\dagger)^N + (a_0^\dagger)^{N-2}\sum_k \lambda_k a_k^\dagger a_{-k}^\dagger + \ldots\right]|0\rangle\,, \tag{1.11}$$

such an energy gain may still arise,

The second way to understand this reduction in energy is by considering the coherent state as a mean-field theory, and then adding

fluctuation corrections. This is discussed in detail in section 6.1. In the presence of the condensate, the normal modes change, becoming the Bogoliubov quasiparticle modes. The quasiparticle creation operators can be written in terms of the particle creation and annihilation operators as:

$$b_k^\dagger = \cosh(\theta_k) a_k^\dagger + \sinh(\theta_k) a_{-k}, \tag{1.12}$$

where θ_k is defined by:

$$\tanh(2\theta_k) = \frac{\epsilon_k + g\rho_0}{g\rho_0}. \tag{1.13}$$

As well as having a different dispersion, this new quasiparticle spectrum has a different ground state. The quasiparticle vacuum is not the particle vacuum. Thus, the new ground state has a population of non-zero momentum modes, and is exactly the state given by eq. (1.10).

Examples of spontaneous coherence

Other than excitons and polaritons, which will be discussed below, there exist a wide variety of systems that show spontaneous phase coherence. The following discussion reviews some of these examples, the experimental difficulties associated with them, and the theoretical models that describe them.

Dilute atomic gases

Of those systems where condensation has unambiguously seen, the preceding discussion applies most closely to condensation of dilute atomic gases [5, 6]. In such systems, the transition temperature is extremely low; typically 10^{-7}K. This temperature is so low partly due to the large mass of the particles involved, but more importantly because of the low densities of the atomic gases. A Bose condensate of most atomic species is not thermodynamically stable; the ground state would be a solid. However, the Bose condensate can be metastable if the density is sufficiently low that three-body collisions

are negligible. Two-body collisions between atoms in their ground states are effectively elastic, and so do not contribute to relaxation to the crystalline ground state.

Such low temperatures are achievable by a mixture of laser cooling [24, 25, 26], and magnetic trapping[27]. Condensation of atomic vapours has now been seen in all stable Alkali metals, and recently also in Ytterbium. A wide variety of experiments have been performed on such condensates. These experiments include interference fringes of two moving condensates [28] , rotating clouds leading to the formation of vortices and vortex lattices *e.g.* [29], and recent experiments on atoms in periodic trapping potentials [30].

Superfluid liquid Helium

Liquid Helium, as discovered by Kapitza [2] and Allen and Misener [3], becomes superfluid at temperatures of around 2.17K. This is a much higher temperature than the dilute atomic condensates, as it is at a much higher density. Higher densities are possible since Helium does not form a solid at any temperature at atmospheric pressure. However, being of much higher density, it is not accurately described by the model of weakly interacting dilute Bose gas — rather it is a Bose liquid. This is immediately evident from its transition temperature, which is less than the 3.1K that would be predicted by eq. (1.5). However, features such as the linear dispersion of low energy modes do survive. Much of the discussion of superfluidity collected in chapter 2 arises from attempts to describe the superfluid behaviour of Helium without assuming weak interactions.

BCS Superconductivity

Superconductivity [1] provides a rather different example of condensation. Most obviously, it involves condensation of pairs of electrons, as electrons are fermionic — however all observed Bose condensates involve bosons that are bound states of fermions. The important difference in BCS superconductors is that the electrons have only weak attractions, so that the formation of bound pairs, and con-

densation of those pairs occurs together. In this weakly interacting limit, where no pairs exist above the transition, the transition temperature is accurately given by a mean-field theory, in terms of an order parameter for the bound pairs.

The theory can be most simply represented starting from the BCS Hamiltonian, describing electrons with an attractive, phonon-mediated interaction

$$H - \mu N = \sum_{k,\sigma} (\epsilon_k - \mu) c^\dagger_{k,\sigma} c_{k,\sigma} - \frac{g}{2} \sum_{k,k',q} c^\dagger_{k',\uparrow} c^\dagger_{q-k',\downarrow} c_{q-k,\downarrow} c_{k,\uparrow}, \quad (1.14)$$

where $c^\dagger_{k,\sigma}$ creates an electron of spin σ. To construct a mean-field theory, this must be rewritten in terms of an order parameter which is a complex field. This is achieved by writing the path integral representation of the free energy, then decoupling the fermionic interaction with a bosonic field:

$$\begin{aligned} e^{-\beta F} &= \int \mathcal{D}(c, c^\dagger) \exp\left(- \int_0^\beta d\tau \left[H - \mu N + \bar{c} \partial_\tau c \right] \right) \\ &= \int \mathcal{D}(c, c^\dagger) \int \mathcal{D}(\Delta) \exp\left(-S[c, \bar{c}, \Delta] \right). \end{aligned} \quad (1.15)$$

The effective action can be written in terms of the two component Nambu spinor,

$$\Psi_{\omega,k} = \begin{pmatrix} c_{\omega,k,\uparrow} \\ \bar{c}_{-\omega,-k,\downarrow} \end{pmatrix}, \quad (1.16)$$

giving:

$$\begin{aligned} S[\Psi, \Delta] &= \sum_q \frac{|\Delta_q|^2}{2g} \\ &+ \sum_{k,k'} \Psi^\dagger_k \begin{pmatrix} i\omega + \epsilon_k - \mu & \Delta_{k-k'} \\ \Delta^*_{k-k'} & i\omega - \epsilon_k + \mu \end{pmatrix} \Psi_{k'}. \end{aligned} \quad (1.17)$$

Integrating over the fermionic fields gives an effective action in terms of Δ_q. Considering only the $\Delta_{q=0}$ term, *i.e.* the mean-field theory, the effective action is

$$S_{\text{eff}}[\Delta_0] = \frac{|\Delta_0|^2}{2g} - \sum_{\omega,k} \ln\left(\omega^2 + (\epsilon_k - \mu)^2 + |\Delta_0|^2 \right). \quad (1.18)$$

Expanding in powers of $|\Delta_0|^2$, the quadratic term — the equivalent of a in eq. (1.1) — is given by:

$$\begin{aligned} a &= \frac{1}{2g} - \sum_{\omega,k} \frac{1}{\omega^2 + (\epsilon_k - \mu)^2} \\ &\approx \frac{1}{2g} - \nu(\mu) \int_{\Omega_D}^{\Omega_D} dx \frac{\tanh(\beta x)}{x}. \end{aligned} \tag{1.19}$$

In the second line, the sum over momenta has been rewritten in terms of energy measured from the chemical potential, $\epsilon_k = \mu + x$, and the integral cut by the Debye frequency Ω_D. For three dimensional systems, the density of states at the chemical potential, $\nu(\mu)$ is proportional to the total density, giving a transition temperature:

$$k_B T_c = \Omega_D \exp\left(-\frac{1}{\rho_0 g}\right), \tag{1.20}$$

Such a treatment is very similar to the mean-field theory of polariton condensation discussed by Eastham and Littlewood [31], and extended in this dissertation. However, there are important differences between the polariton model and the BCS model. The polariton model starts from interacting fermions and bosons — which can be compared to the BCS model after Hubbard-Stratonovitch decoupling — however the polariton model has a dynamic boson mode. There are also differences associated with the fermionic density of states. This comparison is discussed in detail in sections 5.2 and 6.4.

Dilute fermionic atomic gases

Recently, there has been huge interest in cold dilute fermion gases [32, 33, 34, 35] near Feshbach resonance. These are of interest because the Feshbach resonance allows the strength of the inter-atomic interaction to be tuned by applying a magnetic field. The interaction strength changes as a bound state of the fermions in one nuclear spin state is brought into resonance with the zero of energy for fermions in another spin state — the scattering channel state. This is illustrated schematically in figure 1.1. Because the nuclear spin states are not

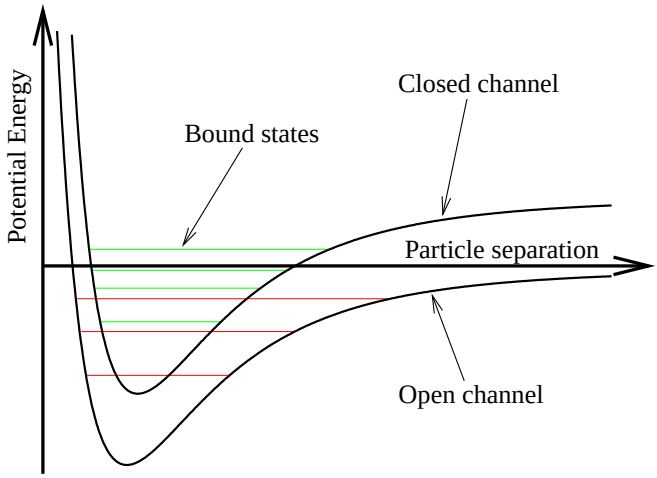

Figure 1.1: Schematic diagram of potential in open (scattering) spin channel and closed channel, showing resonance between bound state and the zero of energy for the open channel.

eigenstates, and couple via the hyperfine interaction, the resonance causes a change of interaction strength in the scattering channel. By adiabatically changing the magnetic field, unbound atoms can be bound into molecules [35]. This allows direct investigation of the crossover between a BCS state for weakly attractive fermions, and a Bose condensate of bound molecules.

There has also been much theoretical activity describing the equilibrium states and dynamics of such systems as the interaction strength is tuned. One proposed model, the Holland-Timmermans model [36, 37], is very similar to the model for polariton condensation discussed in this dissertation:

$$\begin{aligned} H - \mu N &= \sum_{k,\sigma} (\epsilon_k - \mu) c^\dagger_{k,\sigma} c_{k,\sigma} + \sum_k (\epsilon_k + 2\Delta - 2\mu) b^\dagger_k b_k \\ &+ g \sum_{k,q} \left(b^\dagger_q c_{-k+q/2,\downarrow} c_{k+q/2,\uparrow} + c^\dagger_{k+q/2,\uparrow} c^\dagger_{-k+q/2,\downarrow} b_q \right) \end{aligned}$$

$$- \frac{U}{2} \sum_{k,k',q} c^\dagger_{k+q,\uparrow} c^\dagger_{k'-q,\downarrow} c_{k,\downarrow} c_{k',\uparrow}. \tag{1.21}$$

Here, the operator $c^\dagger$ creates a fermion in the scattering channel, and the operator $b^\dagger$ was originally intended as creating a bosonic molecule. The detuning Δ between the fermionic and bosonic channels represents the effect of tuning the resonance by the magnetic field.

This model and the polariton model have in common the presence of a bosonic mode with dynamics and a chemical potential. For the polariton model, this bosonic mode has a clear physical identification as the photon mode in the cavity. In the case of Feshbach resonance, identification of the bosonic field is more subtle. The operators $b^\dagger$ in eq. (1.21) do not create bound molecular states, which would be eigenstates, but rather refer to the closed channel part of a bound molecule — an object that is hard to access experimentally. Integrating out the bosonic mode will lead to a purely fermionic model, but with a frequency and detuning fermion-fermion interaction. For most current experiments, the fraction of population in the closed channel molecular states is small, and it is often sufficient to consider the BCS Hamiltonian, eq. (1.14), but with a detuning dependent interaction (see *e.g.* [38, 39]).

The laser

Finally, there is the laser. Here, a light field is confined in a cavity by partially reflecting mirrors, and interacts with a gain medium. This gain medium is strongly pumped, either electrically or by radiation at a higher energy. Pumping leads to inversion; a non-thermal distribution with higher energy levels occupied more than lower levels. Stimulated emission from the inverted oscillators in the gain medium leads to a coherent photon field, even when pumping is entirely incoherent.

This differs from all of the previous examples in several important regards. Firstly, it is far from thermal equilibrium, and is strongly pumped. Further, in standard laser systems, only the photon field is

coherent, the gain medium shows no phase correlations. As discussed by Szymanska *et al.* [40], polariton condensates with pair-breaking disorder show a crossover from a state with coherence of both excitons and light, to one where only the light is coherent. This does not however directly address how pumping the system out of equilibrium modifies the description of coherence. It remains an open and topical question to model polariton condensation with pumping, and see the crossover thus induced.

1.3 Excitons and polaritons

This section introduces and reviews the history of experimental attempts to produce condensation of excitons and exciton-polaritons. The idea of exciton condensation was first proposed for bulk semiconductors, and later for two-dimensional systems of spatially separated electrons and holes — spatially indirect excitons. While there have been experiments on bulk semiconductors for many years, spatially indirect excitons have been investigated only relatively recently, in coupled quantum well semiconductor heterostructures. Condensation of microcavity polaritons is a more recent idea, driven by the realisation of clear polariton modes for quantum wells in semiconductor microcavities.

Excitons in general

After the observation [2] and characterisation [4] of superfluidity in ^{4}He , excitons were one of the next systems suggested for Bose-Einstein condensation [41, 42, 43, 44]. Excitons are the bound state of an electron and a hole in a semiconductor or semimetal — herein only semiconductors, are considered. They are analogous to the hydrogen atom, with two important differences:

1. The electron and hole masses are typically of the same order of magnitude.

2. The Coulomb attraction is reduced by the semiconductor dielectric constant $\varepsilon \approx 13$.

Thus, the binding energy of an exciton is small compared to that of Hydrogen, and the Bohr radius is large:

$$E_{\rm bind} = \left(\frac{e^2}{4\pi\epsilon}\right)^2 \frac{m}{2\hbar^2} \approx 1 - 100{\rm meV} \tag{1.22}$$

$$a_{\rm bohr} = \frac{4\pi\epsilon}{e^2}\frac{\hbar^2}{m_e} \approx 1 - 100{\rm nm} \tag{1.23}$$

Excitons are an obvious candidate for Bose condensation because of their small mass, typically of the order of the free electron mass. As discussed above, (see eq. (1.5)), transition temperature is inversely proportional to particle mass, so a small mass allows higher transition temperatures or lower densities.

However, Bose condensation of excitons presents several problems. Most obviously excitons have a finite lifetime, typically of the order of nanoseconds, and will decay by photon emission. Excitons can be created by shining light on the sample; the energy needed to create an exciton is given by $\hbar\omega_0 = E_{\rm gap} - E_{\rm bind}$, where $E_{\rm gap}$ is the band gap. Alternatively, higher energy non-resonant illumination creates free electrons and holes, which may bind together to form an exciton. Both resonant and non-resonant pumping result in a population of hot excitons, so to observe condensation it is necessary that excitons can thermalise and cool on timescales shorter than their lifetimes.

A more subtle problem was pointed out independently by Kohn and Sherrington [45] and by Guseĭnov and Keldysh [46]; exciton number is not conserved, and so the phase of any condensate is fixed. As well as radiative recombination, the Coulomb interaction between electrons and holes allows interband transitions, which lead to the creation or annihilation of single excitons and pairs of excitons. Such terms break the symmetry under global changes of the condensate phase. Therefore, even when condensed, the spectrum of low energy modes will be gapped. This would at first seem to destroy superfluidity, however it has been suggested that supercurrents can exist in a model where pairs of excitons can be created or destroyed [47, 48]. Such terms can also be expected to change the form of the phase transition in two dimensions [49, 50].

Exciton condensation has been sought in a variety of systems, in which exciton recombination is suppressed. Recombination can be suppressed for a variety of reasons: it may naturally be dipole forbidden in certain materials, the overlap of electron and hole wavefunctions in momentum space may be reduced by applying magnetic fields (magnetoexcitons), or the overlap in real space may be reduced by using spatially indirect excitons. One of the most promising candidates for exciton condensation was Cu_2O [51], where recombination is dipole forbidden. However at the high densities required for exciton condensation, it appears that recombination by an Auger process becomes important. In such a process two excitons collide, causing one to recombine, and the other to gain energy (see ref. [52] and refs. therein). This density dependent recombination both reduces the possibility for condensation, and provides an alternate explanation for the luminescence observed in such systems.

Coupled quantum well excitons

More recently, experimental efforts have focused on coupled quantum well systems. As first suggested by Lozovik and Yudson [53, 54] and Shevchenko [55], by confining electrons and holes in separate two dimensional layers, the lifetime of excitons is hugely increased. Such systems have a further advantage: as discussed by Lozovik and Yudson [53, 54] the interband transitions that break phase symmetry, discussed above, are smaller in spatially separated electron-hole systems. Because electrons and holes are in separate layers, such interband transitions involve tunnelling between the layers.

Spatially separated electron hole systems can be experimentally realised by coupled quantum wells. By applying a bias field, electrons and holes collect in different quantum wells. Excitons formed from electron and holes in different wells are known as (spatially) indirect excitons, direct excitons have the electron and hole in the same well. This is shown schematically in figure 1.2. Indirect excitons have more features that may favour condensation. As the excitons are confined to two dimensions, momentum conservation perpendicular to the plane of the well is relaxed; this allows excitons to couple

to a continuum of bulk LA phonon modes, increasing the thermalisation rate (see *e.g.* Ivanov *et al.* [56]). Also, the strong repulsive dipole interactions between indirect excitons prevent the formation of biexcitons, and stabilise the system against phase separation into droplets of electron hole liquid[57, 58].

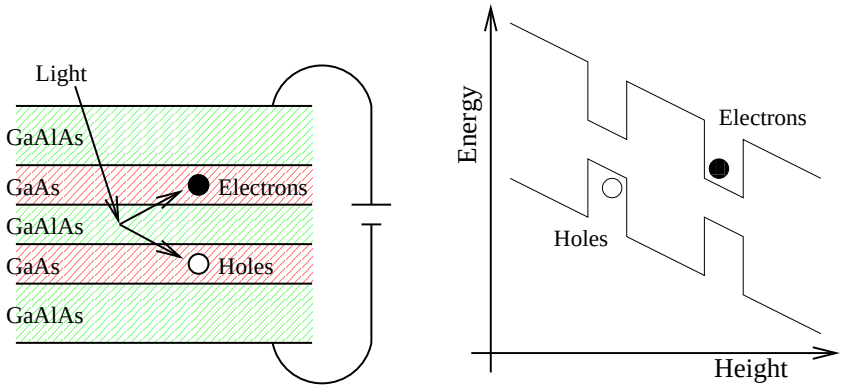

Figure 1.2: Schematic diagrams of a quantum-well bilayer system. The left hand panel shows the geometry normal to the plane of the quantum wells. The right hand shows the energy profile through the layers. An electric field is applied between the two layers, resulting in the energy profile seen. Therefore when pumped the electrons and holes created will move to the separate layers.

Butov [59] provides a detailed review of the properties of indirect excitons in coupled quantum wells, experiments looking for signatures of exciton condensation, and of recent work on pattern formation in a cold exciton gas. Among the many experiments on indirect excitons, a variety of experimental signatures have been investigated. These signatures include changes in the photoluminescence spectrum [60, 61, 62], and in the dynamics of exciton recombination (the "Photoluminescence jump") [63, 64].

In the last few years, there has been much interest in the observation of rings; regions of bright photoluminescence at distances of some 100μm from the laser spot [65, 66, 67]. The existence of

the ring can be explained by a purely classical picture [68], however the fragmentation of the ring into periodic beads at low temperatures suggests an explanation in terms of stimulated process [69, 70]. There have also been recent proposals to study the behaviour of a cold exciton gas in artificially engineered traps [71, 72, 73, 74].

Microcavity polaritons

Microcavity exciton-polaritons are the eigenstates of an exciton coupled to cavity photon modes. The concept of an exciton-polariton was first considered in bulk semiconductors by Pekar [75] and Hopfield [76]. A polariton can be understood as the quantum of light in a dielectric medium, considering the exciton contribution to dielectric response.

Microcavity polaritons can be experimentally realised by placing quantum wells at the antinodes of the photon mode in a cavity created by distributed Bragg reflectors (DBR) [77]. If the coupling between excitons and photons is larger than both their linewidths, then the reflection and photoluminescence spectra will show pronounced anticrossing of the exciton and cavity mode. This is referred to as the strong coupling regime and was observed for quantum wells in DBR microcavities by Weisbuch *et al.* [78]. Figure 1.3 shows a schematic picture of a semiconductor microcavity, and of the upper and lower polariton modes. The small cavity size increases the field strength of the photon mode, increasing its coupling to the exciton. Strong coupling — *i.e.* anticrossing of exciton and photon modes — has also recently been observed for a single quantum dot in a zero-dimension semiconductor microcavity [79] and in a photonic band gap cavity [80].

Current experiments on microcavity polaritons can be divided into two main classes, according to whether pumping is resonant or non-resonant. For non-resonant pumping, two different schemes are commonly used. Either the laser is tuned to energies far above the polariton, creating unbound electrons and holes, which subsequently bind to form high energy and momentum exciton-polaritons. Alternatively, the laser is resonant with high momentum exciton-

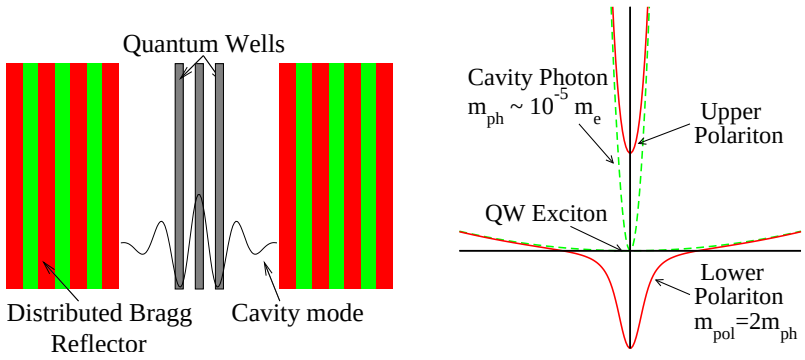

Figure 1.3: (Left) Schematic diagram of a microcavity, formed from two distributed Bragg reflectors, containing quantum wells at the antinodes of the cavity mode. (Right) In plane dispersion of exciton and cavity photon modes, coupled to produce polariton modes.

polaritons, and the pumping is away from normal incidence. For both schemes, a population of incoherent exciton polaritons at large momenta is expected. Such polaritons have predominantly exciton character, and are long lived as they have too large a momentum to allow recombination to bulk photon modes. They may then thermalise by polariton-polariton interactions, and cool by the emission of LA-phonons.

Recent experiments on non-resonantly pumped polaritons have shown a variety of results that suggest stimulated effects. These include nonlinear increase of the occupation of the ground state [81, 82] when pumped beyond some threshold intensity , sub-thermal second order correlation functions [82], changes to the dispersion of polariton luminescence [83, 84, 85] and increased population of low momentum polaritons [83, 86]. Because the low momentum polaritons decay on a picosecond timescale due to the cavity lifetime, and are created at high energies, it is not clear whether polaritons may thermalise within their lifetime. With increasing polariton density, the rate of polariton-polariton scattering increases, and so thermalisation should be faster. Recent data [86] suggest that near the thresh-

old for macroscopic occupation of the ground state the system may approach a thermal state. For lower densities, the occupation shows a maximum away from zero momentum due to a bottleneck in the relaxation process [12, 58, 87]. Even for densities near threshold, it is not expected that the polaritons reach equilibrium at the temperature of the crystal lattice, but rather some quasi-thermal equilibrium at an effective temperature.

There has also been work where the pump laser is resonant with the lower polariton branch. In particular, there exists a "magic angle" where $2E_k = E_{2k} + E_0$, so polariton-polariton scattering, conserving energy and momentum, can directly populate the ground state. In this case the experiment is parametric resonance, with a pump beam creating a "signal" at $k = 0$ and an idler beam at $k = 2k_{\text{pump}}$. Recent experiments on such systems include observation of stimulated scattering [88, 89, 90] and demonstration of second order coherence of the signal beam [91]. Pumping away from the magic angle, the states to which scattering is allowed lie on figure of 8 in momentum space. By pumping at two different azimuthal angles, these allowed scattering curves intersect at two points. Savasta *et al.* [92] have demonstrated coherence between the idler beams of two different pumps when the signal beams intersect, providing a polariton equivalent of the two-slit experiment.

Chapter 2

Superfluidity

Superfluidity describes the ability of a fluid to flow without resistance. At non-zero temperatures, the response of a Bose condensed fluid to forces can be divided into superfluid and normal parts, and can be described by two fluids, with separate normal and superfluid densities. This chapter collects various results defining superfluid density, restricting approximations for its calculation, and relating its definition from response functions to the spectrum of low energy phase modes in a condensed fluid.

Superfluid density plays a particularly important rôle in describing condensation in two dimensions. Although there is no long-range order in two dimensions, interacting bosons can undergo a Kosterlitz-Thouless [18] transition to a superfluid phase. In order to describe this transition it is necessary to map the system of interacting bosons to a problem of interacting vortices, as discussed by Nelson and Kosterlitz [20]. The core energy, and strength of interaction between vortices depend on the dispersion of the phase mode, and thus on the superfluid density. In practical calculations, this mapping therefore relies on using response functions to calculate the superfluid density, which then appears as a parameter describing the model of interacting vortices.

2.1 From Landau's argument to response functions

The name "superfluidity" was first introduced by Kapitza [2] to describe the behaviour of liquid Helium below the λ-transition. Below a temperature of 2.2K, liquid Helium undergoes a phase transition (the λ transition). The most remarkable feature of this low temperature phase is the ability to flow without viscosity. Evidence for such flow was seen independently by Kapitza [2], studying flow between two glass discs, and Allen and Misener [3] studying flow through a capillary.

Landau, in a comprehensive paper [4] in 1941, described this behaviour from a phenomenological picture of helium flowing in a capillary. Starting from a state where the superfluid is flowing in the capillary, viscosity will try to bring the fluid to rest. In the frame of the fluid, the walls are moving, and these moving walls produce a response of the fluid. Neglecting the response of the entire fluid (*i.e.* the condensate response), Landau argued one should consider the energy to create a quasi-particle fluctuation in the moving frame. If this energy, $\epsilon'(\mathbf{p}) = \epsilon(\mathbf{p}) + \mathbf{v}.\mathbf{p}$ is negative, then the walls can create quasi-particles, and destroy the flow. If the spectrum of excitations about the ground state are either gapped, $\epsilon(\mathbf{p}) = \Delta + p^2/2m$, or have a linear dispersion, $\epsilon(\mathbf{p}) = cp$, then there will be a critical velocity required to excite such fluctuations. If the spectrum instead starts with a quadratic dispersion, then no such critical velocity arises.

However, the above argument neglects the possibility of the quantum state of the superfluid changing due to the motion of the walls. In order to address this, one must consider the contributions to momentum current of the superfluid and quasi-particles. The superfluid component, being described by a macroscopic wavefunction, $\Psi = \sqrt{\rho_s} e^{i\phi}$, has a momentum current given by $\mathbf{j}_s = \rho_s \nabla\phi$. The normal component has a momentum given by the sum of momenta of the excited quasi-particles (the phonons and rotons of Landau's description). One can therefore write the total current as $\mathbf{j} = \rho_s \mathbf{v}_s + \rho_n \mathbf{v}_n$. The superfluid velocity, $\mathbf{v}_s = \nabla\phi$, by definition satisfies $\nabla \times \mathbf{v}_s = 0$,

and cannot support circulation.

This distinction leads to a simple, practical test; if a bucket containing helium below the λ point is rotated slowly, the moment of inertia of the helium will be less than expected, and as $T \to 0$ it will vanish. The statement that the superfluid cannot support circulation is an over-simplification; it is possible to create a state where $\phi(\theta + 2\pi) = \phi(\theta) + 2m\pi$ around a point where the superfluid density goes to zero. Therefore, by allowing vortices, a superfluid can rotate. The creation of a vortex core has an energy cost, and so for slow rotations, the vanishing moment of inertia holds.

The separation of ρ_s and ρ_n, and ascribing to them of different motions is the concept of two-fluid hydrodynamics introduced by Landau. This separation should not be thought of as a division of atoms between the superfluid and the normal parts, but that the hydrodynamic behaviour is as if there were two fluids, one of which is irrotational. It is also important to note that the superfluid density must not be identified with the condensate density: as $T \to 0$ the superfluid density always approaches the total density, even when interactions strongly deplete the condensate, as is the case in liquid Helium.

2.2 Response functions and Ward identities

The difference between superfluid and normal-fluid response can be stated in an alternate way, which is more useful for performing calculations. A superfluid has no response to a transverse force, but does have a response to a longitudinal force, with transverse and longitudinal defined as shown in figure 2.1. This distinction can be written more precisely in terms of the current-current response function [9, 93].

In terms of operators $\psi_q^\dagger$ creating a particle of momentum $\mathbf{q}$, the particle current is defined as:

$$\mathbf{J}(\mathbf{q}, 0) = \sum_{\mathbf{k}} \frac{\hbar \mathbf{k}}{m} \psi^\dagger_{\mathbf{k}+\mathbf{q}/2} \psi_{\mathbf{k}-\mathbf{q}/2}. \tag{2.1}$$

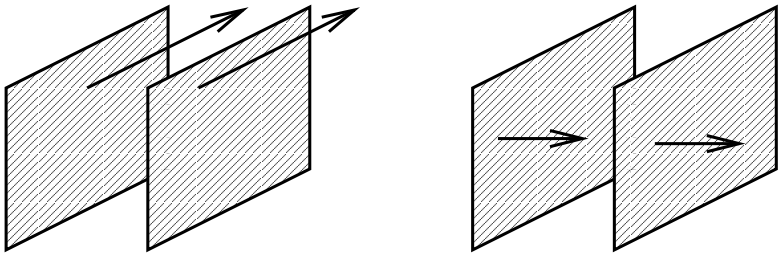

Figure 2.1: Transverse (left) and longitudinal (right) forces applied to a fluid by means of moving plates.

The current-current response function describes how a force, coupling to the current, causes the current to change. A force, $\delta\mathbf{f}$, leads to a perturbation to the Hamiltonian, $\delta H = \delta\mathbf{f}.\mathbf{J}$. The linear response to this force may then be written as $\langle J_i(q,0)\rangle = \chi_{ij}(q)\delta f_j(q)$. Since $J_i^\dagger(q) = J_i(-q)$, if the perturbation is to be Hermitian, then $\delta f_i(q) = \delta f_i(-q)$. By rotational symmetry, the most general response function can be written as:

$$\chi_{ij}(\mathbf{q}) = \chi_{\rm L}(\mathbf{q})\frac{q_i q_j}{q^2} + \chi_{\rm T}(\mathbf{q})\left(\delta_{ij} - \frac{q_i q_j}{q^2}\right). \tag{2.2}$$

To evaluate the linear response function, χ_{ij}, consider the current written in terms of the perturbed states $|n'\rangle$, and energies E'_n:

$$\langle \hat{J}_i(q)\rangle = \frac{1}{\mathcal{Z}}\sum_{n'} e^{-\beta E'_n}\left\langle n'\middle|\hat{J}_i(q)\middle|n'\right\rangle. \tag{2.3}$$

The perturbation δH could cause shifts to the states and the energies. However, as there is no expectation of the current for the unperturbed states, to first order the energies do not shift. Thus, using the perturbed states,

$$\left|n'\right\rangle = |n\rangle + \sum_m |m\rangle\,\frac{\left\langle m\middle|\hat{J}_j(q)\middle|n\right\rangle}{E_n - E_m}\delta f_j(q), \tag{2.4}$$

the linear response is given by:

$$\chi_{ij}(\mathbf{q}) = \frac{2}{\mathcal{Z}} \sum_{n,m} \frac{e^{-\beta E_n}}{E_n - E_m} \left\langle n \middle| \hat{J}_i(-q) \middle| m \right\rangle \left\langle m \middle| \hat{J}_j(q) \middle| n \right\rangle . \qquad (2.5)$$

From the above form, it is possible to construct a sum rule for the longitudinal component of the response function. The discussion here follows that of Pitaevskii and Stringari [9]. If the Hamiltonian depends only on the current operator via the kinetic energy, it follows that: $\left[\hat{H}, \hat{\rho}(q)\right] = -m\mathbf{q}.\hat{\mathbf{J}}(q)$, and so using eq. (2.2) and eq. (2.5):

$$\begin{aligned} \chi_L(q) &= \frac{q_i q_j}{q^2} \chi_{ij}(q) \\ &= \frac{2}{m^2 q^2 \mathcal{Z}} \sum_{n,m} \frac{e^{-\beta E_n}}{E_n - E_m} \left| \left\langle n \middle| \left[\hat{H}, \hat{\rho}(q)\right] \middle| m \right\rangle \right|^2 \\ &= -\frac{1}{m q^2 \mathcal{Z}} \sum_{n} e^{-\beta E_n} \left\langle n \middle| \left[\hat{\rho}(q), \mathbf{q}.\hat{\mathbf{J}}(q)\right] \middle| n \right\rangle . \qquad (2.6) \end{aligned}$$

Evaluating the final commutator gives $\chi_L(q) = -N/m$, or rewriting slightly, $\rho = -m\chi_L(\mathbf{q})/A$. This sum rule is a result of the conservation of particles; it is an expression of the continuity equation for the particle current, and therefore holds for all q.

As discussed above, the superfluid current comes from $\mathbf{j}_s = \rho_s \nabla\phi$, which in momentum space is $(\mathbf{j}_s)_i = i\rho_s q_i \phi(q)$. Therefore, the superfluid contribution will have the symmetry $\chi^s_{ij} \propto q_i q_j$ as $q \to 0$, and so contributes only to the term χ_{L}. Thus the normal density can be defined by the transverse response as $q \to 0$. By analogy to the above sum rule, the normal density is defined by $\rho_{\mathrm{normal}} = -m\chi_{\mathrm{T}}(\mathbf{q} \to 0)/A$. Note that while the longitudinal response at any q is related to the total density, the transverse response reduces to the normal density only as $q \to 0$. At finite q, the superfluid response may have more complicated q dependence, and thus could contribute to both transverse and longitudinal parts. This definition matches the Landau two-fluid hydrodynamic definition of ρ_s and ρ_n. The response to a probe is divided between an irrotational (longitudinal) superfluid response, and the response of the normal fluid.

Ward identities

When attempting to evaluate the response function in some particular approximation scheme, the sum rule $\rho = -m\chi_L(\mathbf{q})/A$ places restrictions on the approximations. To understand these restrictions, consider the response function written in terms of the single particle Green's functions,

$$\chi_{ij}(\mathbf{q}) = \mathrm{Tr}\left[\Gamma_i(\mathbf{k}+\mathbf{q},\mathbf{k})\mathcal{G}(\mathbf{k})\gamma_j(\mathbf{k},\mathbf{k}+\mathbf{q})\mathcal{G}(\mathbf{k}+\mathbf{q})\right]. \tag{2.7}$$

Here $\gamma_i(\mathbf{p},\mathbf{q})$, is the bare coupling of momentum current to the single particle excitations, defined by:

$$\hat{J}_i(q) = \sum_k \hat{\Psi}^\dagger(\mathbf{k})\gamma_i(\mathbf{k},\mathbf{k}+\mathbf{q})\hat{\Psi}(\mathbf{k}+\mathbf{q}), \tag{2.8}$$

where

$$\hat{\Psi}(\mathbf{k}) = \begin{pmatrix} \psi(\mathbf{k}) \\ \psi^\dagger(-\mathbf{k}) \end{pmatrix} \quad \text{so,} \quad \gamma_i(\mathbf{k},\mathbf{k}+\mathbf{q}) = \sigma_3\frac{2k_i+q_i}{2m} \tag{2.9}$$

The Pauli matrix σ_3 acts on this Nambu space of creation and annihilation operators.

The expression $\Gamma_i(p,q)$ is a dressed version of this vertex; *i.e.* it includes corrections due to interactions between particles. This expression is shown diagrammatically in figure 2.2. In order to sat-

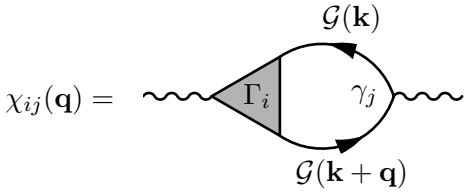

Figure 2.2: Current-current response function in terms of dressed propagators and vertices

isfy current conservation, and hence fulfil the sum rule on χ_L, it is necessary to make consistent approximations for Γ and $\mathcal{G}$.

In the following, the amputated vertex function, Γ, will be defined in terms of correlation functions, and current conservation used

to produce an identity relating Γ and $\mathcal{G}$. This scheme was first applied in the study of Quantum Electrodynamics by Ward [94] and generalised by Takahashi [95] (as discussed in *e.g.* Section 10.4 of Weinberg's book [96]). It was then applied by Nambu [97] to the calculation of the current-current response in the theory of BCS superconductivity (discussed in *e.g.* Chapter 8 of Schrieffer's book [1]). The discussion below is similar to that of Schrieffer.

The amputated vertex function, Γ is the full vertex, Λ, with external propagators removed, thus:

$$\begin{aligned} \Lambda_i(x,y,z) &= \langle T(\hat{J}_i(x)\psi(y)\psi^\dagger(z))\rangle & (2.10)\\ &= \int dy' \int dz' \mathcal{G}(y,y')\mathcal{G}(z',z)\Gamma_i(x,y',z') & (2.11)\end{aligned}$$

The Ward-Takahashi identity results from differentiating this equation with respect to x. Acting on the right hand side of eq. (2.10), this results in three terms: one term associated with the divergence of the current, and two terms associated with commutators when time ordering changes. If the current is conserved, the divergence term vanishes. Assuming translational invariance, and Fourier transforming w.r.t. $x-y$ and $x-z$ leads to the function $\Gamma_i(\mathbf{p},\mathbf{q})$, and yields the equation:

$$q_i\Gamma_i(\mathbf{k}+\mathbf{q},\mathbf{k}) = \sigma_3\mathcal{G}^{-1}(\mathbf{k}) - \mathcal{G}^{-1}(\mathbf{k}+\mathbf{q})\sigma_3. \qquad (2.12)$$

This is the Ward-Takahashi identity that must be satisfied in order to fulfil the sum rule for χ_{ij}.

To see that this identity is sufficient for the sum rule, consider the expression for the response function in eq. (2.7):

$$\begin{aligned} q_i\chi_{ij}(\mathbf{q}) = q_j\chi_L(q) &= \\ &= \mathrm{Tr}\left[\left(\sigma_3\mathcal{G}^{-1}(\mathbf{k}) - \mathcal{G}^{-1}(\mathbf{k}+\mathbf{q})\sigma_3\right)\mathcal{G}(\mathbf{k})\gamma_j(\mathbf{k},\mathbf{k}+\mathbf{q})\mathcal{G}(\mathbf{k}+\mathbf{q})\right] \\ &= \mathrm{Tr}\left[\left(\gamma_j(\mathbf{k}-\mathbf{q},\mathbf{k}) - \gamma_j(\mathbf{k},\mathbf{k}+\mathbf{q})\right)\sigma_3\mathcal{G}(\mathbf{k})\right] \\ &= -\frac{q_j}{m}\mathrm{Tr}\left[\mathcal{G}(\mathbf{k})\right] = -q_j\frac{N}{m}, \qquad (2.13)\end{aligned}$$

making use of the Ward Identity, cyclic permutations within the trace, relabelling $\mathbf{k}$, and the form of the bare vertex, $\gamma_i(\mathbf{k},\mathbf{k}+\mathbf{q})$.

Zero-loop order calculation

This section discusses the form of the vertex corrections consistent with calculation of the fluctuation Green's function at zero-loop order. These vertex corrections are calculated for a weakly interacting dilute Bose gas:

$$H - \mu N = \sum_k (\epsilon_k - \mu)\psi_k^\dagger \psi_k + \frac{g}{2}\sum_{k,k',q} \psi_{k+q}^\dagger \psi_{k'-q}^\dagger \psi_k \psi_{k'}. \qquad (2.14)$$

Considering fluctuations about a uniform condensed solution, with condensate density $\rho_0 = \mu/g$, the inverse Green's function can be written in the Nambu space of eq. (2.9) as:

$$\begin{aligned} \mathcal{G}^{-1}(\mathbf{q},\omega) &= \mathcal{G}_0^{-1}(\mathbf{q},\omega) + \Sigma \qquad (2.15)\\ &= \begin{pmatrix} i\omega + \epsilon_{\mathbf{k}} - \mu + 2g\rho_0 & g\rho_0 \\ g\rho_0 & -i\omega + \epsilon_{\mathbf{k}} - \mu + 2g\rho_0 \end{pmatrix}. \end{aligned}$$

Therefore, the Ward identity (eq. (2.12)) becomes:

$$q_i \Gamma_i(\mathbf{k}+\mathbf{q},\mathbf{k}) = \begin{pmatrix} \epsilon_{\mathbf{k}+\mathbf{q}} - \epsilon_{\mathbf{k}} & -2g\rho_0 \\ 2g\rho_0 & -\epsilon_{\mathbf{k}+\mathbf{q}} + \epsilon_{\mathbf{k}} \end{pmatrix}. \qquad (2.16)$$

The diagonal terms in this expression are exactly those from the bare current vertex:

$$q_i \gamma_i(\mathbf{k}+\mathbf{q},\mathbf{k}) = \sigma_3 \mathbf{q}\cdot(2\mathbf{k}+\mathbf{q})\frac{1}{2m} = \sigma_3\left(\epsilon_{\mathbf{k}+\mathbf{q}} - \epsilon_{\mathbf{k}}\right). \qquad (2.17)$$

It is therefore necessary to find off-diagonal vertex corrections, where the current couples to the creation or annihilation of pairs of bosons.

The diagrams responsible for these corrections are shown in figure 2.3. Such diagrams involve vertices proportional to $\sqrt{\rho_0}$ where a condensate particle is created or annihilated. The right hand vertex, where three non-condensate lines meet behaves differently for the anomalous and normal vertex corrections. For the anomalous vertex correction, shown in fig. 2.3, two non-condensed particles are created at this right hand vertex. This requires that the internal propagator must create a particle at the right hand vertex.

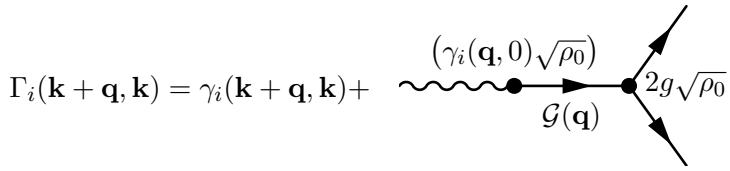

Figure 2.3: Vertex corrections for weakly interacting Bose gas at zero-loop order, anomalous contribution.

By inverting eq. (2.15) to give the fluctuation Green's function:

$$\mathcal{G}(\mathbf{q},\omega) = \frac{1}{\omega^2 + \epsilon_{\mathbf{q}}(\epsilon_{\mathbf{q}} + 2g\rho_0)} \begin{pmatrix} -i\omega + \epsilon_{\mathbf{k}} + g\rho_0 & -g\rho_0 \\ -g\rho_0 & +i\omega + \epsilon_{\mathbf{k}} + g\rho_0 \end{pmatrix} \tag{2.18}$$

the diagram in fig. 2.3 may be evaluated to give:

$$\begin{aligned} \Delta\Gamma_i(\mathbf{k}+\mathbf{q},\mathbf{k})_{12} &= \sqrt{\rho_0}\,(1,1)\left(\frac{q_i}{2m}\sigma_3\right)\mathcal{G}(\mathbf{q},0)\begin{pmatrix} 0 \\ 1 \end{pmatrix} 2g\sqrt{\rho_0} \\ &= \frac{q_i}{2m} 2g\rho_0 \frac{-(\epsilon_{\mathbf{q}} + 2g\rho_0)}{\epsilon_{\mathbf{q}}(\epsilon_{\mathbf{q}} + 2g\rho_0)} = -\frac{q_i}{q^2} 2g\rho_0. \end{aligned} \tag{2.19}$$

In contrast, for the normal vertex correction, the internal propagator can either create or destroy a non-condensed particle. The contributions from these two processes cancel:

$$\begin{aligned} \Delta\Gamma_i(\mathbf{k}+\mathbf{q},\mathbf{k})_{11} &= \sqrt{\rho_0}\,(1,1)\left(\frac{q_i}{2m}\sigma_3\right)\mathcal{G}(\mathbf{q},0)\begin{pmatrix} 1 \\ 1 \end{pmatrix} g\sqrt{\rho_0} \\ &= \frac{q_i}{2m} g\rho_0 \frac{(1-1)(\epsilon_{\mathbf{q}} + 2g\rho_0)}{\epsilon_{\mathbf{q}}(\epsilon_{\mathbf{q}} + 2g\rho_0)} = 0 \end{aligned} \tag{2.20}$$

Including such corrections will not yet satisfy the sum rule on the longitudinal response function. The vertex corrections above ensure that the longitudinal response evaluated from eq. (2.7) gives the correct density of non-condensed particles. To correctly include the condensate density requires the diagram shown in figure 2.4. This diagram gives a contribution ρ_0/m to the longitudinal response. This point is discussed again in chapter 3 in terms of amplitude and phase variables.

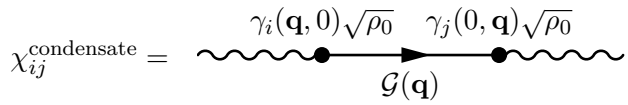

Figure 2.4: Single particle contribution to the current-current response function, giving a contribution proportional to the condensate density, ρ_0.

The detailed evaluation of these vertex corrections and extra diagrams can however be avoided. Note that the vertex corrections found can be written in the form:

$$\Gamma_i(\mathbf{p},\mathbf{q}) = \gamma_i(\mathbf{p},\mathbf{q}) + (p_i - q_i)f(p,q). \tag{2.21}$$

This form of the vertex correction only affects the longitudinal response. Therefore, the the normal density can be evaluated from the transverse linear response without vertex corrections. By comparing this to the total density evaluated directly from the free energy, the superfluid density can be found.

Following this procedure, the transverse response function, without vertex corrections, is given by:

$$\chi^T(q\to 0) = \frac{1}{\beta}\sum_{\mathbf{k},\omega}\frac{\hbar^2 k_i k_j}{m^2}\mathrm{Tr}\left(\mathcal{G}(\mathbf{k})\sigma_3\mathcal{G}(\mathbf{k})\sigma_3\right), \tag{2.22}$$

and so, taking the continuum limit and restoring factors of $\hbar$, the normal density is given by

$$\rho_{\mathrm{n}} = \int_0^\infty \frac{d^2k}{(2\pi)^2}\frac{\hbar^2k^2}{2m}\frac{1}{\beta}\sum_{\omega}\mathrm{Tr}\left(\mathcal{G}(\mathbf{k})\sigma_3\mathcal{G}(\mathbf{k})\sigma_3\right). \tag{2.23}$$

2.3 Relating definitions of superfluid density

The previous section describes a definition, and prescription for calculating, the superfluid density, in agreement with Landau's definition of two-fluid hydrodynamics. When considering two-dimensional systems, an alternate definition of the superfluid density is important. The low energy fluctuations of a condensed system, which will

lead to logarithmic divergences of correlation functions, are expected to have an effective action:

$$\mathcal{Z} = e^{-S_0} \int \mathcal{D}\phi \exp\left(-\int_0^\beta d\tau \int d^2 r \rho_s \frac{(\nabla\phi)^2}{2m}\right) \tag{2.24}$$

where ϕ is the phase of the order parameter, and $\phi \equiv \phi + 2\pi$. That this definition of ρ_s, controlling the low energy fluctuations of the system, and the previous definition, in terms of response functions, agree is an important result. This section will show why this is so, following closely the detailed discussion of Griffin [93], relating the response functions to a microscopic description of a condensed Bose gas.

Before discussing how this result follows from a microscopic picture, it is instructive to show how it follows from a phenomenological description. As discussed by Pitaevskii and Stringari [9, section 6.7], the phenomenological action describing two-fluid hydrodynamics contains a term corresponding to slow phase variations of the order parameter, and a term corresponding to quasi-particles:

$$S = \int d^d r \left(\rho_s \frac{(\nabla\phi)^2}{2m} + \rho_n \frac{m v_n^2}{2}\right), \tag{2.25}$$

where v_n is the normal component velocity. Note that ρ_s and ρ_n are, as throughout this chapter, the number densities, while Pitaevskii and Stringari [9] use mass densities. Treating ϕ and v_n as the dynamical variables of this theory, it can be seen that their contributions to the current response (where $J = (i\nabla\phi + v_n)/m$), take the form:

$$\chi_{ij}(q) \propto \rho_s \frac{q_i q_j}{q^2} q^2 \left\langle \phi(q)^2 \right\rangle + \rho_n \delta_{ij} \left\langle v_n(q)^2 \right\rangle. \tag{2.26}$$

At high temperatures these expectations can be evaluated by the equipartition theorem, giving

$$\frac{q^2}{2m} \left\langle \phi(q)^2 \right\rangle = \frac{d}{2} k_B T = \frac{1}{2m} \left\langle v_n(q)^2 \right\rangle, \tag{2.27}$$

where d is the spatial dimension. Thus at high temperatures, in this phenomenological theory, the difference of longitudinal and transverse response is controlled by the same density as controls the low energy phase fluctuations.

To derive this result from the quantum fluctuations in a microscopic picture relies on two statements about a condensed Bose gas:

1. The two-particle response functions, and single particle Green's function of a condensed gas depend on one another, and share the same poles.

2. The difference between transverse and longitudinal responses as $q \to 0$ depends only on diagrams where all momentum is carried by a single particle excitation.

If these statements are true, then the density that controls the difference in longitudinal and transverse response will necessarily control the low energy single particle excitations. The remainder of this section will summarise the arguments of Griffin [93, 98, 99, 100, 101, 102] that justify this argument in general. Chapter 3 will then explicitly show them to hold at one-loop order for a weakly interacting Bose gas.

General method: Regular and irregular parts

In order to understand how response functions and single particle Green's functions are related, it is convenient to divide the response functions into parts which are irreducible with respect to cutting either a single interaction line, or a single particle line. This method was first applied to a condensed Bose gas by Ma and Woo [103] in the context of a charged Bose gas, and later applied by Griffin to the study of excitation spectra and response functions in liquid Helium [93]. Following the common notation, diagrams not separated by cutting an interaction line will be termed "irreducible" and represented by a bar, *e.g.* $\bar{\chi}$. Diagrams not separated by cutting a particle line will be termed "regular" and represented by a superscript R, *e.g.* χ^R.

Because the interaction couples to density, not momentum current, it is also convenient to discuss the decomposition of the density-density response function, χ_{nn}, rather than the current-current response function χ_{JJ}. However, these can be related by the continuity

equation [103, 104]:

$$\chi_{nn}(q,\omega) = \frac{q^2}{m^2\omega^2}\left(\chi^L_{JJ}(q,\omega) + \frac{\rho}{m}\right) \tag{2.28}$$

Note again that the response functions and density here refer to number density, not mass density. The interaction will be written as a general, momentum dependent $V(q)$, where for the weakly interacting dilute Bose gas $V(q) = g$, suitably regularised.

The irreducible density response function can be re-summed with interaction lines to give the full density response:

$$\chi_{nn} = \frac{\bar{\chi}_{nn}}{\epsilon} = \frac{\bar{\chi}_{nn}}{1 - V(q)\bar{\chi}_{nn}(q)}. \tag{2.29}$$

For the current-current response, the equivalent formula is more complicated because the interaction couples to density, not current:

$$\chi^L_{JJ} = \bar{\chi}^L_{JJ} + \frac{\bar{\chi}^L_{Jn}V(q)\bar{\chi}^L_{nJ}}{\epsilon}, \tag{2.30}$$

where χ_{Jn} is the mixed current-density response. However, the continuity equation, eq. (2.28), also holds with with irreducible response functions.

Taking the irreducible version of eq. (2.28) at $\omega = 0$ gives an alternate expression for the longitudinal response sum rule,

$$\bar{\chi}^L_{JJ}(q,0) = -\frac{\rho}{m}. \tag{2.31}$$

One can then divide irreducible response into regular and single-particle mediated parts:

$$\bar{\chi}^L_{JJ}(q) = \bar{\chi}^{L,R}_{JJ}(q) + \bar{\Lambda}^L_\alpha \mathcal{G}_{\alpha\beta}\bar{\Lambda}^L_\alpha, \tag{2.32}$$

where the index structure, $\alpha\beta$ of $\mathcal{G}$ refers to the standard particle-hole Nambu space, see *e.g.* eq. (2.9). The vertices, $\bar{\Lambda}^L_\alpha$ represent the full coupling of current to single particle excitations, including all vertex corrections.

In contrast to the longitudinal current response, the transverse response has only regular, irreducible parts:

$$\chi^T_{JJ}(q) = \bar{\chi}^T_{JJ}(q) = \bar{\chi}^{T,R}_{JJ}(q). \tag{2.33}$$

This is because any coupling of current to single particle excitations brings a factor of $\mathbf{q}$, thus giving a contribution to only the longitudinal part. Further, the regular irreducible diagrams for transverse and longitudinal current response differ only in their external vertices coupling to current. This means that, as $q \to 0$:

$$\lim_{q\to 0}\left(\bar{\chi}^{T,R}_{JJ}(q)\right) = \lim_{q\to 0}\left(\bar{\chi}^{T,L}_{JJ}(q)\right) = -\frac{\rho_{\text{normal}}}{m} \tag{2.34}$$

This leads immediately to the conclusion:

$$\begin{aligned}\lim_{q\to 0}&\left(\bar{\chi}^{L}_{JJ}(q,0) - \bar{\chi}^{L,R}_{JJ}(q,0)\right) = \\ &= \lim_{q\to 0}\left(\bar{\Lambda}^L_\alpha(q,0)\mathcal{G}_{\alpha\beta}(q,0)\bar{\Lambda}^L_\alpha(q,0)\right) = -\frac{\rho_s}{m}\end{aligned} \tag{2.35}$$

This formally establishes the connection of the superfluid response to the low energy behaviour of the single particle Green's function.

2.4 Shared poles of Green's function and response function

The above results might suggest that the response function can be divided into a part due to the superfluid and a part due to the normal fluid. However, as stressed by Griffin [98, 100], such an identification is difficult, as both parts share the same poles. This is most easily seen in terms of the density response function. The following summarises the argument of Griffin [93, Section 5.1] showing that the poles are shared.

For density-density response, the equivalent of eq. (2.32) is:

$$\bar{\chi}_{nn}(q) = \bar{\chi}^R_{nn}(q) + \bar{\Lambda}_\alpha \bar{\mathcal{G}}_{\alpha\beta}\bar{\Lambda}_\beta. \tag{2.36}$$

Adopting the notation of Ma and Woo [103], the Green's function (and similarly the irreducible Green's function) can be written in the form:

$$\mathcal{G}_{\alpha\beta}(q) = \frac{N_{\alpha\beta}(q)}{D(q)}, \qquad D(q) = -\det\left(\mathcal{G}^{-1}(q)\right) \tag{2.37}$$

In terms of this parameterisation, equations (2.36) and (2.29) can be combined to give:

$$\chi_{nn} = \frac{\bar{\chi}^R_{nn}\bar{D} + \bar{\Lambda}_\alpha \bar{N}_{\alpha\beta}\bar{\Lambda}_\beta}{\bar{D}\epsilon} \tag{2.38}$$

Therefore, the poles of this expression are controlled by the zeros of $\bar{D}\epsilon$.

To relate this to the poles of the Green's function, consider the self energy. The self energy is necessarily regular, since it is resummed with single particle propagators in the full Green's function. However, it can be divided into irreducible and interaction mediated parts.

$$\Sigma_{\alpha\beta} = \bar{\Sigma}_{\alpha\beta} + \frac{\bar{\Lambda}_\alpha V(q)\bar{\Lambda}_\beta}{\epsilon^R} \tag{2.39}$$

The expression ϵ^R is the regular part of the ϵ defined in eq. (2.29):

$$\epsilon^R = 1 - V(q)\bar{\chi}^R_{nn} = \epsilon + V(q)\bar{\Lambda}_\alpha \bar{\mathcal{G}}_{\alpha\beta}\bar{\Lambda}_\beta. \tag{2.40}$$

Again, following directly Ma and Woo [103], one can relate the reducible and irreducible Green's function denominators. Define

$$\Sigma^C_{\alpha\beta} = \frac{\bar{\Lambda}_\alpha V(q)\bar{\Lambda}_\beta}{\epsilon^R}. \tag{2.41}$$

In terms of this, and the irreducible inverse Green's function expressed in terms of $\bar{N}_{\alpha\beta}$, the full Green's function denominator is:

$$\begin{aligned} D \;=\; -\Big[&(\bar{N}_{11} + \Sigma^C_{22})(\bar{N}_{22} + \Sigma^C_{11}) \\ &- (\bar{N}_{12} - \Sigma^C_{21})(\bar{N}_{21} + \Sigma^C_{12})\Big]. \end{aligned} \tag{2.42}$$

Using the result, $\Sigma^C_{22}\Sigma^C_{11} = \Sigma^C_{21}\Sigma^C_{12}$, which follows immediately from the definition, eq. (2.41), one can then write:

$$D = \bar{D} - \bar{N}_{\alpha\beta}\Sigma^C_{\alpha\beta} = \bar{D} - \bar{N}_{\alpha\beta}\frac{\bar{\Lambda}_\alpha V(q)\bar{\Lambda}_\beta}{\epsilon^R}. \tag{2.43}$$

Finally, combining this with eq. (2.40), gives

$$\epsilon_R D = \left(\epsilon + V(q)\bar{\Lambda}_\alpha\bar{\mathcal{G}}_{\alpha\beta}\bar{\Lambda}_\beta\right)\bar{D} - \bar{N}_{\alpha\beta}\bar{\Lambda}_\alpha V(q)\bar{\Lambda}_\beta = \epsilon\bar{D} \tag{2.44}$$

Thus, the poles of χ_{nn}, given by the zeros of $\epsilon\bar{D}$, and the poles of $\mathcal{G}$, given by the zeros of D are the same.

Chapter 3

One loop superfluid density

As an example of the discussion in chapter 2, it is illustrative to relate the response functions, and effective action for phase fluctuations, at one loop order. This chapter presents such a calculation, working in terms of density and phase variables. Similar one-loop calculations, but in terms of particle creation and annihilation operators, are presented in Talbot and Griffin [100]. The task at hand is to show that the effective action for the phase mode involves the superfluid density, defined at one-loop order, rather than the condensate density as would appear at zero-loop order. Considering the previous discussion, this is a result of the connection between the self-energy and the response functions. Therefore, this result may be achieved by writing the phase fluctuation self-energy in terms of the current-current response function.

3.1 Effective action and current density.

Starting from the Bose gas Hamiltonian of eq. (2.14), the particle creation operator can be written in terms of density and amplitude and phase fluctuations as:

$$\psi = \sqrt{\rho_0 + \pi} e^{i\phi}. \tag{3.1}$$

In terms of these fields, and making use of $g\rho_0 = \mu$, the action becomes:

$$\begin{aligned} S[\phi,\pi] &= \sum_{\omega,k} \frac{1}{2} \begin{pmatrix} \phi_k & \pi_k \end{pmatrix} \begin{pmatrix} 2\rho_0\epsilon_k & -i\omega \\ i\omega & \frac{1}{2\rho_0}(\epsilon_k + 2g\rho_0) \end{pmatrix} \begin{pmatrix} \phi_k \\ \pi_k \end{pmatrix} \\ &+ \int d^d r \frac{1}{2m} \left\{ \frac{1}{4} \left[\frac{(\nabla\pi)^2}{\rho_0+\pi} - \frac{(\nabla\pi)^2}{\rho_0} \right] + (\nabla\phi)^2\pi \right\}. \end{aligned} \tag{3.2}$$

The terms in the second line, still written in position space, produce density-density and density-phase interactions. Expanding the denominator for small π/ρ_0 (which can be shown to be equivalent to an expansion for small g, since $\rho_0 = \mu/g$), and Fourier transforming the second line becomes:

$$S_{\text{int.}}[\phi,\pi] = \frac{1}{2m} \sum_{k,k'} (\mathbf{k}\cdot\mathbf{k}') \left(\frac{\pi_k \pi_{k'} \pi_{-k-k'}}{4\rho^2} - \phi_k \phi_{k'} \pi_{-k-k'} \right), \tag{3.3}$$

where for compactness of notation, the label k should be interpreted as (k,ω), but the scalar product refers only to the momentum part of k.

It is clear that at zero-loop order, the effective quadratic action for the phase involves the condensate density. By including density-phase interaction terms, this will be modified. The resultant self energy diagrams can be related to the current-current response function, and thus to the superfluid density.

In order to use the current-current response function, it is necessary to express it in terms of density and phase operators. Using eq. (3.1), then eq. (2.1) may be rewritten in real space as:

$$\mathbf{J}(r,0) = \frac{1}{2m} \left[\left(\sqrt{\rho_0+\pi} e^{-i\phi} \right) (-i\nabla) \left(\sqrt{\rho_0+\pi} e^{i\phi} \right) + \text{c.c.} \right], \tag{3.4}$$

which, in terms of the Fourier components of ϕ and π can be written

$$J_i(q,0) = \frac{i}{m} \left(\rho_0 q_i \phi_q + \sum_k k_i \phi_k \pi_{q-k} \right). \tag{3.5}$$

Any diagram involving the first term in parentheses necessarily contributes to the longitudinal response, due to the factor of q_i. In

order to find a contribution to the transverse response function, it is necessary to consider the contributions from the second term:

$$\chi_{ij}^{T,\text{one loop}}(q,0) = -\frac{1}{m^2}\Big[k_i k_j \mathcal{G}_{\pi\pi}(q-k)\mathcal{G}_{\phi\phi}(k) + k_i(q_j-k_j)\mathcal{G}_{\pi\phi}(q-k)\mathcal{G}_{\phi\pi}(k)\Big]. \quad (3.6)$$

These contributions are shown diagrammatically in figure 3.1.

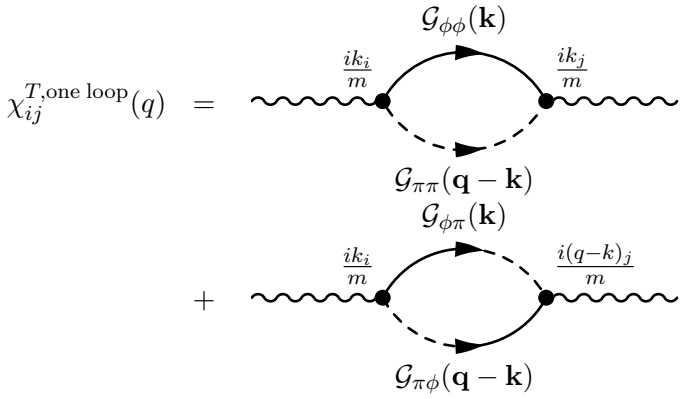

Figure 3.1: One-loop order contributions to the transverse current-current response function, in terms of the phase (solid line) and density (dashed line) propagators, and momentum current vertices as described in eq. (3.5)

3.2 Calculating phase self-energy.

Armed with this knowledge, it is possible to calculate the phase self-energy at one-loop order, and relate this to the one-loop response function. By considering a path integral formulation with action (3.2), one can write:

$$\mathcal{Z} \approx \int \mathcal{D}(\phi,\pi) e^{-S_{\text{eff}[\phi,\pi]}}$$

$$\approx \int \mathcal{D}(\phi,\pi) e^{-S_0[\phi,\pi]} \left(1 - S_{\rm int}[\phi,\pi] + \frac{1}{2!} S_{\rm int}[\phi,\pi]^2\right) \quad (3.7)$$

where S_0 is the quadratic part, and so to second order,

$$S_{\rm eff} = S_0 + \langle S_{\rm int}\rangle_c - \frac{1}{2}\left\langle S_{\rm int}^2\right\rangle_c . \quad (3.8)$$

Because the interaction contains odd powers of fields, the first order term will vanish, and $\left\langle S_{\rm int}^2\right\rangle_c = \left\langle S_{\rm int}^2\right\rangle$. Thus, using the obvious notation for the two terms in eq. (3.3) the phase self energy is:

$$\frac{1}{2}\phi_q\phi_q\Sigma_{\phi\phi}(q) = -\left\langle S_{\rm int}^{\phi\phi\pi} S_{\rm int}^{\pi\pi\pi}\right\rangle - \frac{1}{2}\left\langle S_{\rm int}^{\phi\phi\pi} S_{\rm int}^{\phi\phi\pi}\right\rangle \quad (3.9)$$

Taking contractions using Wick's theorem, this becomes:

$$\begin{aligned}
\frac{1}{2}\phi_q\phi_q\Sigma_{\phi\phi}(q) = -\phi_q\phi_q \frac{1}{4m^2}\sum_k \Bigg\{ & \\
& \left[\frac{-1}{4\rho^2}\left\langle\pi(0)\pi(0)\right\rangle\left\langle\pi(k)\pi(k)\right\rangle\left(2(\mathbf{0}\cdot\mathbf{k}) + k^2\right)q^2\right] \\
& + \frac{1}{2}\Bigg[\left\langle\pi(0)\pi(0)\right\rangle\left\langle\phi(k)\phi(k)\right\rangle 2q^2k^2 \\
& \quad + \left\langle\pi(0)\phi(0)\right\rangle\left\langle\phi(k)\pi(k)\right\rangle 2q^2(\mathbf{q}\cdot\mathbf{0}) \\
& \quad + \left\langle\pi(q-k)\pi(q-k)\right\rangle\left\langle\phi(k)\phi(k)\right\rangle 4(\mathbf{q}\cdot\mathbf{k})^2 \\
& \quad + \left\langle\pi(q-k)\phi(q-k)\right\rangle\left\langle\phi(k)\pi(k)\right\rangle 4(\mathbf{q}\cdot\mathbf{k})(\mathbf{q}\cdot(\mathbf{q}-\mathbf{k}))\Bigg]\Bigg\}
\end{aligned} \quad (3.10)$$

The two sets of square brackets in eq. (3.10) correspond to the two terms in eq. (3.9). Each line in eq. (3.10) corresponds to a diagram shown in figure 3.2.

Eliminating those terms which vanish, and expressing the correlations as Green's functions, this becomes:

$$\frac{1}{2}\Sigma_{\phi\phi}(q) = \sum_k \Bigg\{ \frac{1}{4\rho_0^2}\epsilon_k\epsilon_q\mathcal{G}_{\pi\pi}(0)\mathcal{G}_{\pi\pi}(k) - \epsilon_k\epsilon_q\mathcal{G}_{\pi\pi}(0)\mathcal{G}_{\phi\phi}(k)$$

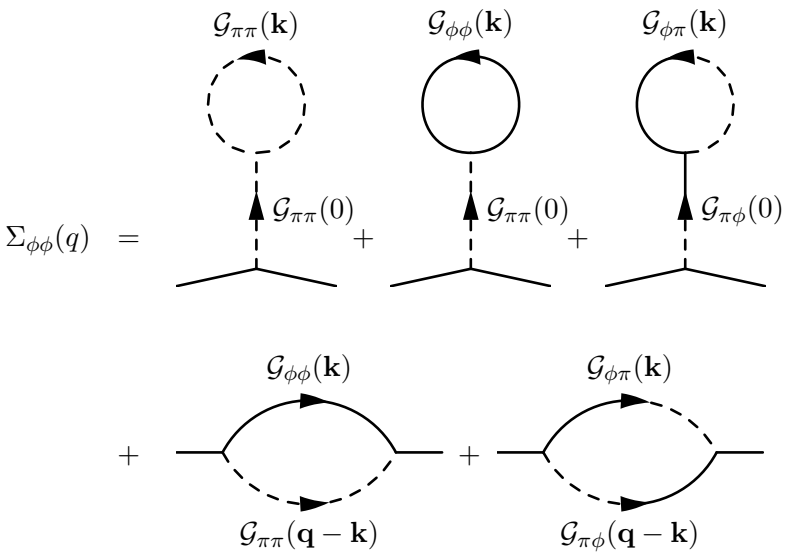

Figure 3.2: One-loop contribution to phase self-energy, in terms of the phase (solid line) and density (dashed line) propagators. Each diagram corresponds to a line in eq. (3.10); combinatoric factors, and factors associated with the three-field vertices are as described in that equation.

$$
\begin{aligned}
& - \frac{1}{2m^2}\Big[(\mathbf{q}\cdot\mathbf{k})^2 \mathcal{G}_{\pi\pi}(q-k)\mathcal{G}_{\phi\phi}(k) \\
& \qquad + (\mathbf{q}\cdot\mathbf{k})(\mathbf{q}\cdot(\mathbf{q}-\mathbf{k}))\mathcal{G}_{\pi\phi}(q-k)\mathcal{G}_{\phi\pi}(k)\Big]\Big\} \\
= \; & -\epsilon_q \sum_k \epsilon_k \left(\mathcal{G}_{\phi\phi}(k) - \frac{\mathcal{G}_{\pi\pi}(k)}{4\rho_0^2}\right)\mathcal{G}_{\pi\pi}(0) \\
& + \frac{q_i q_j}{2}\chi_{ij}^{T,\text{one loop}}(q). \qquad (3.11)
\end{aligned}
$$

It remains then to identify the first expression in the final form for eq. (3.11). As discussed in depth in section 6.1, the total density must be evaluated by taking the total derivative of the free energy

with respect to chemical potential, including the implicit dependence of ρ_0 on μ. From the quadratic part of the action, S_0 in eq. (3.2) its derivative with respect to chemical potential takes the following form:

$$\frac{dS_0[\phi,\pi]}{d\mu} = \frac{1}{2}\frac{d\rho_0}{d\mu}\sum_k \left(\phi_k^2 2\epsilon_k - \pi_k^2 \frac{\epsilon_k}{2\rho_0^2}\right). \tag{3.12}$$

Therefore, the derivative of Gaussian contribution to the free energy can be written as:

$$\frac{dF_{\text{quad.}}}{d\mu} = \left\langle \frac{dS_0[\phi,\pi]}{d\mu} \right\rangle = \frac{1}{g}\sum_k \epsilon_k \left(\mathcal{G}_{\phi\phi}(k) - \frac{\mathcal{G}_{\pi\pi}(k)}{4\rho_0^2}\right). \tag{3.13}$$

This expression is the density of non-condensed particles, and is exactly the expression appearing in eq. (3.11).

Using $\mathcal{G}_{\pi\pi}(0) = 1/g$, as can be readily identified from the form of the inverse Green's function at $\omega = 0$, $q = 0$, this gives a self energy:

$$\Sigma_{\phi\phi}(q) = -2\epsilon_q \rho_{\text{uncondensed}} + q_i q_j \chi_{ij}^{T,\text{one loop}}(q). \tag{3.14}$$

Taking the asymptotic form of χ_{ij}^T, this becomes:

$$\Sigma_{\phi\phi}(q \to 0) = \frac{q^2}{m}\left(-\rho_{\text{uncondensed}} + \rho_{\text{normal}}\right). \tag{3.15}$$

Thus, using the asymptotic form of the self energy, the phase component of the inverse Green's function becomes:

$$\begin{aligned} \mathcal{G}_{\phi\phi}^{-1}(q \to 0) &= \mathcal{G}_{\phi\phi,0}^{-1}(q \to 0) - \Sigma_{\phi\phi}(q \to 0) \\ &= \frac{q^2}{m}\left(\rho_0 + \rho_{\text{uncondensed}} - \rho_{\text{normal}}\right) = \frac{q^2 \rho_s}{m}, \end{aligned} \tag{3.16}$$

which is the required result.

Part II

Signatures of exciton condensation

Chapter 4

Angular distribution of photoluminescence from trapped excitons

Bose condensation of trapped excitons confined to two dimensions leads to a change in the angular distribution of their photoluminescence. For weakly interacting bosons in a trap, condensation would lead to spatial condensation — a characteristic change in the spatial distribution at the transition temperature. For excitons in in-plane traps in quantum well bilayer systems, the traps are relatively shallow, and interactions between excitons relatively strong. Therefore, there is no dramatic change of the spatial profile at the transition temperature.

However, since condensation leads to phase coherence between excitons at opposite sides of the trap, radiation emitted from different parts of the trap will have fixed phase relationships. This leads to strong beaming of radiation in a direction normal to the plane in the condensed state. Such behaviour can easily be described at zero temperature. At finite temperature it is necessary to consider the excitation spectrum of a trapped condensate. Excitations can be divided into low energy phase fluctuations, and higher energy density

fluctuations. Thermal occupation of the phase fluctuations is sufficient to destroy the angular beaming well before density fluctuations become important.

In this chapter the quantum-well bilayer systems studied experimentally are modelled as a gas of bosons. The spatial distribution is shown to have no significant change at condensation, but condensation causes the angular distribution to become strongly peaked. By considering phase fluctuations, the angular distribution at non-zero, but low temperatures is found.

4.1 The system and the model

As discussed in the introduction (see sec. 1.3), quantum-well bilayer systems are currently the most likely candidate for observing exciton condensation. At low densities, when the average exciton separation is much larger than the exciton size (set here by the inter-well spacing), the excitons may be modelled as bosons, confined to a two-dimensional plane:

$$H[\psi] = \int \left[\psi^* \left(-\frac{\nabla^2}{2m} + V(\mathbf{r}) - \mu \right) \psi + \frac{\lambda}{2} |\psi|^4 \right] d^2\mathbf{r}. \tag{4.1}$$

Here, $V(r)$ is the in-plane trap potential, which will be assumed to be harmonic, $V(r) = \frac{1}{2}u_0 r^2$. The effective interaction $\lambda\delta(r)$ is a momentum independent approximation to the dipole-dipole interaction between two excitons. The interaction strength, λ, may be found either by calculating the capacitance of the bilayer device, or from the small momentum part of the dipole-dipole interaction. For this latter case, the dipole-dipole interaction:

$$u_{\text{int}}(\mathbf{r}, \mathbf{r}') = 2 \times \frac{e^2}{4\pi\varepsilon_0\varepsilon_r} \left(\frac{1}{|\mathbf{r} - \mathbf{r}'|} - \frac{1}{\sqrt{|\mathbf{r} - \mathbf{r}'|^2 + d^2}} \right) \tag{4.2}$$

can be Fourier transformed to give,

$$u_{\text{int}}(q) = \frac{e^2}{\varepsilon_0\varepsilon_r} \left(\frac{1}{q} - \frac{e^{-qd}}{q} \right) \approx \frac{e^2 d}{\varepsilon_0\varepsilon_r} + \mathcal{O}(qd^2), \tag{4.3}$$

with the higher order terms negligible for $q \leq 1/d$. For GaAs wells, with an interwell spacing of 5nm, this gives a value $\lambda \approx 7.0\text{nm}^2\text{eV}$. A characteristic scale for the trap potential is $u_0 \approx 10^{-12}\text{eVnm}^{-2}$, (i.e. $\Delta V = 0.1\,\text{meV}$ for $\Delta r = 10\,\mu\text{m}$, [72]).

4.2 Spatial distribution

In order to show that no change of spatial profile occurs at condensation, consider the three lengthscales that control the size of a cloud of bosons. Thermally occupying the potential trap gives a lengthscale:

$$R_{\text{thermal}} \approx \sqrt{\frac{k_{\text{B}}T}{u_0}}. \tag{4.4}$$

The harmonic oscillator ground state in the trap has size:

$$R_{\text{H.O.}} \approx \sqrt[4]{\frac{\hbar^2}{mu_0}}. \tag{4.5}$$

Finally, balancing inter-particle repulsion with the trap profile gives the Thomas-Fermi profile size:

$$R_{\text{T.F.}} \approx \sqrt[4]{\frac{\lambda N}{u_0}}. \tag{4.6}$$

Without interactions, at condensation, the cloud changes from the a thermal size to the size of the ground-state mode, which is macroscopically occupied. However, with interactions, and large numbers of particles, the ground state size is instead set by the Thomas-Fermi profile. Therefore, between condensing and $T = 0$, the cloud size remains fixed at the Thomas-Fermi lengthscale.

4.3 Angular distribution

Although the spatial distribution does not change significantly, the angular distribution may be expected to change. At temperatures well below the transition, radiation emitted from opposite sides of

the cloud of trapped excitons will be coherent. This means it can interfere constructively in a direction normal to the trap, and destructively at angles away from the normal. This leads to a peak of radiation on an angular scale set by $\lambda_{\rm rad}/R$, where $\lambda_{\rm rad}$ is the wavelength of radiation, and R the cloud size.

To generalise this result to finite temperatures, it is necessary to consider how the angular distribution depends on the state of the excitons. The angular distribution of radiation from excitons trapped in a quantum well reflects the momentum distribution of the excitons, due to conservation of in-plane momentum in photoluminescence. Including factors due to the photon final density of states, and polarisation of the emitted radiation, this gives [105, 106, 107, 108]:

$$I(\mathbf{k}_\parallel) \propto N_{\rm ex}(\mathbf{k}_\parallel)\rho_{\rm ph}(\mathbf{k}_\parallel, k_0) \sum_{\mathbf{e_k}} |\langle f| \, \mathbf{e_k}.\hat{\mathbf{p}} \, |i\rangle|^2 \, . \tag{4.7}$$

Here, $k_0 = 2\pi/\lambda_{\rm rad}$ is photon wavenumber, $\mathbf{e_k}$, the direction of polarisation, $\rho_{\rm ph}(\mathbf{k}_\parallel, k_0)$ the photon density of states, and $|i\rangle$ and $|f\rangle$ represent the initial and final electronic states. The momentum distribution of excitons depends on the state of the Bose gas:

$$N_{\rm ex}(\mathbf{k}_\parallel) = \left\langle |\psi(\mathbf{k}_\parallel)|^2 \right\rangle = \sum_{\mathbf{r},\mathbf{r}'} \left\langle \psi^\dagger(\mathbf{r})\psi(\mathbf{r}') \right\rangle e^{i\mathbf{k}_\parallel.(\mathbf{r}-\mathbf{r}')} \tag{4.8}$$

Matrix element, polarisation, density of states

Before discussing how the exciton distribution is changed by the presence of a condensate, it is important to understand the angular dependence of the other terms in eq. (4.7). The result of this section will be that the angular dependence of these other terms can be neglected for small angles, $\theta \ll 1$, where θ is defined by $|\mathbf{k}_\parallel| = k_0 \sin\theta$. Since the exciton distribution produces features on a scale $\theta \approx \lambda_{\rm rad}/R$, the terms discussed in this section are unimportant, but included for completeness.

The matrix element $\langle f| \, \mathbf{e_k}.\hat{\mathbf{p}} \, |i\rangle$ gives an angular dependence due to the possible polarisation directions of emitted radiation. The sum over polarisations, $\mathbf{e_k}$, is over directions perpendicular to the photon

wavevector. For a bulk semiconductor, the matrix element would be isotropic. In a quantum well, the electron states have broken symmetry, and so $\mathbf{p}$ has different expectations for directions in-plane and perpendicular to the plane.

In terms of the emission angle, θ, and the angle of polarisation measured with respect to the plane containing the z axis, χ, as shown in figure 4.1, one may write the polarisation direction:

$$\mathbf{e} = \sin\chi \begin{pmatrix} \cos\phi \\ -\sin\phi \\ 0 \end{pmatrix} + \cos\chi \begin{pmatrix} \cos\theta\sin\phi \\ \cos\theta\cos\phi \\ -\sin\theta \end{pmatrix} \tag{4.9}$$

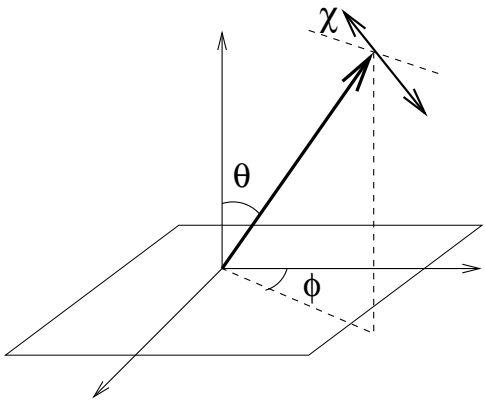

Figure 4.1: Angles of emitted radiation and polarisation of radiation with respect to the plane in which excitons may move.

The expectation of the momentum for transitions between conduction and valence electron states can be written in terms of the direction of the electron wavevector with respect to the Γ point. This wavevector is parameterised in terms of a polar angle, Ω, measured with respect to the normal to the quantum well plane, and an azimuthal angle, ξ. Following Chuang [106, Section 9.5], for the optically allowed transitions between a $J = 3/2$ valence band and

$J = 1/2$ conduction band these matrix elements are:

$$\left\langle \frac{1}{2}, \pm\frac{1}{2} \middle| \mathbf{p} \middle| \frac{3}{2}, \pm\frac{1}{2} \right\rangle \propto \begin{pmatrix} \pm\cos\Omega\cos\xi - i\sin\xi \\ \pm\cos\Omega\sin\xi + i\cos\xi \\ \mp\sin\Omega \end{pmatrix}. \tag{4.10}$$

Taking the scalar product of this with the polarisation vector, $\mathbf{e}$, and averaging over the polarisation direction, and the azimuthal electron direction, gives the form:

$$\sum_{\mathbf{e_k}} |\langle f| \mathbf{e_k}.\hat{\mathbf{p}} |i\rangle|^2 \propto \left[\left(\cos^2\theta + 1\right)\left(\cos^2\Omega + 1\right) + 2\sin^2\theta\sin^2\Omega\right] \tag{4.11}$$

In a bulk semiconductor, the polar angle of the electron wavevector, Ω should be averaged over solid angles, and this expression would not depend on θ. However, in a quantum well, the electron wavevector is confined by the boundary conditions, and so, for small exciton centre of mass motion ($k_{\rm ex} \ll 1/d$ where d is quantum well size), one can instead approximate $\Omega \approx 0$. In this case, the matrix element becomes:

$$\sum_{\mathbf{e_k}} |\langle f| \mathbf{e_k}.\hat{\mathbf{p}} |i\rangle|^2 \propto \left(1 + \cos^2\theta\right) \tag{4.12}$$

The photon density of states in eq. (4.7) contains both the density of states of photons at energy ω_0, and a constraint on total photon wavevector:

$$\begin{aligned} \rho_{\rm ph}(\mathbf{k}_\parallel, k_0) &= \rho_{\rm ph}(\omega_0)\delta\left(k_0 - |\mathbf{k}|\right) \\ &= \rho_{\rm ph}(\omega_0)\frac{k_0}{\sqrt{k_0^2 - |\mathbf{k}_\parallel|^2}}\delta\left(k_z - \sqrt{k_0^2 - |\mathbf{k}_\parallel|^2}\right) \end{aligned} \tag{4.13}$$

In eq. (4.13), the δ-function has been rewritten in terms of a constraint on the perpendicular momentum. As a result of the Jacobian of this change of variables, there is an angular dependence $\rho_{\rm ph}(\mathbf{k}_\parallel, k_0) \propto 1/\cos\theta$.

Combining these factors, the total angular dependence is:

$$I(\theta) \propto \frac{\left(1 + \cos^2\theta\right)}{\cos\theta} N_{\rm ex}(k_0 \sin\theta) \tag{4.14}$$

As promised, for $\theta \ll 1$, only the exciton distribution will have a significant angular dependence.

Zero temperature: Thomas-Fermi limit

At zero temperature, the order parameter can be approximated by the Thomas-Fermi limit [9], neglecting the term due to curvature in eq. (4.1). Then, the total energy is a functional of the density only, and can be minimised to give:

$$|\psi(|\mathbf{r}| < R)|^2 = \frac{2N}{\pi R^4}(R^2 - \mathbf{r}^2), \quad R = \left(\frac{4\lambda N}{\pi u_0}\right)^{1/4}. \tag{4.15}$$

If the wavefunction is assumed phase coherent across the entire cloud, then it is just the square root of the expression in eq. (4.15). Taking the Fourier transform, the momentum space profile is thus given by:

$$N_{\rm ex}(\mathbf{k}) = 8\pi R^2 N \left(\frac{\sin kR}{(kR)^3} - \frac{\cos kR}{(kR)^2}\right)^2 \tag{4.16}$$

(here, and afterwards, $\mathbf{k} = \mathbf{k}_\parallel$ is used for brevity). This expression shows oscillations in (kR) which result from the sharp edge of the Thomas-Fermi distribution, and so are not expected to occur in a better approximation.

The important feature of eq. (4.16) is the existence of a sharp peak in the photoluminescence profile if $R > \lambda_{\rm rad}$. For the indirect exciton line $\lambda_{\rm rad} \approx 800\,{\rm nm}$ [72]. Using the numbers discussed in section 4.1, the Thomas-Fermi radius is approximately $R \sim 1.5\,N^{1/4}\mu{\rm m}$, so a peak should be visible even for small particle numbers.

4.4 Finite temperatures: phase fluctuations

For a uniform density system in two dimensions, fluctuations lead to power law correlations at long distances. Therefore, the coherence between opposite sides of the traps is reduced by a factor $e^{-\alpha \ln R/\xi_T}$, with $\alpha = \frac{mT}{2\pi\rho}$ [7], R the cloud size, ξ_T a thermal length. This length, $\xi_T = (\lambda\rho/4m)^{1/2}/k_{\rm B}T$ corresponds to the energy cutoff in the Planck

distribution of phase fluctuations [7]. When the coefficient $\alpha = \frac{1}{4}$ at $T_{\rm BEC} = \pi\rho/2m$, there is a Kosterlitz-Thouless transition [18, 20].

For temperatures, $T \ll T_{\rm BEC}$, density fluctuations and vortices are negligible compared to phase fluctuations. Therefore, there exist a range of phase fluctuations with a range of wavenumbers $R^{-1} < k < \xi_T^{-1}$. The depletion argument, applied to the trapped condensate, gives a temperature-dependent momentum distribution

$$N_{\rm ex}(\mathbf{k}) = \left| \int \left(\frac{\lambda\rho(\mathbf{r})}{mR^2T^2} \right)^{mT/8\pi\rho(\mathbf{r})} \sqrt{\rho(\mathbf{r})} e^{i\mathbf{k}\mathbf{r}} d^2\mathbf{r} \right|^2 . \tag{4.17}$$

This expression has the form of replacing the condensate density with a "coherent particle density" $\tilde{\rho}(\mathbf{r}) = (\rho(\mathbf{r})/\rho_B)^{\rho_A/\rho(\mathbf{r})}\,\rho(\mathbf{r})$. For a harmonic trap, with the numbers discussed above,

$$\frac{\rho_A}{\rho_0} = \frac{mk_{\rm B}T}{8\pi\hbar^2}\sqrt{\frac{\pi\lambda}{2u_0N}} \sim 30 \times \frac{T[{\rm K}]}{\sqrt{N}},$$
$$\frac{\rho_0}{\rho_B} = \frac{u_0 2\pi\hbar^2}{m(k_{\rm B}T)^2} \sim \left(\frac{10^{-2}}{T[{\rm K}]}\right)^2 .$$

The temperature dependence of the PL peak is shown in fig. 4.2. Qualitatively, the peak is suppressed at

$$T \simeq T_* = T_{\rm BEC}/\ln(R/\xi_T), \tag{4.18}$$

i.e. well below $T_{\rm BEC}$.

The next step is to verify eq. (4.17) obtained in a local density approximation for the fluctuations. In a spatially inhomogeneous condensate, since at low temperatures (4.18) the phase fluctuations are Gaussian and the density fluctuations can be ignored, one can write an exact expression for the temperature-dependent momentum distribution as

$$N_{\rm ex}(\mathbf{k}) = \sum_{\mathbf{r},\mathbf{r}'} (\rho(\mathbf{r})\rho(\mathbf{r}'))^{1/2} e^{-\frac{1}{2}D_{\mathbf{r},\mathbf{r}'}} e^{i\mathbf{k}(\mathbf{r}-\mathbf{r}')}, \tag{4.19}$$

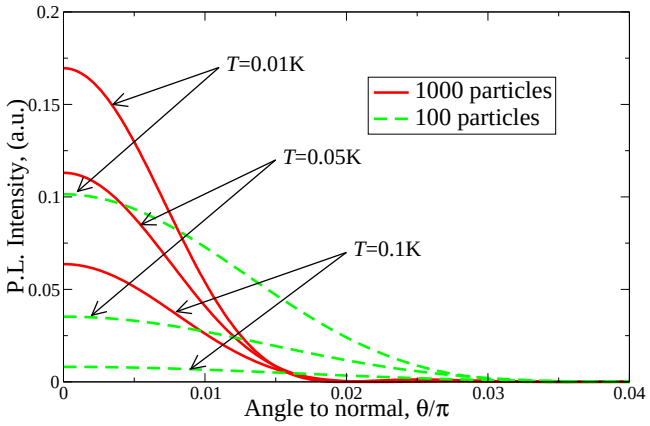

Figure 4.2: Temperature dependence of the angular profile. Plotted for two different numbers of particles in the trap: 10^3 (solid lines), 10^2 (dashed lines), with the larger peak rescaled by 1/20 for easier comparison.

with $D_{\mathbf{r},\mathbf{r}'} = \left\langle (\phi(\mathbf{r}) - \phi(\mathbf{r}'))^2 \right\rangle$. The phase fluctuations are determined by the energy functional

$$H[\phi] = \int \frac{\rho(\mathbf{r})}{2m} \left(\nabla\phi(\mathbf{r})\right)^2 d^2\mathbf{r}, \tag{4.20}$$

so that the Green's function $G(\mathbf{r},\mathbf{r}') = \langle\phi(\mathbf{r})\phi(\mathbf{r}')\rangle$ obeys

$$-\frac{\beta}{m}\nabla_{\mathbf{r}}\left(\rho(\mathbf{r})\nabla_{\mathbf{r}}G(\mathbf{r},\mathbf{r}')\right) = \delta(\mathbf{r}-\mathbf{r}'), \tag{4.21}$$

while $D_{\mathbf{r},\mathbf{r}'} = G(\mathbf{r},\mathbf{r}) + G(\mathbf{r}',\mathbf{r}') - 2G(\mathbf{r},\mathbf{r}')$.

For uniform density ρ, the solution of eq. (4.21) is $G(\mathbf{r},\mathbf{r}') = -\alpha \ln|\mathbf{r}-\mathbf{r}'|/R$, $\alpha = \frac{m}{2\pi\beta\rho}$, which gives

$$\frac{1}{2}D_{|\mathbf{r}-\mathbf{r}'|\gg\xi_T} = \frac{m}{2\pi\beta\rho}\ln\left(\frac{|\mathbf{r}-\mathbf{r}'|}{\xi_T}\right), \quad D_{\mathbf{r}=\mathbf{r}'} = 0, \tag{4.22}$$

where the equal point contribution is evaluated at the thermal length cutoff $|\mathbf{r}-\mathbf{r}'| \approx \xi_T$. When this result is used to estimate the effect of fluctuations on $N_{\rm ex}(\mathbf{k})$, one notes that the behavior of the

peak is determined by $|\mathbf{k}| \approx R^{-1}$ so the typical separation $\mathbf{r} - \mathbf{r}'$ in eq. (4.19) is of the order of the cloud radius R. For such separations, the equal point term $G(\mathbf{r}, \mathbf{r}) \simeq \alpha \ln R/\xi_T$ is much larger than the term $G(\mathbf{r}, \mathbf{r}') \leq \alpha$. This shows that the phase fluctuations are dominated by the equal point contribution, and allows to replace the 'Debye-Waller factor' $e^{-\frac{1}{2}D_{\mathbf{r},\mathbf{r}'}}$ in eq. (4.19) by $e^{-\frac{1}{2}G(\mathbf{r},\mathbf{r})-\frac{1}{2}G(\mathbf{r}',\mathbf{r}')}$, reproducing the local density approximation result, eq. (4.17).

This local-density-approximation can be further justified by finding the asymptotic form of the Green's function in a harmonic trap. As shown in Appendix A, the asymptotic form as two points approach each other is given by:

$$\lim_{\epsilon \to 0} G(r + \delta, r - \delta) = \frac{-m}{2\pi\beta\rho(r)} \ln\left(\frac{2\delta}{r}\right). \tag{4.23}$$

This matches both the nature of the divergence, and the pre-factor $m/2\pi\beta\rho$ seen in eq. (4.22), and supports the local density approximation eq. (4.17) for a finite system, with ρ replaced by $\rho(\mathbf{r})$. From the asymptotes of the trapped gas Green's functions, eq. (4.23), cutting the logarithmic divergence with the thermal length, the expression in eq. (4.19) for momentum distribution due to far separated excitons becomes identical to eq. (4.17).

Part III

Thermodynamics and signatures of condensation of microcavity polaritons

Chapter 5

Mean field theory and fluctuation spectrum

Polariton condensation can be described by a model of localised excitons coupled to propagating photons [31, 109]. This chapter presents the extended Dicke model that will be studied in this and the next chapter, and discusses the mean field results and fluctuation spectrum. A model of localised excitons is motivated by systems such as organic semiconductors [110, 111], quantum dots [79, 80, 112] and disordered quantum wells [113]. In addition, the predictions of such a model are expected to be similar to those for a model of mobile excitons, since a typical exciton mass is several orders of magnitude larger than the typical photon mass.

The Hamiltonian studied here is similar to that proposed by Holland [37] and Timmermans [36] in the context of Feshbach resonances in atomic gases. However, there are a number of important differences between the two models; most notably the absence of a direct four-fermion interaction, and the bare fermion density of states. How these differences affect the mean-field results is discussed in section 5.2 and their effect on the fluctuation spectrum in sections 5.3 and 5.4.

5.1 The model

The model describes localised two-level systems, coupled to a continuum of radiation modes in a two-dimensional microcavity. Considering only two levels describes a hard-core repulsion between excitons on a single site. Static Coulomb interactions between different sites are neglected. The two-level systems may either be represented as fermions with an occupancy constraint, as will be described below, or as spins with magnitude $|\mathbf{S}| = 1/2$. In the latter case, the generalised Dicke Hamiltonian [13] is:

$$\begin{aligned} H &= \sum_{j=1}^{j=nA} 2\epsilon_j S_j^z + \sum_{k=2\pi l/\sqrt{A}} \hbar\omega_k \psi_k^\dagger \psi_k \\ &+ \frac{g}{\sqrt{A}} \sum_{j,k} \left(e^{2\pi i \mathbf{k}\cdot\mathbf{r}_j} \psi_k S_j^+ + e^{-2\pi i \mathbf{k}\cdot\mathbf{r}_j} \psi_k^\dagger S_j^- \right). \end{aligned} \tag{5.1}$$

Here $A \to \infty$ is the quantisation area and n the areal density of two-level systems, *i.e.* sites where an exciton may exist. Without inhomogeneous broadening, the energy of a bound exciton is $2\epsilon = \hbar\omega_0 - \Delta$, defining the detuning Δ between the exciton and the photon. When later an inhomogeneously broadened band of exciton energies is introduced, Δ will represent the detuning between photon and centre of the exciton band. The photon dispersion, for photons in an ideal 2D cavity of width w, and relative permittivity ε_r is

$$\hbar\omega_k = \hbar \frac{c}{\sqrt{\varepsilon_r}} \sqrt{k^2 + \left(\frac{2\pi}{w}\right)^2} \approx \hbar\omega_0 + \frac{\hbar^2 k^2}{2m}, \tag{5.2}$$

so the photon mass is $m = (\hbar\sqrt{\varepsilon_r}/c)(2\pi/w)$.

The coupling constant, g, written in the dipole gauge is,

$$g = d_{ab} \sqrt{\frac{e^2}{2\varepsilon_0 \varepsilon_r} \frac{\hbar\omega_k}{w}}, \tag{5.3}$$

where d_{ab} is the dipole matrix element. For small photon wavevectors (w.r.t. $1/w$), it is justified to neglect the k dependence of g, *i.e.* to

take $\omega_k = \omega_0$. The factor of $1/\sqrt{w}$ is due to the quantisation volume for the electric field.

The grand canonical ensemble, $\tilde{H} = H - \mu N$, allows the calculation of equilibrium for a fixed total number of excitations, N, given by;

$$N = \sum_{j=1}^{nA} \left(S_j^z + \frac{1}{2} \right) + \sum_{k=2\pi l/\sqrt{A}} \psi_k^\dagger \psi_k. \tag{5.4}$$

It is therefore convenient to define $\hbar\tilde{\omega}_k = \hbar\omega_k - \mu$ and $\tilde{\epsilon} = \epsilon - \mu/2$. Expressing all energies in terms of the scale of the Rabi splitting, $g\sqrt{n}$, and all lengths via the two-level system density n, there remain only two dimensionless parameters that control the system, the detuning $\Delta^* = \Delta/g\sqrt{n}$ and the photon mass $m^* = mg/\hbar^2\sqrt{n}$. Typical values for current experiments [83, 85] are $g\sqrt{n} \approx 10\text{meV}$, $m \approx 10^{-5} m_{\text{electron}}$, and taking $n \approx 1/a_{\text{Bohr}}^2 \approx 10^{12}\text{cm}^{-2}$ leads to an estimate of $m^* \approx 10^{-3}$.

This model is similar to that studied by Hepp and Lieb [16]. They considered the case $\mu = 0$, *i.e.* without a bath to fix the total number of excitations. The transition studied by Hepp and Lieb was later shown by Rzążewski *et al.* [114] to be an artefact of neglecting A^2 terms in the coupling to matter. However, see also the discussion in chapter 7. Independent of such discussion, the model discussed in this chapter, when $\mu \neq 0$, does not suffer the same fate [31]: the sum rule of Rzążewski *et al.* which prevents condensation no longer holds when $\mu \neq 0$.

In order to integrate over the two-level systems, it is convenient to represent them as fermions, $S^z = \frac{1}{2}(b^\dagger b - a^\dagger a)$ and $S^+ = b^\dagger a$. For each site there then exist four states, the two singly occupied states, $a^\dagger |0\rangle$, $b^\dagger |0\rangle$, and the unphysical states $|0\rangle$ and $a^\dagger b^\dagger |0\rangle$.

Following Popov and Fedotov [115] the sum over states may be restricted to the physical states by inserting a phase factor:

$$\mathcal{Z} = \int \mathcal{D}(a,b) e^{-S[a,b]} e^{i(\pi/2)(b^\dagger b + a^\dagger a)}. \tag{5.5}$$

Since the Hamiltonian has identical expectations for the two unphysical states, this phase factor causes the contribution of zero occupied

and doubly occupied sites to cancel, so the partition sum includes only physical states. Such a phase factor may then be incorporated as a shift of the Matsubara frequencies for the fermion fields, using instead $\omega_n = (n + 3/4)2\pi T$. Thus, from here the two-level systems will be described as fermions.

High energy properties, ultraviolet divergences

The Hamiltonian (5.1) is a low energy effective theory, and will fail at high energies. This theory is not renormalisable; there exist infinitely many divergent one particle irreducible diagrams, and so would need infinitely many renormalisation conditions. These divergent diagrams lead to divergent expressions for the free energy and density.

To treat this correctly, it would be necessary to restore high energy degrees of freedom, which lead to a renormalisable theory. Integrating over such high energy degrees of freedom will recover, for low energies, the theory of eq. (5.1). One may then calculate the free energy for the full theory, with appropriate counter terms. The low energy contributions will be the same as before, but the high energy parts differ, however such high energy parts are not relevant at low temperatures. Since only the low energy properties of the theory are being considered, a cutoff K_{m} will be introduced. The coupling g is assumed to be zero between excitons and those photons with $k > K_{\mathrm{m}}$.

A number of candidates for this cutoff exist; the reflectivity bandwidth of the cavity mirrors, the Bohr radius of an exciton (where the dipole approximation fails), and the momentum at which photon energy is comparable to higher energy excitonic states (for which the two-level approximation fails). Which of these scales becomes relevant first depends on the exact system, however changes in K_{m} will lead only to logarithmic errors in the density.

5.2 Summary of mean field results

Before discussing the fluctuation spectrum, the mean-field results of Eastham and Littlewood [31, 109] are presented. Integrating over the fermion fields yields an effective action for photons:

$$\begin{aligned} S[\psi] &= \int_0^\beta d\tau \sum_k \psi_k^\dagger \left(\partial_\tau + \hbar\tilde{\omega}_k\right)\psi_k + N\mathrm{Tr}\ln\left(\mathcal{M}\right) \qquad (5.6)\\ \mathcal{M}^{-1} &= \begin{pmatrix} \partial_\tau + \tilde{\epsilon} & \frac{g}{\sqrt{A}}\sum_k e^{2\pi i \mathbf{k}\cdot\mathbf{r_j}}\psi_k \\ \frac{g}{\sqrt{A}}\sum_k e^{-2\pi i \mathbf{k}\cdot\mathbf{r_j}}\psi_k^\dagger & \partial_\tau - \tilde{\epsilon} \end{pmatrix}. \end{aligned}$$

The partition function is dominated by the values of ψ that minimise $S[\psi]$. Therefore, thermodynamic properties may be found by considering such a minimum saddle point, and integrating over Gaussian fluctuations around it. The static, uniform, minimum, ψ_0, satisfies the equation:

$$\hbar\tilde{\omega}_0\psi_0 = g^2 n\frac{\tanh(\beta E)}{2E}\psi_0, \quad E = \sqrt{\tilde{\epsilon}^2 + g^2\frac{|\psi_0|^2}{A}}. \qquad (5.7)$$

which describe a mean-field condensate of coupled coherent photons and exciton polarisation. The mean-field expectation of the density is given by

$$\rho_{\mathrm{M.F.}} = \frac{|\psi_0|^2}{A} + \frac{n}{2}\left[1 - \frac{\tilde{\epsilon}}{E}\tanh(\beta E)\right]. \qquad (5.8)$$

Note that the photon field acquires an extensive occupation. The intensive quantity $\rho_0 = |\psi_0|^2/A$ may be defined as the density of photons in the condensate. This corresponds to an electric field strength of $\sqrt{\hbar\omega_0\rho_0/2\varepsilon_0}$.

For an inhomogeneously broadened band of exciton energies, eq. (5.7) should be averaged over exciton energies. In this case condensation will introduce a gap in the excitation spectrum of single fermions [31]: whereas when uncondensed there may be single particle excitations of energy arbitrarily close to the chemical potential, now the smallest excitation energy is $2g|\psi|/\sqrt{A}$. The existence of this gap is reflected by features of the collective mode spectrum discussed below.

Connection to Dicke Superradiance

It is interesting to compare this mean-field condensed state, described by eq. (5.7), to the superradiant state originally considered by Dicke [13]. Dicke considered a Hamiltonian similar to eq. (5.1), but with a single photon mode. Constructing eigenstates $|L, m\rangle$ of the modulus and z component of the total spin, $\mathbf{S} = \sum_j \mathbf{S}_j$, Dicke showed that for N particles, the state $|N/2, 0\rangle$ has the highest radiation rate.

Taking the state described by the mean-field condensate, as described in eq. (5.7), and considering the limit as $\psi_0 \to \infty$ and $T \to 0$, the equilibrium state may be written as

$$|\psi_{\text{cond.}}\rangle = \frac{1}{2^{N/2}} \prod_j (|\uparrow\rangle_j + |\downarrow\rangle_j) \tag{5.9}$$

$$= \frac{1}{2^{N/2}} \sum_{p=0}^{N} \sqrt{\binom{N}{p}} \left| \frac{N}{2}, \frac{N}{2} - p \right\rangle, \tag{5.10}$$

i.e. a binomial distribution of angular momentum states.

As N tends to infinity, this becomes a Gaussian centred on the Dicke super-radiant state, with a width that scales like $\sqrt{N}$. However, it should be noted that the above state represents only the exciton part; this should be multiplied by a photon coherent state. In the self consistent state, there exists a sum of terms with different divisions of excitation number between the photons and excitons. These different divisions have a fixed phase relationship. Such a statement would remain true even if projected onto a state of fixed total excitation number. This is different from the Dicke superradiant state, which has no photon part. In the Dicke state, the only important coherence is that between the different ways of distributing excitations between the two-level systems.

Comparison of Mean-Field results with other boson-fermion systems

The mean-field equations (5.7), (5.8) have a form that is common to a wide range of fermion systems. However, the form of the density of states, and the nature of fermion interactions can significantly alter the form of the mean-field phase boundary. It is of interest to compare the extended Dicke model discussed here to other systems in which BCS-BEC crossover has been considered, and to note that even at the mean-field level, important differences emerge. To this end, one may compare the mean-field equations for the modified Dicke model to the Holland-Timmermans Hamiltonian [36, 37, 116], and to BCS superconductivity [1].

For a gas of fermionic atoms, or BCS, the density of states is non-zero for all energies greater than zero, whereas for localised excitons, without inhomogeneous broadening, it is a δ function. One immediate consequence is a difference of interpretation of the mean-field equations; the number equation and the self consistent condition for the anomalous Green's function. For a weakly interacting fermion system the number equation alone fixes the chemical potential [15], and the self-consistent condition can then be solved to find the critical temperature. For localised fermions, the chemical potential lies below the band of fermions, and so the density is controlled by the tail of the Fermi distribution, so temperature and chemical potential cannot be so neatly separated. This can remain true even in the presence of inhomogeneous broadening; the majority of density may come from regions of large density of states in the tail of the Fermi distribution.

Differences also exist in the density dependence of the mean-field transition. The absence of a direct four-fermion interaction means that the effective interaction strength is entirely due to photon mediated interactions. Since the model discussed here has the photons at chemical equilibrium with the excitons, this effective interaction strength depends strongly upon the chemical potential.

For BCS superconductors, and the BCS limit for weakly interacting fermionic atoms, the dependence of critical temperature upon

density is due to the changing density of states, which appears in the self consistent equation as a pre-factor of the logarithm in the BCS equation $1/g = \rho_s \ln(\omega_D/T_c)$. In contrast, the density dependence of T_c for the Dicke model is due to the changing coupling strength and occupation of two-level systems with changing chemical potential. Such a change of coupling strength with chemical potential also occurs in the Holland-Timmermans model, near Feshbach resonance, where the boson mediated interaction is not dominated by the direct four-fermion term. Even with inhomogeneous broadening of energies, unless the chemical potential remains fixed at low densities, there will be a strong density dependence of T_c as the effective interaction strength changes. The resultant phase boundary with inhomogeneous broadening, at low densities, is given in section 6.4.

5.3 Effective action for fluctuations

Including fluctuations about the saddle point, $\psi = \psi_0 + \delta\psi$, one may write the two-level system inverse Green's function as $\mathcal{M}^{-1} = \mathcal{M}_0^{-1} + \delta\mathcal{M}^{-1}$, where

$$\delta\mathcal{M}^{-1} = \frac{g}{\sqrt{A}} \sum_k \begin{pmatrix} 0 & e^{2\pi i \mathbf{k}\cdot\mathbf{r}_j}\delta\psi_k \\ e^{-2\pi i \mathbf{k}\cdot\mathbf{r}_j}\delta\bar{\psi}_k & 0 \end{pmatrix}, \tag{5.11}$$

thus eq. (5.6) can be expanded to quadratic order as

$$\begin{aligned} S &= S[\psi_0] + \beta \sum_{i\omega} \sum_k (i\omega + \hbar\tilde{\omega}_k)|\delta\psi_{\omega,k}|^2 \\ &- \frac{N}{2}\mathrm{Tr}\left(\mathcal{M}_0\delta\mathcal{M}^{-1}\mathcal{M}_0\delta\mathcal{M}^{-1}\right) \qquad (5.12) \\ &= S[\psi_0] + \frac{\beta}{2}\sum_{i\omega,k} \delta\bar{\Psi}_{\omega,k}\mathcal{G}^{-1}(\omega,\mathbf{k})\delta\Psi_{\omega,k} \qquad (5.13) \end{aligned}$$

where $\delta\Psi$ is in a particle/hole Nambu space:

$$\delta\Psi_{\omega,k} = \begin{pmatrix} \delta\psi_{\omega,k} \\ \delta\bar{\psi}_{-\omega,-k} \end{pmatrix} \tag{5.14}$$

and the inverse photon Green's function is given by:

$$\mathcal{G}^{-1}(\omega,\mathbf{k}) = \begin{pmatrix} i\omega + \hbar\tilde{\omega}_k + K_1(\omega) & K_2(\omega) \\ K_2^*(\omega) & -i\omega + \hbar\tilde{\omega}_k + K_1^*(\omega) \end{pmatrix} \quad (5.15)$$

The exciton contribution to the inverse Green's function (with $\nu = (n+3/4)2\pi T$) is

$$\begin{aligned} K_1(\omega) &= \frac{g^2}{A}\sum_j\sum_\nu \frac{(i\nu+\tilde{\epsilon})\,(i\nu+i\omega-\tilde{\epsilon})}{(\nu^2+E^2)\,((\nu+\omega)^2+E^2)} \\ &= g^2 n\frac{\tanh(\beta E)}{E}\left(\frac{i\tilde{\epsilon}\omega - E^2 - \tilde{\epsilon}^2}{\omega^2+4E^2}\right) - |\alpha|\delta_\omega, \quad (5.16) \\ K_2(\omega) &= \frac{g^2}{A}\sum_j\sum_\nu \frac{g^2\psi_0^2/A}{(\nu^2+E^2)\,((\nu+\omega)^2+E^2)} \\ &= g^2 n\frac{\tanh(\beta E)}{E}\left(\frac{g^2\psi_0^2/A}{\omega^2+4E^2}\right) - \alpha\delta_\omega, \quad (5.17) \\ \alpha &= g^2 n\beta\frac{\mathrm{sech}^2(\beta E)}{4E^2}g^2\frac{\psi_0^2}{A}, \quad (5.18) \end{aligned}$$

where the sum over sites assumed no inhomogeneous broadening, and ω is a bosonic Matsubara frequency, $2\pi nT$. The mean-field action, $S[\psi_0]$, is given by:

$$S[\psi_0] = \hbar\tilde{\omega}_k|\psi_0|^2 - \frac{\mu N}{2} - \frac{N}{\beta}\ln\left[\cosh\left(\beta E\right)\right]. \quad (5.19)$$

The terms $\alpha\delta_\omega$ occur when the sum over fermionic frequencies in eqs. (5.16)(5.17) have second order poles. These terms must be included in the thermodynamic Green's function at $\omega = 0$. However, they do not survive analytic continuation, and so do not appear in the retarded Green's function or in the excitation spectrum. This is discussed in Appendix B.

Even considering inhomogeneous broadening of exciton energies, such terms remain as δ_ω, rather than some broadened peak. This can be understood by considering which transitions contribute to the excitons' response to a photon, *i.e.* between which exciton states there

is a matrix element due to the photon. If uncondensed, the photon couples to transitions between the exciton's two energy states, $\pm\epsilon$. In the presence of a coherent field, these energy states mix. The photon then couples both to transitions $E \to -E$ and also to the degenerate transition $E \to E$. Since this transition is between the two levels on a single site, inhomogeneous broadening does not soften the δ_ω term.

This conclusion differs for models with transitions between two bands of fermion states. If transitions are allowed between any pair of lower and upper band states, the degenerate transition above is replaced by a continuum of intra-band transitions. In the extended Dicke model all intra-band excitations are of zero energy. If there exists a range of low energy intra-band transitions, these allow the Goldstone mode to decay, giving rise to Landau damping [116, 117]. For the extended Dicke model, as there is no continuum of modes, no such damping occurs.

In order to consider fluctuations for an inhomogeneously broadened system of excitons, a correct treatment requires calculating for a given realisation of disorder, and then averaging the final results. Because the position of an exciton matters in its coupling to light, it would be necessary to include averaging over disorder in both energy and position of excitons. However, for low energy modes, the expressions for K_1, K_2 will be averaged over exciton energies.

This approximation is equivalent to the assumption that the energies and positions of excitons sampled by photons of different momenta are independent and uncorrelated. Such an approximation evidently cannot hold for high momenta, as otherwise the number of random variables would become greater than the number of excitons. This approximation will also necessarily neglect scattering between polariton momenta states. However, such effects involve high energy states (since they require momenta on the order of the inverse exciton spacing), and can be neglected in discussing the low energy behaviour.

5.4 Fluctuation spectrum

Inverting the matrix in the effective action for fluctuations, eq. (5.13), one finds the fluctuation Green's function. The location of the poles of this Green's function give the spectrum of those excitations which can be created by injecting photons, measured relative to the chemical potential.

These poles come from the denominator:

$$\begin{aligned} \det\left(\mathcal{G}^{-1}\right) &= |i\omega + \hbar\tilde{\omega}_k + K_1(\omega)|^2 - |K_2(\omega)|^2 \\ &= \frac{\left(\omega^2 + \xi_1^2\right)\left(\omega^2 + \xi_2^2\right)}{(\omega^2 + 4E^2)}, \end{aligned} \tag{5.20}$$

where, as discussed above, the δ_ω terms have been ignored, and no inhomogeneous broadening of excitons is assumed.

In the condensed state the poles are:

$$\xi_{1,2}^2 = \frac{1}{2}\left\{A(k) \pm \sqrt{A(k)^2 - B(k)}\right\}, \tag{5.21}$$

where

$$A(k) = 4E^2 + (\hbar\tilde{\omega}_k)^2 + 4\tilde{\epsilon}\hbar\tilde{\omega}_0, \tag{5.22}$$

$$B(k) = 16\frac{\hbar^2 k^2}{2m}\left(E^2\hbar\tilde{\omega}_k - \tilde{\epsilon}^2\hbar\tilde{\omega}_0\right). \tag{5.23}$$

In the normal state, the denominator simplifies further, as K_2 is zero, and eq. (5.20) is replaced by:

$$|i\omega + \hbar\tilde{\omega}_k + K_1(\omega)|^2 = \left|\frac{(i\omega + E_+)(i\omega + E_-)}{(i\omega + 2\tilde{\epsilon})}\right|^2. \tag{5.24}$$

There are two poles, the upper and lower polariton;

$$E_\pm = \frac{1}{2}\left((\hbar\tilde{\omega}_k + 2\tilde{\epsilon}) \pm \sqrt{(\hbar\tilde{\omega}_k - 2\tilde{\epsilon})^2 + 4g^2 n\tanh(\beta\tilde{\epsilon})}\right). \tag{5.25}$$

The polariton dispersion (5.25) from localised excitons has the same structure as from propagating excitons, since the photon dispersion dominates. The spectra, both condensed and uncondensed, are shown in figure 5.1.

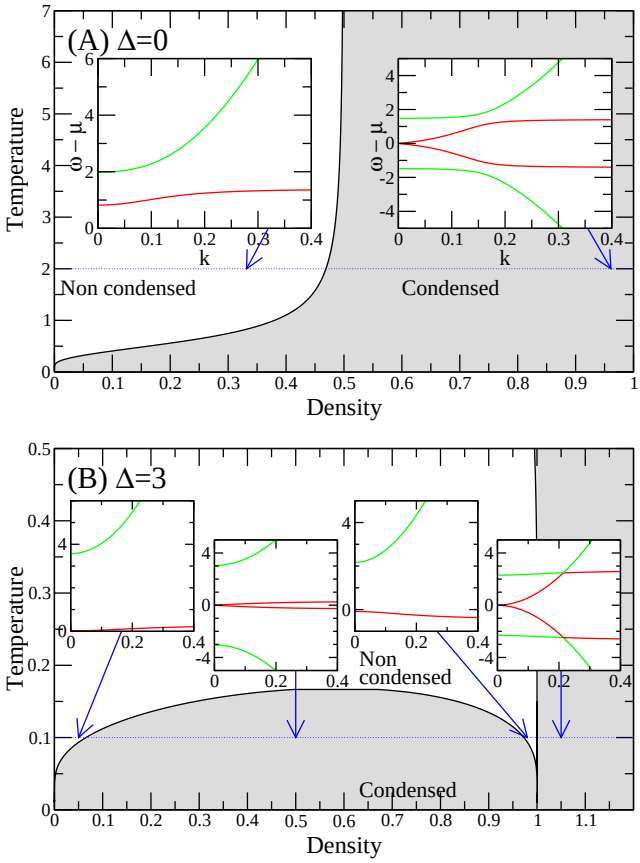

Figure 5.1: Excitation spectra in the condensed and uncondensed states, superimposed on the mean-field phase diagram, to show choice of density and temperature. Panel A is for the resonant case, the two spectra are for $T = 2g\sqrt{n}$ and $\mu/g\sqrt{n} = -1.4$ and -0.24. Panel B has the exciton detuned by $3g\sqrt{n}$ below the photon, and the spectra are for $T = 0.1g\sqrt{n}$ and $\mu/g\sqrt{n} = -3.29$, -3.01, -2.54 and -0.37. The photon mass is $m^* = 0.01$. Temperatures and energies plotted in units of $g\sqrt{n}$, densities in units of n, and wavevectors in units of $\sqrt{n}$.

The difference between condensed and uncondensed spectra is dramatic: two new poles appear. These arise because the off diagonal terms in eq. (5.13) mix photon creation and annihilation operators. Such a spectrum may be observed in polariton condensation experimentally, as one may probe the response to inserting a real photon, and observing its emission at a later time. In the presence of a condensate, the polariton is not a quasi-particle. Creating a photon corresponds to a superposition of creating and destroying quasi-particles. At non-zero temperature, a population of quasi-particles exists, so processes where a quasi-particle is destroyed are possible. This means that a process in which a photon, with energy less than the chemical potential, is added to the system is possible (*i.e.* P_{absorb} as defined in eq. (B.9)). However, if the system is experimentally probed with photons of energy less than the chemical potential, what will be observed is gain, since the absorption of photons is more than cancelled by spontaneous and stimulated emission.

At small momentum, ξ_1 corresponds to phase fluctuations of the condensate, *i.e.* it is the Goldstone mode, and has the form $\xi_1 = \pm\hbar c k$, with,

$$c = \sqrt{\frac{1}{2m}\left(\frac{4\hbar\tilde{\omega}_0 g^2 n}{\xi_2(0)^2}\right)\left(\frac{|\psi_0|^2}{N}\right)} \approx \sqrt{\frac{\lambda}{2m}\frac{\rho_0}{n}}. \tag{5.26}$$

The second expression is, for comparison, the form of the Bogoliubov mode in a dilute Bose gas, of interaction strength λ. As ψ_0 increases, the phase velocity first increases, then decreases. The decrease is due to the saturation of the effective exciton-photon interaction.

The leading order corrections $\xi_1 = \pm ck + \alpha k^2$ are of interest for considering Beliaev decay of phonons [118]. If $\alpha < 0$, kinematic constraints prevent the decay of phonons. For the Bogoliubov spectrum in a dilute Bose gas, $\alpha = 0$, and the cubic term becomes relevant. Here, both signs are possible; according to whether the spectrum crosses over to the quadratic lower polariton dispersion before this crosses over to a flat exciton dispersion. In most cases, $\alpha > 0$ and ξ_1 will have a point of inflection, but if the exciton is detuned below

the photon, then for certain densities, $\alpha < 0$, and the curvature is always negative.

The modes may also be compared to the Cooperon modes in BCS theory. At small momenta, although the mode ξ_1 becomes a pure phase fluctuation, the other mode ξ_2 is not an amplitude fluctuation. To see why this is so, it is helpful to rewrite the action in equation (5.13) in terms of the Fourier components of the transverse and longitudinal fluctuations of the photon field. These components, at quadratic order, are equivalent to the phase and amplitude components, and are given by:

$$\begin{aligned} \delta\psi_{\omega,k} &= \psi_L(\omega,k) + i\psi_T(\omega,k), \\ \delta\bar{\psi}_{\omega,k} &= \psi_L(-\omega,-k) - i\psi_T(-\omega,-k). \end{aligned} \tag{5.27}$$

In terms of these new variables, the action may be written:

$$S = S[\psi_0] + \beta \sum_{i\omega,k} \Psi^T_{-\omega,-k} \mathcal{G}^{-1}(\omega,\mathbf{k}) \Psi_{\omega,k} \tag{5.28}$$

where now

$$\Psi_{\omega,k} = \begin{pmatrix} \psi_L(\omega,k) \\ \psi_T(\omega,k) \end{pmatrix} \tag{5.29}$$

and the rotated inverse Green's function is:

$$\mathcal{G}^{-1}(\omega,\mathbf{k}) = \begin{pmatrix} \hbar\tilde{\omega}_k + \Re(K_1) + K_2 & -\omega - \Im(K_1) \\ \omega + \Im(K_1) & \hbar\tilde{\omega}_k + \Re(K_1) - K_2 \end{pmatrix} \tag{5.30}$$

Due to the off-diagonal components, the eigenstates are mixed amplitude and phase modes. This mixing vanishes only where ω is small, which means that the lowest energy parts of the Goldstone mode are purely phase fluctuations. Since the amplitude mode at $k = 0$ has a non-zero frequency, it will mix with the phase mode.

The off diagonal terms come from two sources. The dynamic photon field leads to the term ω. The fermion mediated term $\Im(K_1)$ will be non zero if the density of states is asymmetric about the chemical potential. For the Dicke model, both terms contribute to mixing since:

$$\Im(K_1) = g^2 n \frac{\tanh(\beta E)}{E} \left(\frac{\tilde{\epsilon}\omega}{\omega^2 + 4E^2} \right). \tag{5.31}$$

Unless $\tilde{\epsilon} = 0$, the density of states is not symmetric about the chemical potential, and so this term is non-zero.

For BCS superconductivity the pairing field is not dynamic, so there is no off diagonal ω term. However there can still be mixing due to $\Im(K_1)$, which is given by:

$$\Im(K_1) = \sum_{i\nu,q} \frac{\nu(\epsilon_q - \epsilon_{q+Q}) + \omega\epsilon_q}{(\nu^2 + \epsilon_q^2 + \Delta^2)((\nu+\omega)^2 + \epsilon_{q+Q}^2 + \Delta^2)}, \tag{5.32}$$

in which ν is a fermionic Matsubara frequency, $(2n+1)\pi T$, and Δ the superconducting gap. Note that this coupling now depends on the momentum transfer Q as well as energy ω. If the density of states is symmetric, *e.g.* $\epsilon_q = v_F q$, then at $Q = 0$, $\Im(K_1)$ will be zero, and as the boson field has no dynamics, the modes will then entirely decouple. In real superconductors, symmetry of the density of states about the chemical potential is only approximate, and so some degree of mixing will occur.

5.5 Inhomogeneous luminescence spectrum

Although four poles exist, they may have very different spectral weights. At high momentum, the weights of all poles except the highest vanish, and the remaining pole follows the bare photon dispersion.

Such effects can be seen more clearly by plotting the incoherent luminescence spectrum. As discussed in appendix B, this can be found from the Green's function as

$$P_{\text{emit}}(x) = 2n_{\text{B}}(x)\Im\left[\mathcal{G}_{00}(i\omega = x + i\eta)\right]. \tag{5.33}$$

It is easier to observe how the spectral weight associated with poles changes after adding inhomogeneous broadening. Figures 5.2 and 5.3 plot the luminescence spectrum for the same parameters as in figure 5.1, but with inhomogeneous broadening. This will broaden the poles, except for the Goldstone mode (labelled (d) in figure 5.2), as discussed above. The distribution of energies used is, for numerical

efficiency, a cubic approximation to a Gaussian, with standard deviations $0.1g\sqrt{n}$ and $0.3g\sqrt{n}$. The results with a Gaussian density of states have been compared to this cubic approximation, and no significant differences occur.

In the condensed case, a third pair of lines are visible, (labelled (c) in figure 5.2). These correspond to the minimum energy for a neutral excitation, $2g\sqrt{n}\psi_0$, *i.e.* flipping the spin on a single site. They are analogous to a particle-hole excitation in BCS, which have twice the energy of the gap for adding a single particle. This energy is the smallest "inter-band excitation". If the inhomogeneous broadening is small compared to the gap then these extra lines will be less visible, as seen in panel B of figure 5.2. For large inhomogeneous broadening , the peak at the edge of the gap (c) and the upper polariton (b) will merge, as shown by (e) in panel B of figure 5.3. This will result in a band of incoherent luminescence separated from the coherent emission at the chemical potential by the gap. Such structure, although associated with the internal structure of a polariton, can be seen even at densities where the transition temperature is adequately described by a model of structureless polaritons.

It is also interesting to consider the uncondensed cases. In panel A of figure 5.2, with the smaller broadening, three lines are visible; the upper and lower polariton, and between them luminescence from excitons weakly coupled to light (labelled (a)). These weakly coupled states arise from excitons further away from resonance with the photon band. Although there may be a large density of such states, they make a much smaller contribution to luminescence than the polariton states, because of their small photon component. With larger broadening, these weakly coupled excitons form a continuum stretching between the two modes, as seen in panel A of figure 5.3.

5.6 Momentum distribution of photons

From the Green's function for photon fluctuations, one can calculate the momentum distribution of photons in the cavity. For a two-dimensional cavity coupled via the mirrors to three-dimensional

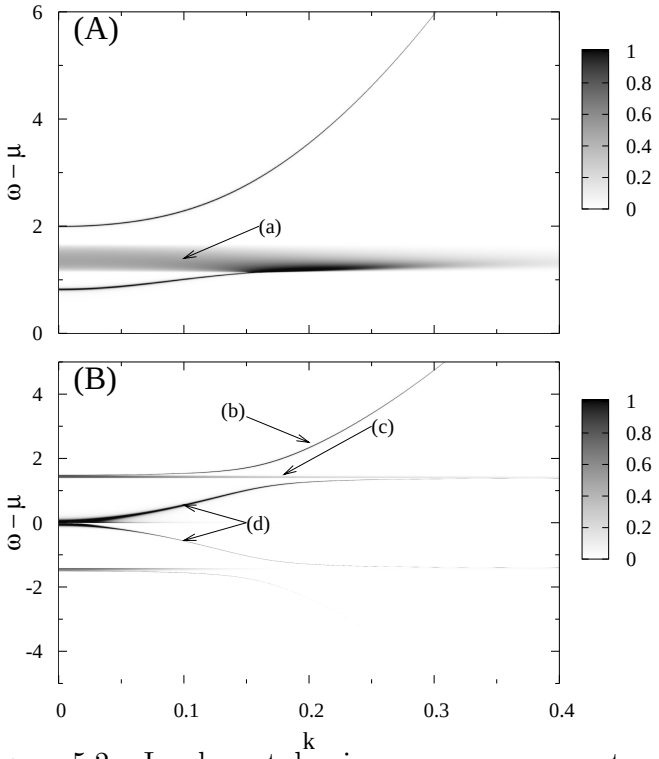

Figure 5.2: Incoherent luminescence vs momentum (x axis) and energy (y axis) calculated above (panel A) and below (panel B) phase transition. Inhomogeneous broadening of $0.1g\sqrt{n}$, all other parameters are the same as in the unbroadened case shown in panel A of figure 5.1. Colour allocated as tanh(Intensity), energies are in units of $g\sqrt{n}$, and wavevectors in units of $\sqrt{n}$.

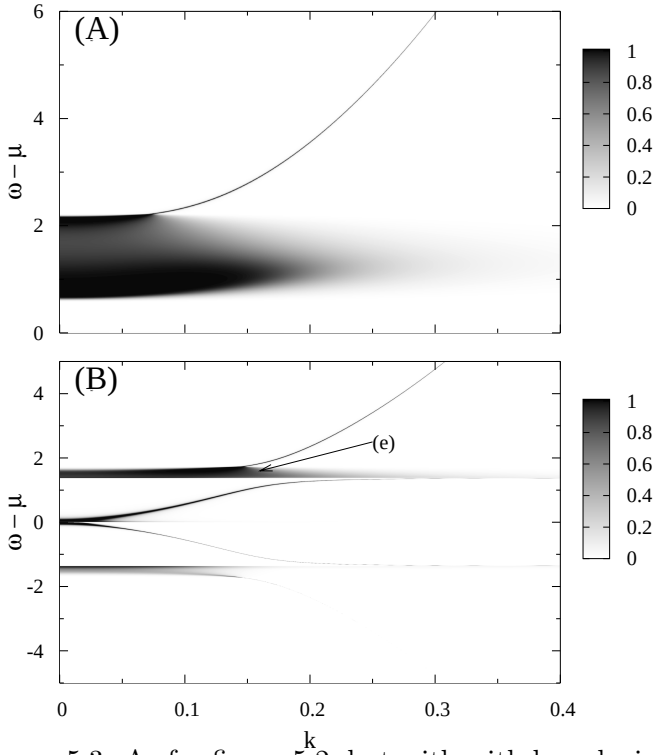

Figure 5.3: As for figure 5.2, but with with broadening of $0.3g\sqrt{n}$. Colour allocated as tanh(Intensity), energies are in units of $g\sqrt{n}$, and wavevectors in units of $\sqrt{n}$.

photons outside, the momentum distribution may be observed experimentally from the angular distribution [83].

When uncondensed, $N(p)$ is given by

$$\begin{aligned} N(p) &= \lim_{\delta\to 0^+} \left\langle \psi_p^\dagger(\tau+\delta)\psi_p(\tau)\right\rangle \\ &= \lim_{\delta\to 0^+} \beta \oint \frac{dx}{2\pi i} n_B(z) e^{\delta z} \mathcal{G}_{11}(iz,p). \end{aligned} \tag{5.34}$$

However when condensed, since the system is two-dimensional, it is necessary to treat fluctuations more carefully. Writing $\psi(r) =$

$\sqrt{\rho_0 + \pi(r)}e^{i\phi(r)}$, the action involves only derivatives of the phase, showing that large phase fluctuations are possible. For quadratic fluctuations, one can use the matrix in eq. (5.28) describing transverse and longitudinal modes, and relate these to the phase and amplitude excitations.

At low enough temperatures, it is possible to calculate $N(p)$ by considering only the phase mode, as discussed in section 4.4. Thus, neglecting amplitude fluctuations gives;

$$\begin{aligned} N(p) &= \frac{1}{A}\int d^2r \int d^2r' e^{i\mathbf{k}\cdot(\mathbf{r}-\mathbf{r}')}\rho_0 \left\langle e^{i(\phi(\mathbf{r})-\phi(\mathbf{r}'))}\right\rangle \\ &= \rho_0 \frac{1}{A}\int d^2R \int d^2t e^{i\mathbf{k}\cdot\mathbf{t}} e^{-D(\mathbf{R}+\mathbf{t}/2,\mathbf{R}-\mathbf{t}/2)}, \end{aligned} \tag{5.35}$$

where ρ_0 is taken as the mean-field photon density. The phase correlator, found by inverting the amplitude/phase action, is:

$$\begin{aligned} D(\mathbf{r},\mathbf{r}') &= \int \frac{d^2k}{(2\pi)^2}\left[1-\cos\left(\mathbf{k}.(\mathbf{r}-\mathbf{r}')\right)\right]\frac{m}{\beta\rho_0\hbar^2k^2} \\ &\approx \frac{m}{2\pi\beta\rho_0\hbar^2}\ln\left(\frac{|\mathbf{r}-\mathbf{r}'|}{\xi_T}\right). \end{aligned} \tag{5.36}$$

The thermal length is $\xi_T = \beta c$, where c is the velocity of the sound mode from eq. (5.26). This comes from the energy scale at which fluctuations become cut by the thermal distribution.

In this approximation, eq. (5.35) may be evaluated exactly [119] giving

$$\begin{aligned} N(p) &= 2\pi\rho_0\frac{(p\xi_T)^\eta}{p^2}\int_0^\infty x^{1-\eta}J_0(x)dx \\ &= 2\pi\rho_0\frac{\xi_T^\eta}{p^{2-\eta}}2^{1-\eta}\frac{\Gamma(1-\eta/2)}{\Gamma(\eta/2)}, \end{aligned} \tag{5.37}$$

where $\eta = m/2\pi\beta\rho_0\hbar^2$ controls the power law decay of correlations. The second line follows from an identity (see ref. [120] exercise XVII.32). This is valid only for small η, far from the transition. The Kosterlitz-Thouless transition [18] occurs when η becomes large, an approximate estimate of the transition is at $\eta = 2$.

The momentum distribution can therefore be calculated both at low temperatures, where such a scheme holds, and at high temperatures, when uncondensed. This is shown in figure 5.4. When condensed, the power law divergence leads to a peak normal to the plane. This peak reflects coherence between distant parts of the system, so in a finite system this peak is cut at small momenta.

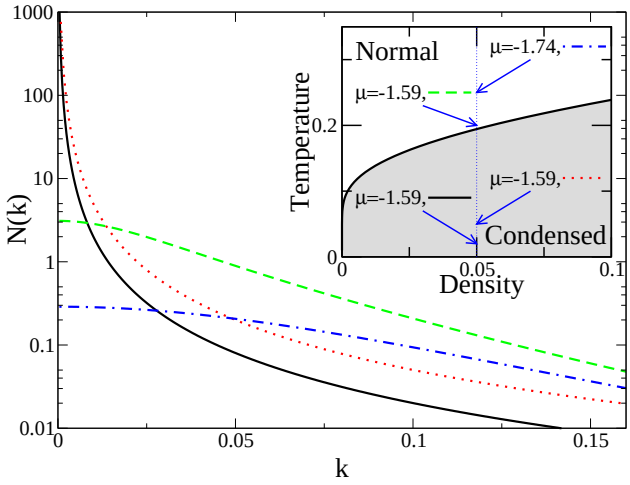

Figure 5.4: Momentum distribution of photons, plotted for two temperatures below and two above transition. The inset illustrates the choices of density and temperature. (Parameters $\Delta^* = 1$, $m^* = 0.01$, wavevector plotted in units of $\sqrt{n}$, temperature in units of $g\sqrt{n}$, density in units of n, and $N(k)$ in arbitrary units.)

Chapter 6

Fluctuation corrections to mean-field phase boundary

From the spectrum of fluctuations it is possible to calculate a correction to the mean-field density, and thus to the mean-field phase boundary. The method used is similar to that of Nozières and Schmitt-Rink [14], who studied fluctuation corrections to the BCS mean-field theory for a model of interacting, propagating fermions. However, because the model studied here differs from that of Nozières and Schmitt-Rink, the approach to including second order fluctuations will also differ. The remainder of this introduction first presents a brief summary of the method used by Nozières and Schmitt-Rink, further developed by Randeria [15], and then presents the differences in approach from these works.

Fluctuation corrections in three dimensions

To consider fluctuation corrections to a mean field-theory, one first needs to find the partition function in terms of a coherent state path integral for a bosonic field,

$$\mathcal{Z} = \int \mathcal{D}\psi \exp(-S[\psi])$$

For the Dicke model, $S[\psi]$ is given in eq. (5.6). In the work of Nozières and Schmitt-Rink, $S[\psi]$ resulted from decoupling a four-fermion interaction, and then integrating over the fermions. This effective action may be understood as a Ginzburg-Landau theory, with coefficients that are functions of temperature and chemical potential as well as the parameters in the Hamiltonian. To find the mean-field phase boundary, one needs both to find the values of temperature and chemical potential where the transition occurs, and to calculate the density evaluated at these parameters.

For the mean-field theory, the action is evaluated for a static uniform field, ψ_0, and minimised w.r.t. this field. At the critical temperature, a second order phase transition occurs, and the minimum action moves to a non-zero ψ_0. The density is found by differentiating the free energy w.r.t. chemical potential. For the mean field theory, the free energy is approximated by the action evaluated at ψ_0.

To go beyond the mean field theory, one can expand the effective action about the saddle point:

$$\mathcal{Z} \approx e^{-S[\psi_0]} \int \mathcal{D}\delta\psi \exp\left(-\frac{1}{2}\left.\frac{\partial^2 S}{\partial\psi^2}\right|_{\psi_0} (\delta\psi)^2\right) \tag{6.1}$$

This gives an improved estimate of the free energy, from which follows an improved estimate of the density, and thus of the phase boundary. In three dimensions (but not in two, as discussed below), one only needs an estimate of the density at the mean-field critical temperature. It is therefore sufficient to consider an expansion about the normal state saddle point, $\psi = 0$. For a model derived from interacting fermions, such fluctuations may be understood as the contribution to the density from non-condensed pairs of particles, whereas the mean-field estimate of density included only unpaired fermions. These corrections will increase the density at a fixed critical temperature, or equivalently decrease the critical temperature for a given density.

The extended Dicke model studied here differs from the model studied by Nozières and Schmitt-Rink; two differences are of partic-

ular importance. Firstly, the extended Dicke model boson field is dynamic, and there exists a chemical potential for bosons. In this respect, the extended Dicke model is closer to the boson-fermion models [36, 37] studied in the context of Feshbach resonances, for which Ohashi & Griffin [116] have studied fluctuation corrections. The second important difference is that the polariton system modelled is two-dimensional. This requires calculation of fluctuations in the presence of a condensate, as discussed next.

Fluctuations in two dimensions

To find the fluctuation-correction to the mean-field phase boundary in two dimensions, it is necessary to consider fluctuations in the presence of a condensate. Considering fluctuations in the normal state would lead to the conclusion that the normal state can support any density: as one approaches the mean-field critical temperature, the fluctuation density will become infra-red divergent, allowing any density. This correctly indicates that no long-range order exists in two dimensions; however a Kosterlitz-Thouless [18, 20] transition does occur.

Instead one must start by considering fluctuations in the presence of a condensate. This gives a density, defined by the total derivative of free energy w.r.t. chemical potential, of the form:

$$\rho = -\frac{dF}{d\mu} = -\frac{\partial F}{\partial \mu} - \frac{\partial F}{\partial \psi_0}\frac{d\psi_0}{d\mu}. \tag{6.2}$$

When considering fluctuation corrections in the presence of a condensate, in any dimension, one must take care to consider the depletion of the order parameter due to the interaction between condensed and uncondensed particles. This is discussed in detail in section 6.1. Such a depletion means that, for a fixed temperature, the critical value of the chemical potential changes; at the mean-field critical chemical potential the formula for total density may become negative. It is therefore necessary to make a separate estimate of the order parameter in the presence of fluctuations, and define the phase boundary where the order parameter goes to zero.

In three dimensions such a calculation can be achieved by identifying parts of the density as the population of the ground state and of fluctuations (as discussed below in section 6.1). In two dimensions, no true condensate exists, but a quasi-condensate with a cutoff k_0 can be considered. As discussed by Popov [7, Chapter 6], the quasi-condensate and fluctuation densities both contain terms which diverge logarithmically as $k_0 \to 0$, but these divergences cancel in the total density.

Instead, in two dimensions, one must consider an alternate definition for the location of the phase boundary. Since the transition is a Kosterlitz-Thouless transition, one should map the problem to the two-dimensional Coulomb Gas [121]. This requires the vortex core energy and strength of vortex-vortex interactions, which both scale as $\hbar^2\rho_s/2m$, where ρ_s is a superfluid response density. The phase transition thus occurs when $\rho_s = \#2mT/\hbar^2$. The numerical pre-factor depends on the vortex core structure. However, approximating the critical condition by $\rho_s = 0$ leads to only a small shift to T_C.

6.1 Total derivatives and negative densities

This section discusses the effects and interpretation of the second term in eq. (6.2). In ref. [116], Ohashi & Griffin define the density as the partial derivative of free energy w.r.t. chemical potential, neglecting the second term in eq. (6.2), which they describe as a higher-order correction under the Gaussian fluctuation approximation. As shown below in sec. 6.1, the contribution of the second term in eq. (6.2) to the density should not necessarily be neglected in the Gaussian fluctuation approximation. Section 6.1 shows explicitly that the two terms in eq. (6.2) are of the same order. The existence of the second term is crucial in finding a finite density in two dimensions, however may be less important in three dimensions.

Gaussian fluctuation approximation

Before showing that the second term in eq. (6.2) is of the same order as the first, it is shown why the second term of eq. (6.2) should not be automatically neglected. Even though it is of the form $\partial^3 S/\partial\psi_0^3$, such terms are not necessarily small, and can contribute to the density at quadratic order.

To see that a Gaussian theory may be correct even if such third order terms are not small, consider an expansion of the effective action,

$$S = S[\psi_0] + \frac{d^2S}{d\psi_0^2}\delta\psi^2 + \frac{d^3S}{d\psi_0^3}\delta\psi^3 + \dots \tag{6.3}$$

A Gaussian approximation is justified if, using this action, the expectation of the cubic term is less than the quadratic term. This condition can be written as

$$\left(\frac{d^2S}{d\psi_0^2}\right)^{3/2} \gg \frac{d^3S}{d\psi_0^3}. \tag{6.4}$$

This need not require that the coefficient of the cubic term is smaller, *i.e.* that

$$\frac{d^2S}{d\psi_0^2} \gg \frac{d^3S}{d\psi_0^3}.$$

In fact, if both terms are of the same order, but large; $d^2S/d\psi_0^2 \simeq d^3S/d\psi_0^3 \gg 1$, then the condition (6.4) is fulfilled.

Writing the free energy including fluctuations schematically as

$$F = S[\psi_0] + \ln\left[\int \mathcal{D}\delta\psi \exp\left(-\frac{d^2S}{d\psi_0^2}\delta\psi^2\right)\right], \tag{6.5}$$

the fluctuation contribution to the second term in eq. (6.2) will take the form

$$\rho = \dots + \left\langle \frac{d^3S}{d\psi_0^3}\delta\psi^2 \right\rangle \frac{d\psi_0}{d\mu}, \tag{6.6}$$

where $\langle\dots\rangle$ signifies averaging over the fluctuation action. Thus, in calculating the condensate density, there is a term which depends on $\partial^3 S/\partial\psi_0^3$ but only involves second order expectations of the fields.

Since $\partial^3 S/\partial\psi_0^3$ is not necessarily small, and it contributes to the density at quadratic order, there is no a priori argument for neglecting this term. In the following it is shown explicitly that this term should be included.

Total derivatives for a dilute Bose gas

The following discussion will show explicitly that the two terms in equation (6.2) are of the same order for a weakly interacting dilute Bose gas,

$$H - \mu N = \sum_k (\epsilon_k - \mu) a_k^\dagger a_k + \frac{g}{2} \sum_{k,k',q} a_{k+q}^\dagger a_{k'-q}^\dagger a_k a_{k'}. \tag{6.7}$$

Further, the terms in eq. (6.2) will be interpreted by considering the Hugenholtz-Pines relation at one loop order, as discussed in ref. [7, Chapter 6]

Saddle point and fluctuations.

To find the free energy, consider the static uniform saddle point, $\langle a_0^\dagger a_0 \rangle = |A|^2 = \mu/g$, and quadratic fluctuations, which are governed by the Hamiltonian:

$$\begin{aligned} H_{\text{eff}} &= \sum_k (\epsilon_k - \mu + 2gA^2) a_k^\dagger a_k \\ &+ \frac{gA^2}{2} \left(a_k^\dagger a_{-k}^\dagger + a_k a_{-k} \right). \end{aligned} \tag{6.8}$$

Thus, by a Bogoliubov transform, the free energy and density become

$$\begin{aligned} F &= -\mu A^2 + \frac{g}{2} A^4 \\ &+ \sum_k \left(\frac{1}{\beta} \ln\left(1 - e^{-\beta E_k}\right) + \frac{1}{2}(E_k - \epsilon_k - \mu) \right), \end{aligned} \tag{6.9}$$

$$\rho = A^2 - \sum_k \left(n_B(E_k) \frac{\epsilon_k}{E_k} + \frac{\epsilon_k - E_k}{2E_k} \right), \tag{6.10}$$

where $E_k = \sqrt{\epsilon_k(\epsilon_k + 2\mu)}$.

The total density is thus less than the saddle point A^2, and could be negative. From the form of the fluctuation Hamiltonian, eq. (6.8), using $gA^2 = \mu$, it can be seen that the fluctuation contribution is:

$$\rho_f = -\sum_k \left\{ \left\langle a_k^\dagger a_k \right\rangle + \frac{1}{2}\left(\left\langle a_k^\dagger a_{-k}^\dagger \right\rangle + \left\langle a_k a_{-k} \right\rangle \right) \right\}. \tag{6.11}$$

Using the results:

$$\left\langle a_k^\dagger a_k \right\rangle = n_B(E_k)\frac{\epsilon_k + \mu}{E_k} + \frac{\epsilon_k + \mu - E_k}{2E_k}, \tag{6.12}$$

$$\left\langle a_k^\dagger a_{-k}^\dagger \right\rangle = \left\langle a_k a_{-k} \right\rangle = -\frac{\mu}{E_k}\left(n_B(E_k) + \frac{1}{2} \right), \tag{6.13}$$

it is clear this matches eq.(6.10).

In contrast, taking partial derivatives, and neglecting the second term in eq. (6.2) gives $\rho_f = \sum_k \left\langle a_k^\dagger a_k \right\rangle$. In two dimensions, for $\mu \neq 0$, this expression will be infra-red divergent, while eq. (6.10) is not.

Hugenholtz-Pines relation To identify the meaning of the terms in eq. (6.11), one can consider the Hugenholtz-Pines relation for the normal and anomalous self energies $A(\omega, k)$, $B(\omega, k)$ respectively:

$$A(0,0) - B(0,0) = \mu, \tag{6.14}$$

The approximations in the previous section are equivalent to evaluating A and B at one-loop order. As explained by Popov [7, Chapter 6], this becomes

$$\begin{aligned} \mu &= 2g(\rho_0 + \rho_1) - g(\rho_0 + \tilde{\rho_1}) \\ &- 2g^2\rho_0 \sum_k (\mathcal{G}(k)\mathcal{G}(-k) - \mathcal{G}_1(k)\mathcal{G}_1(-k)). \end{aligned} \tag{6.15}$$

Here ρ_0 is the one-loop calculation of condensate density, ρ_1 the density of non-condensed particles, and $\tilde{\rho}_1$ is an anomalous particle

density, $\tilde{\rho}_1 = \sum_k \mathcal{G}_1(k)$, with $\mathcal{G}_1$ the anomalous Green's function. The last term is a second order correction due to the three boson vertices of the form $gA(a^\dagger a^\dagger a + a^\dagger aa)$. This last term in eq. (6.15) can be evaluated to be $2g\tilde{\rho}_1$, leading to the result

$$\rho_0 = \frac{\mu}{g} - (2\rho_1 + \tilde{\rho}_1), \tag{6.16}$$

showing that $\rho_0 + \rho_1$ is less than the saddle point density.

Compare this expression for the total density to that from saddle point and fluctuations,

$$\rho = \rho_0 + \rho_1 = \rho_{\text{s.p.}} - \frac{\partial F_{\text{fluct}}}{\partial \mu} - \frac{d\psi_0}{d\mu}\frac{\partial F_{\text{fluct}}}{\partial \psi_0}, \tag{6.17}$$

where $\rho_{\text{s.p.}} = \mu/g$ is the saddle point expectation of the density, and F_{fluct} is the free energy from the fluctuation contributions. Since ρ_1, the density of non-condensed particles can be identified as

$$\rho_1 = \sum_k \left\langle a_k^\dagger a_k \right\rangle = -\frac{\partial F_{\text{fluct}}}{\partial \mu}, \tag{6.18}$$

one must identify the depleted condensate density, eq. (6.16) with

$$\rho_0 = \frac{\mu}{g} - \frac{d\psi_0}{d\mu}\frac{\partial F_{\text{fluct}}}{\partial \psi_0}. \tag{6.19}$$

The derivatives w.r.t. the order parameter therefore describe a depletion of the order parameter due to fluctuations. Physically, interactions between the condensate and the finite population of non-condensed particles (at finite temperature) push up the chemical potential. With such a theory, there now exists a region of parameter space where which is not condensed, but $\mu > 0$. In such a region it is essential to include modifications of the particle spectrum due to interactions to describe the normal state.

Comparison of methods The phase boundary for the weakly interacting dilute Bose gas model with static interactions is peculiarly

insensitive to the calculation scheme. This can be seen by considering the Hugenholtz-Pines relation at the transition. In general, the anomalous self energy vanishes at the transition, so $\mu = A(0,0)$. Since $\rho_0 = 0$, the total density is ρ_1, which may be found from the fluctuation Green's function, $\rho = \sum_{\omega,k} \mathcal{G}(\omega, k)$,

$$\mathcal{G}(\omega, k) = \left[i\omega + \epsilon_k - A(0,0) + A(\omega, k) \right]^{-1}, \tag{6.20}$$

where $\mu = A(0,0)$ has been used. If the self energy is static, then $A(\omega, k) = A(0,0)$, and so at the transition the quasi particles are exactly free. Any approximation scheme which gives $B(0,0) = 0$ when $\rho_0 = 0$ will then reproduce this result. For this reason, partial derivatives will give correct calculations of the phase boundary for a dilute Bose gas, but this does not remain true for dynamic self energies.

For a boson-fermion model, such as polaritons, because of the dynamic self energy, total and partial derivatives will give different answers. For the three-dimensional case studied by Ohashi and Griffin, this will lead to critical temperatures differing by a numerical factor, but in two dimensions using partial derivatives gives divergent answers. Were one to use partial derivatives, the density calculated from the condensed and non-condensed phases would agree at the critical chemical potential. However, for the total derivative, the density calculated at the new critical potential need not agree with that calculated from the non-condensed phase. A difference between these results reflects the fact that both are approximations of the phase boundary, and is indicative of the Ginzburg criterion.

6.2 Total density for condensed polaritons

From the effective action, eq. (5.13), the free energy per unit area, including quadratic fluctuations may be written as:

$$\begin{aligned} \frac{F}{A} &= \frac{S[\psi_0]}{A} + \mathrm{Tr} \ln \left(|i\omega + \hbar\omega_k + K_1(\omega)|^2 - |K_2(\omega)|^2 \right) \quad (6.21) \\ &= \left\{ \hbar\tilde{\omega}_k \frac{|\psi_0|^2}{A} - \frac{\mu n}{2} - \frac{n}{\beta} \ln \left[\cosh \left(\beta E \right) \right] \right\} \end{aligned}$$

$$
\begin{aligned}
&+ \quad \left\{ \frac{1}{\beta} \int_0^\infty \frac{d^2k}{(2\pi)^2} \ln\left[1 - e^{-\beta\hbar\tilde{\omega}_k}\right] \right\} \\
&+ \quad \frac{1}{\beta} \int_0^{K_\mathrm{m}} \frac{d^2k}{(2\pi)^2} \ln\left[\frac{\sinh(\beta\xi_1/2)\sinh(\beta\xi_2/2)}{\sinh(\beta E)\sinh(\beta\hbar\tilde{\omega}_k/2)} \right] \\
&+ \quad \frac{1}{\beta} \int_0^{K_\mathrm{m}} \frac{d^2k}{(2\pi)^2} \frac{1}{2} \ln\left[1 - \frac{\alpha 4E^2}{2\left(\hbar\tilde{\omega}_k E^2 - \hbar\tilde{\omega}_0 \tilde{\epsilon}^2\right)} \right]. \qquad (6.22)
\end{aligned}
$$

The trace in the first line represents the sum over Matsubara frequencies and momenta,

$$
\mathrm{Tr} = \int_0^\infty \frac{d^2k}{(2\pi)^2} \frac{1}{\beta} \sum_\omega . \qquad (6.23)
$$

The terms E, α and $\xi_{1,2}$ are defined as in section 5.3. The first term in braces is $S[\psi_0]$, the others together are the fluctuation corrections. As discussed in section 5.1, the interaction has been cut off at a scale K_m, so for $k > K_\mathrm{m}$, the action is that of a free gas of photons, *i.e.* the second term in braces. The final term is due to the δ_ω terms in eq. (5.13), as discussed further in the appendix B.2.

The total density is then given by:

$$
\begin{aligned}
\rho &= \frac{|\psi_0|^2}{A} + \frac{n}{2}\left[1 - \frac{\tilde{\epsilon}}{E}\tanh(\beta E)\right] \\
&+ \int_0^{K_\mathrm{m}} \frac{d^2k}{(2\pi)^2} \left\{ f[\xi_1] + f[\xi_2] - f[2E] + \frac{1}{2} + g(k) \right\} \\
&+ \int_{K_\mathrm{m}}^\infty \frac{d^2k}{(2\pi)^2} n_\mathrm{B}(\hbar\tilde{\omega}_k), \qquad (6.24)
\end{aligned}
$$

where

$$
\begin{aligned}
f[x] &= \left(n_\mathrm{B}(x) + \frac{1}{2}\right)\left(-\frac{dx}{d\mu}\right), \\
g(k) &= -\frac{1}{2\beta}\frac{1}{(1-C)}\frac{dC}{d\mu}, \\
C &= \frac{\beta \mathrm{sech}^2(\beta E) g^2 n}{2\left(\hbar\tilde{\omega}_k E^2 - \hbar\tilde{\omega}_0\tilde{\epsilon}^2\right)} \frac{g^2|\psi_0|^2}{A}.
\end{aligned}
$$

In going from eq. (6.22) to eq. (6.24) the two integrals have been re-arranged, the second now describing only the free, high energy photons. Again, the last term, $g(k)$, arises due to the δ_ω terms.

The derivatives of polariton energies that arise in calculating the density may be given in terms of the expressions $A(k)$, $B(k)$ as defined in eq. (5.21):

$$\begin{aligned}\frac{2\xi_{1,2}}{d\mu} &= \frac{1}{4\xi_{1,2}}\left[\frac{dA(k)}{d\mu} \pm \frac{1}{\sqrt{A(k)^2 - B(k)}}\times\right. \\ &\qquad \left.\times\left(2A(k)\frac{dA(k)}{d\mu} - \frac{dB(k)}{d\mu}\right)\right], \qquad (6.25)\\ \frac{dA(k)}{d\mu} &= 8E\frac{dE}{d\mu} - 2\hbar\omega_k - 4\tilde{\epsilon} - 2\hbar\tilde{\omega}_0, \qquad (6.26)\\ \frac{dB(k)}{d\mu} &= 16\frac{\hbar^2k^2}{2m}\left(2E\frac{dE}{d\mu}\tilde{\omega}_k - E^2 + \tilde{\epsilon}\hbar\tilde{\omega}_0 + \tilde{\epsilon}^2\right). \qquad (6.27)\end{aligned}$$

To find $dE/d\mu$ in the presence of a condensate, one can differentiate the gap equation, eq. (5.7), giving

$$-1 = \frac{dE}{d\mu}\frac{g^2n}{2E^2}\left(\beta E\,\mathrm{sech}^2(\beta E) - \tanh(\beta E)\right). \qquad (6.28)$$

6.3 Two dimensions, superfluid response

Having found an expression for the total density including fluctuations, it is necessary to consider how fluctuations change the critical chemical potential. As discussed in the introduction to this section, in two dimensions this requires consideration of the Kosterlitz-Thouless phase transition. The phase boundary is approximated from the condensed state by the chemical potential at which the superfluid response vanishes. The normal and superfluid responses must therefore be calculated in the presence of a condensate.

Calculating normal response density

Following the discussion in Chapter 2, the normal density, as defined by the response function, is given by equation (2.23). Using the

polariton Green's functions, this expression becomes:

$$\rho_{\rm n} = {\rm Tr}\left(\frac{\hbar^2k^2}{2m}\frac{A(\omega,k)^2+A(\omega,k)^{*2}-2\left|K_2(\omega)\right|^2}{\left(\left|A(\omega,k)\right|^2-\left|K_2(\omega)\right|^2\right)^2}\right) \quad (6.29)$$

where

$$A(\omega,k) = i\omega + \hbar\tilde{\omega}_k + K_1(\omega) \quad (6.30)$$

and Tr again signifies the sum over momenta and frequencies, as in eq. (6.23). Writing the terms K_1, K_2 explicitly, this can be simplified to reveal its pole structure, as:

$$\rho_n = {\rm Tr}\left(\frac{\hbar^2k^2}{2m}\left\{\frac{\left[2\tilde{\omega}_0(i\tilde{\epsilon}\omega - E^2 - \tilde{\epsilon}^2) + (i\omega+\tilde{\omega}_k)(\omega^2+4E^2)\right]^2}{(\omega^2+\xi_1^2)^2(\omega^2+\xi_2^2)^2}\right.\right.$$
$$\left.\left. - \frac{\left[2\tilde{\omega}_0(E^2-\tilde{\epsilon}^2)\right]^2}{(\omega^2+\xi_1^2)^2(\omega^2+\xi_2^2)^2} + {\rm C}_0(k)\right\}\right). \quad (6.31)$$

Again, in evaluating the Matsubara sum, one must consider the δ_ω terms. The term ${\rm C}_0(k)$ is the difference between the true term at $\omega = 0$, and the analytic continuation appearing in the Matsubara sum in eq. (6.31), and is given by:

$${\rm C}_0(k) = 2\alpha \times \left[\left(\frac{\hbar^2k^2}{2m}\right)\left(\frac{\hbar^2k^2}{2m} + \frac{g^2|\psi_0|^2}{A}\frac{\hbar\tilde{\omega}_0}{E^2}\right)\right.$$
$$\left. \times \left(\frac{\hbar^2k^2}{2m} + \frac{g^2|\psi_0|^2}{A}\frac{\hbar\tilde{\omega}_0}{E^2} - 2\alpha\right)\right]^{-1}, \quad (6.32)$$

with α as defined in eq. (5.18).

Total photon density

For the polariton system there is an added complication. Equation (6.31) gives the density of normal photons, but equation (6.24) is the total excitation density (including excitons). It is therefore necessary to calculate the total photon density.

This can be done by considering separate chemical potentials for photons and excitons, which are set equal at the end of the calculation. This means making the change,

$$\mu N \to \mu_{\text{ex.}} \sum_{j=1}^{j=nA} \left(S_j^z + \frac{1}{2} \right) + \mu_{\text{phot.}} \sum_k \psi_k^\dagger \psi_k, \tag{6.33}$$

in the action. The photon density is then total derivative w.r.t. the photon chemical potential, $\mu_{\text{phot.}}$.

This density is given by equation (6.24) with two changes. Firstly, the mean-field exciton density,

$$\frac{n}{2} \left[1 - \frac{\tilde{\epsilon}}{E} \tanh(\beta E) \right], \tag{6.34}$$

should be removed. Secondly, in $f[x]$,$g(k)$ derivatives should be taken w.r.t $\mu_{\text{phot.}}$. This means replacing equations (6.26) and (6.27) by:

$$\frac{dA(k)}{d\mu_{\text{phot.}}} = 8E\frac{dE}{d\mu} - 2\hbar\omega_k - 4\tilde{\epsilon}, \tag{6.35}$$

$$\frac{dB(k)}{d\mu_{\text{phot.}}} = 16\frac{\hbar^2 k^2}{2m} \left(2E\frac{dE}{d\mu}\tilde{\omega}_k - E^2 + \tilde{\epsilon}^2 \right). \tag{6.36}$$

This makes use of the fact that $dE/d\mu_{\text{phot.}} = dE/d\mu$, as can be seen from the gap equation.

6.4 Phase boundary including fluctuations

Combining the results of this chapter so far, the phase boundary is found by plotting the total density (eq. (6.24)) at the value of chemical potential where the normal photon density (eq. (6.31)) matches the total photon density (discussed in section 6.3). The phase boundaries found in this way are plotted in figure 6.1 and figure 6.3. The form of the phase boundary can be explained by considering how, at finite temperatures, the occupation of excited states of the system depletes the condensate. Which excited states are relevant changes with density.

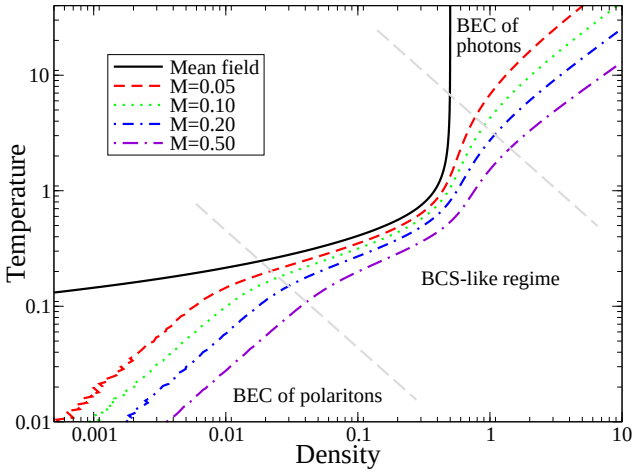

Figure 6.1: Mean-field phase boundary, and phase boundaries including fluctuation correction for four values of photon mass, on a logarithmic scale. Plotted for the resonant case, $\Delta = 0$. Temperature plotted in units of $g\sqrt{n}$ and density in units of n.

Resonant case

When condensed, the lowest energy mode is the phase mode, described by eq. (5.26). At low density, this has a shallow slope, and consequently a large density of states. Such excitations are described in a model of point bosons. The phase boundary can therefore be estimated from the degeneracy temperature of a gas of polaritons, of mass $2m$, where m is the bare photon mass:

$$T_{deg} = \frac{2\pi\hbar^2}{2(2m)}\rho = g\sqrt{n}\frac{\pi}{2m^*}\frac{\rho}{n}. \tag{6.37}$$

As the density increases, the phase mode becomes steeper, and so has a smaller density of states. The relevant excitations are then single particle excitations across the gap. Such excitations are accounted for in the mean-field theory. Combining equations (5.7) and

(5.8) gives the mean field result:

$$T_c = g\sqrt{n}\frac{\sqrt{1-2\rho/n}}{2\tanh^{-1}(1-2\rho/n)} \approx \frac{g\sqrt{n}}{-\ln(\rho/n)}. \tag{6.38}$$

As seen in figure 6.1, the mean-field boundary is effectively constant on the scale of the boundary for BEC of point bosons, and so the crossover to mean-field always occurs near $T \approx g\sqrt{n}$, the Rabi splitting. The density at which this crossover occurs depends on the photon mass. Comparing equations (6.37) and (6.38), this crossover occurs at a density $\rho_{\text{crossover}} \approx nm^*$.

In terms of the measurable Rabi splitting, $g\sqrt{n}$ and polariton mass m, this gives the density:

$$\rho_{\text{crossover}} = \frac{mg\sqrt{n}}{\hbar^2} \tag{6.39}$$

For the structures studied by Yamamoto *et al.* [82, 83, 84], $g\sqrt{n} \approx$ 7meV and $m \approx 10^{-5}m_{\text{electron}}$. These values give a crossover density of $\rho_{\text{crossover}} = 2.6 \times 10^8\text{cm}^{-2}$. This is both much less than the estimates of experimentally achieved density, $n \sim 10^{11}\text{cm}^{-2}$ per pulse, and also much less than the Mott density in this structure, $n_{\text{Mott}} \approx 3.6 \times 10^{13}\text{cm}^{-2}$. For the structures studied by Dang *et al.* [81, 85] $g\sqrt{n} \approx 13$meV, and $m \approx 3 \times 10^{-5}m_{\text{electron}}$, so crossover densities are again of the same order, $\rho_{\text{crossover}} = 5 \times 10^8\text{cm}^{-2}$. Dang *et al.* also presents results for the detuned case [85], discussed below, with a range dimensionless detunings $0.5 > \Delta^* > -0.7$.

Equation (6.39) describes the crossover in terms of properties measurable for a given microcavity. However, to understand what fundamental lengthscales control this crossover density, it is necessary to write the coupling strength and polariton mass in terms of the dimensions of the cavity and properties of the excitons. Using the expressions in section 5.1 for photon mass and coupling strength g, this gives the crossover density as:

$$\rho_{\text{crossover}} = 4\pi^2\sqrt{\frac{e^2}{4\pi\varepsilon_0\hbar c}}\frac{1}{\varepsilon_r^{1/4}}\frac{d_{ab}\sqrt{n}}{w^2}. \tag{6.40}$$

The crossover density is therefore controlled by two parameters: the width of the cavity, w, and the ratio of electron-hole separation to average two-level system separation, $d_{ab}\sqrt{n} = d_{ab}/r_{\text{separation}}$. If the average two-level system separation ($r_{\text{separation}}$) is less than the electron-hole separation (d_{ab}), then the model of localised two-level systems will break down. Therefore, within this extended Dicke model the largest possible crossover density scale is $1/w^2$. This lengthscale occurs because the cavity size controls the wavelength of the lowest radiation mode. Crossover to a BCS-like mean-field regime occurs when the density approaches a scale set by the wavelength of light, rather than one set by the exciton Bohr radius. Therefore, in general this crossover density is much less than the Mott density.

At yet higher densities, the single particle excitations are saturated, and so the condensate becomes photon dominated. In this regime, the transition temperature is that for a gas of massive photons. If the photon mass is large ($m^* > 1$), a mean-field regime never exists, instead the phase boundary changes directly from polariton condensation to a photon condensation. However, since for experimental parameters the dimensionless mass is only of the order of 10^{-3}, a mean-field regime will exist. These various crossovers are illustrated schematically in figure 6.2.

Effects of detuning

If the excitons are detuned below the photon (positive detuning), it becomes possible for the system to reach half filling while remaining uncondensed. For positive detunings greater than $2g\sqrt{n}$ the mean-field phase boundary becomes re-entrant, as shown in panel B of figure 6.3. For smaller but still positive detunings, the mean-field boundary has a maximum critical density at a finite temperature, but no maximum of critical temperature. The opposite case, of excitons detuned above photons, shows no interesting features; the system will always condense before half filling.

This multi-valued phase boundary is discussed in ref. [31], and can be explained in terms of phase locking of precessing spins [122],

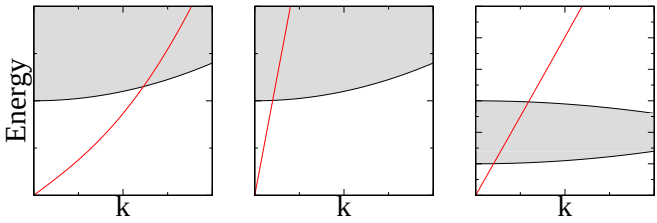

Figure 6.2: A schematic picture of how the relevant excitations change between the polariton BEC, the BCS-like mean-field and the photon BEC regimes. In the low density limit, a shallow sound mode exists. At higher densities, this becomes steeper, and the relevant excitations are gapped single particle excitations. At yet higher densities, these modes are saturated, and the high k photon modes become relevant.

either about spin down (low density) or spin up (high density) states. Above inversion, increasing the density reduces the extent to which a spin may precess. For very large detunings, at low temperatures, the phase diagram therefore becomes symmetric about half filling.

When $\Delta \geq 2g\sqrt{n}$, the re-entrance leads to a point at zero temperature where two second order phase boundaries meet. Including fluctuations, as shown in the panel B of figure 6.3, these phase boundaries no longer meet, but instead there is a region where two different condensed solutions coexist. In this region, there are two minima of the free energy, and so a first-order phase boundary between them can be expected. Although this boundary could be calculated by comparing the free energies including fluctuations, its form may be altered significantly by higher order corrections.

In the mean-field theory, at zero temperature, the chemical potential jumps discontinuously at the point where the two branches of the phase boundary meet. This can be understood by the chemical potential locking to the lower polariton for the lower density transitions, and to the upper polariton at higher densities. This can be seen in the panel B of figure 6.4, which plots the value of the

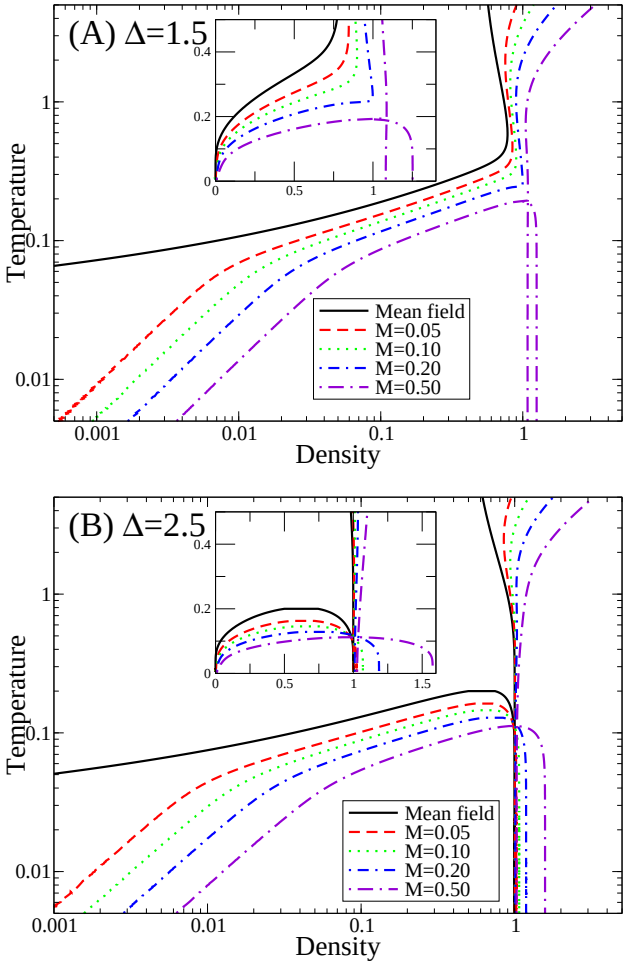

Figure 6.3: Phase boundary with exciton detuned below the photon by $\Delta = 1.5g\sqrt{n}$ and $\Delta = 2.5g\sqrt{n}$ respectively. Main graph are on a logarithmic scale, insets are on a linear scale. Plotted with the exciton detuned below the photon band by $\Delta = 1.5g\sqrt{n}$ (panel A) and $\Delta = 2.5g\sqrt{n}$ (panel B). Temperature plotted in units of $g\sqrt{n}$ and density in units of n.

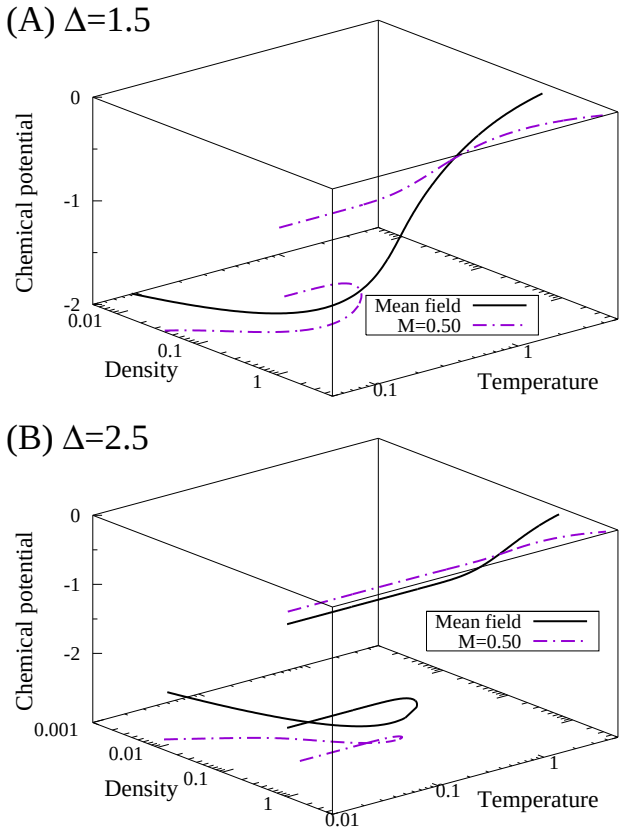

Figure 6.4: Chemical potential vs density and temperature at the phase boundary, for the mean-field phase boundary, and $m^* = 0.50$ fluctuation corrections. Plotted for detunings of $\Delta = 1.5g\sqrt{n}$ and $\Delta = 2.5g\sqrt{n}$, with all other parameters as in figure 6.1. Temperature and chemical potential plotted in units of $g\sqrt{n}$, and density in units of n.

chemical potential at the phase boundary. Including fluctuations, the jump in chemical potential has a similar form, and is somewhat larger. In the region of coexistence discussed above, the two minima of free energy have different chemical potentials, so at the first-order transition, the chemical potential will jump.

At smaller detunings, as shown in panel A of figure 6.3, although the mean-field phase boundary is single valued, adding fluctuations can reproduce the same coexistence regions. For this to occur, the photon mass must be large — *i.e.* there must be a significant density of states for fluctuations. As shown in panel A of figure 6.4, this coexistence is also characterised by two minima of the free energy, with different chemical potentials, and so is also expected to become a first-order transition in the same manner.

To explain how fluctuations lead to the introduction of multiple phase boundaries at a single temperature, it is necessary to consider the upper branch of excitations, $\xi_2(k)$. With positive detuning, the energy of this mode (w.r.t. chemical potential) can continue to fall as the chemical potential increases in the condensed state. This has two effects, it makes the sound velocity larger (as can be seen from eq. (5.26)), and increases the population of this "pair-breaking" upper mode. The combination of these effects is responsible for the creation of the coexistence region by fluctuations.

Effects of inhomogeneous broadening

It is interesting to consider how a small inhomogeneous broadening will modify the phase boundary. Exact calculations with a continuum of exciton energies are technically challenging and not particularly illuminating, so the following presents a discussion of the main effects expected. The following discussion is for a Gaussian distribution of energies, centred at the bottom of the photon band, with a standard deviation much less than $g\sqrt{n}$.

The most significant change to the boundary is due to the existence of a low energy tail of excitons. This means that, even at low densities, the chemical potential lies within the exciton band, and a

BCS-like form of T_c will be recovered. Consider the density of states,

$$\nu_s(\epsilon) = \frac{\exp\left(-\epsilon^2/2\sigma^2\right)}{\sqrt{2\pi}\sigma}. \tag{6.41}$$

For large negative chemical potentials, at low temperatures and densities, the saddle point equation (5.7) becomes

$$\begin{aligned} \frac{\hbar\omega_0}{g^2} = \frac{1}{g_{\text{eff}}} &= \int_{-\infty}^{\infty} \frac{\tanh(\beta\tilde{\epsilon})}{2\tilde{\epsilon}} \nu_s(\epsilon) d\epsilon, \\ &\approx \nu_s\left(\frac{\mu}{2}\right)\left[1 + \ln\left(\frac{\Lambda}{T}\right)\right], \end{aligned} \tag{6.42}$$

and the mean-field density (5.8), using the asymptotic form of the error function, is

$$\rho_{\text{M.F.}} = \nu_s\left(\frac{\mu}{2}\right)\left(\frac{\sigma^2}{-\mu}\right). \tag{6.43}$$

The cutoff, Λ is approximately $2\sigma^2/\mu$, but appears only as a pre-exponential factor, and so the density dependence it gives to T_c will be neglected. Thus, the mean-field transition temperature at low densities then becomes

$$T_c = \Lambda \exp\left(-\frac{2\sigma^2}{g^2\rho}\right). \tag{6.44}$$

For low densities, this result is very different to the mean-field theory without broadening, eq. (6.38). Whereas before the mean-field boundary was approximately constant, it now drops rapidly to zero. If one now considers how fluctuations will modify this boundary, it is more helpful to consider the density as a function of temperature. At low temperatures, fluctuations increase the density by a small amount, $\Delta\rho \propto T$. Without broadening, the mean-field critical density is approximately $\rho \approx ne^{-g\sqrt{n}/T}$ and goes to 0 faster than the fluctuation corrections, $\Delta\rho$. Therefore, as shown in figure 6.1, at low temperatures the fluctuation contribution controls the phase boundary. With broadening the mean-field critical density at low temperature is approximately $\rho \approx 2\sigma^2/g^2 \ln(\Lambda/T)$, which goes to

zero more slowly than $\Delta\rho$. Therefore, including fluctuations in this regime does not change the form of the phase boundary drastically. Hence at very low densities, the boundary is again well described by a mean-field theory.

Relation to alternate models and experimental systems

The model studied here describes two-level systems with a finite total density of states — the density of states, per unit area, integrated over all energies, is finite. As will be explained below, this finite total density of states is responsible for the re-entrant behaviour seen in the mean-field theory for detunings $\Delta \geq 2g\sqrt{n}$. In the preceding sections, the finite total density of states has also been implicated in explaining the existence of a photon dominated region at high temperature, and the multi-valued phase boundary in the presence of fluctuations. This section discusses how these effects may change in alternate models which do not have saturable two-level systems. Although the multi-valued phase boundary is expected only to occur for a finite band of two-level systems, the existence of a photon dominated regime at high densities is more general.

Before discussing the more involved question of how changing the density of states affects fluctuations, its effect on the mean-field theory [31, 109, 123] is summarised. Consider the highest possible density achievable in the normal state. Since there exists a bosonic mode, the chemical potential cannot exceed the energy of this mode if the system is to remain normal. Therefore at zero temperature, only exciton modes below the boson mode are relevant. Regardless of whether the total density of states is finite, the density of states below the bosonic mode will be finite. However, at non-zero temperatures, exciton modes above the chemical potential can be occupied by the tail of the Fermi distribution. If there is a finite total density of states, there will be a maximum density of excitons that can be occupied thermally. This is what is referred to as "saturation" below. Note that for an exciton band centred at the bottom of the photon band, this maximum density of excitons is half the density of two-level systems — the system saturates at half filling. If the total

density of states is not finite, it is possible to support any total density in the normal state by making the temperature high enough.

This saturation is responsible for the multi-valued phase boundary in the mean-field theory. If the density is close to total inversion of the two-level systems, all two-level systems must be in the up state. This makes it hard for them to produce a macroscopic polarisation — viewed as spins, this is to say that if $S_z \approx +1/2$, then S_x will be small. Hence, the system becomes uncondensed near total inversion. If the excitation density is greater than the density of two-level systems, the mean-field theory requires a coherent photon density. Hence, the system condenses again, giving a re-entrant boundary. Without saturable excitons, neither the uncondensing due to reduction of mean-field polarisation, or the re-condensation due to exciton saturation will occur. With fluctuations, the multi-valued phase boundary is analogous to the mean-field re-entrance, and appears to require saturable excitations in the same manner. Therefore, such multi-valued phase boundaries are not expected in a general model with a continuum of exciton states.

Let us now consider the case where there is a finite density of exciton states, separated by the exciton binding energy from a continuum of electron-hole states. In such a case, if the continuum is well separated from bound states, it may only affect the phase boundary at densities larger than those where the features discussed above occur. Well separated here means that the exciton binding energy is much larger than the energy scales in the model, in particular, much larger than $g\sqrt{n}$. If the continuum only has effects at very high densities, the exotic multi-valued phase boundary described in previous sections will be realisable. For the systems studied by Yamamoto *et al.* [83], $g\sqrt{n} \approx 7$meV, and the exciton binding energy $Ryd^* \approx 10$meV. For Dang *et al.* [81], $g\sqrt{n} \approx 13$meV, and $Ryd^* \approx 25$meV. In neither case can the effects of the continuum be avoided. Reducing the Rabi splitting, $g\sqrt{n}$, might allow the multi-valued phase boundary to be observed. However, reducing the Rabi splitting will decrease the transition temperature in the region of interest. In addition, to have strong coupling, the Rabi splitting must remain larger than the polariton linewidth due to photon lifetimes.

The existence of a photon dominated region at high densities is however generic, and does not rely on a model with a finite total density of states. In an electron-hole plasma model [119, 124], such a regime is also predicted. At large densities, as the chemical potential (lying within the exciton band) approaches the bottom of the photon band, the photon density increases much faster than the exciton density. The result in ref. [119] only describes a photon dominated regime at zero temperature. For the two-level system model, at high densities, the system remains photon dominated, and with increasing temperature changes from coherent to incoherent photons. Such a change from coherent to incoherent photons is also expected to occur in the electron-hole model, due to the large occupation of bosonic modes near the chemical potential, but further work is required here.

This discussion of how the extended Dicke model relates to experimental systems has so far concentrated on what happens at high densities. At lower densities (including the densities of current experiments), no such significant differences are expected. This is because, at low densities, higher energy exciton modes would not be occupied, even if they exist. In particular, the angular distribution of radiation (figure 5.4) and excitation spectrum (figures 5.1 and 5.2) should remain unchanged for generic models. Such signatures should therefore be expected for equilibrium condensation in the systems currently studied.

The signatures of condensation presented in this paper are calculated for a system in thermal equilibrium, while current experiments are pumped. For non-resonantly pumped experiments [81, 82, 83, 84, 85], one must consider how pumping will modify the excitation spectrum and the occupation of modes. This can be described by coupling the system to baths describing pumping of excitons and decay of photons. For systems near equilibrium, with small coupling to baths, one expects the excitation spectrum to remain close to the equilibrium case, but with non-thermal occupations. Even with non-thermal occupation, the large density of states for excitations near the chemical potential can be expected to produce a peak in the angular distribution of radiation. For strong coupling to baths, the spectrum of excitations will also change. One particularly significant

change is the possibility of giving a finite lifetime to the Goldstone mode. In this strongly pumped region, the signatures predicted in this paper can be expected to change significantly.

It is also of interest to discuss how these signatures are related to the behaviour seen in resonantly pumped cavities [88, 89, 90]. In these experiments pumping at a critical angle excites polaritons at momentum k_p, causing emission from signal, $k = 0$, and idler, $k = 2k_p$, modes. Such a system may be described as an optical parametric oscillator. Above a threshold, the luminescence from the signal increases superlinearly, and the signal linewidth narrows dramatically. In such a system, the occupation of the signal mode obeys a self-consistency condition, and the relative phase between the pump and signal mode is free. However, the nature of this self-consistency differs from that for an equilibrium condensate, and thus the signatures of equilibrium condensation are no longer immediately applicable.

The form of the condensed luminescence spectrum, and the angular distribution of polaritons depend on the existence of the low energy Goldstone mode. The energy of this mode vanishes as $k \to 0$ as a consequence of the gap equation, eq. (5.7), which means that global phase rotations cost no energy. In a laser, the coherent field is also set by a self-consistency condition, balancing pumping and decay. Like condensation, the laser transition can also be described as symmetry breaking [125]. However, because the self-consistency relates imaginary parts of the self energy, the dynamics of modes near the lasing mode is diffusive. Therefore a free global phase and a self-consistency condition are not sufficient for the signatures described in this paper.

For the optical parametric oscillator experiments, the condition of self-consistency is complicated by the existence of a coherent idler field [126, 127]. Since such experiments are strongly pumped it is expected that, despite the free phase and self-consistency, the luminescence spectrum and angular distribution of radiation as described in this paper will not be applicable. The laser and the equilibrium condensate are extreme cases, and the distinction in practice is less clear [89, 122]. For example, adding decoherence [40, 128] to an equi-

librium condensate causes a crossover to a regime better described as a laser.

Chapter 7

Hepp and Lieb transition and the no-go theorem

As was first shown by Hepp and Lieb[16, 17], and later reformulated in terms of Glauber's coherent states by Wang and Hioe[129], the Dicke model undergoes a phase transition to a condensed state at low temperatures. It was shown by Rzążewski *et al.*[114, 130, 131] that in its original context, the Hepp and Lieb transition is an artefact of the model.

As discussed earlier, in section 5.1, this chapter does not affect the results of the extended Dicke model studied in the rest of this dissertation. Because the Dicke model is exactly solvable in the limit that the number of two-level systems, $N \to \infty$, analogues of the Hepp and Lieb transition have been considered in a variety of other systems[31, 132, 133, 134]. Therefore, this chapter is of wider interest, and also partially addresses how including direct interactions between excitons may modify the extended Dicke model studied in the rest of this dissertation.

Considered as an approximation of light-matter interaction in the Coulomb gauge, the Dicke model neglects A^2 terms in the light-matter coupling. These A^2 terms prevent the phase transition. In this chapter, it is shown that adding direct Coulomb interactions

between electric dipoles leads to a phase transition, which, in the electric dipole gauge is the Hepp and Lieb transition. However, due to the gauge dependent meaning of the bosonic mode in the Dicke model, this transition does not lead to a macroscopic electric field.

Similar results, *i.e.* the phase transition due to the Coulomb interaction of electric dipoles in an extended Dicke model, were derived by Emeljanov and Klimontovich [135], prior to the work of Rzążewski *et al.* They did not however consider how this transition can be undertsood as the Hepp and Lieb transition when the model is written in the electric dipole gauge.

7.1 Introduction

The Dicke model describes a collection of two-level systems (TLS) coupled via a single bosonic mode. Writing a TLS as a spin, magnitude $|S| = 1/2$ the Dicke model is:

$$H = \epsilon \sum_j S_j^z + \hbar\omega_0 \psi^\dagger \psi + \frac{g}{\sqrt{V}} \sum_j i(S_j^+ - S_j^-)(\psi + \psi^\dagger). \qquad (7.1)$$

If understood as an approximation of the light-matter Hamiltonian written in the Coulomb gauge, the Dicke Hamiltonian includes the coupling $\mathbf{A} \cdot \mathbf{p}$, but neglects the A^2 terms. As first stated by Rzążewski *et al.*[114, 130], including such terms prevents the Hepp and Lieb phase transition. The A^2 terms increase the energy required to occupy the bosonic mode. The Hepp and Lieb transition requires a sufficiently strong coupling of light and matter, which requires a large density of TLS. However, at high densities, the effect of the A^2 term also becomes large, and prevent the phase transition.

Whether a phase transition occurs is gauge independent. However, if the Dicke model is instead understood to result from the light-matter Hamiltonian written in the electric dipole gauge, no A^2 terms were neglected. This would suggest that the Hepp and Lieb transition can describe a physical phase transition. The resolution of this apparent paradox lies in the Coulomb interactions between

separated TLS. These terms cause a transition to a state with macroscopic polarisation in the Coulomb gauge, which in the electric dipole gauge is exactly the transition of Hepp and Lieb.

The bosonic field, ψ, appearing in a Dicke-like model has different interpretations in different gauges. In the Coulomb gauge it corresponds to the transverse electric field. In the electric dipole gauge it is the electric displacement. Whether ψ acquires a macroscopic expectation depends on the gauge; $\psi = 0$ in the Coulomb gauge, but is non-zero in the electric dipole gauge. There is thus no spontaneous transverse electric field, so this transition is thus not in contradiction with other no-go theorems[131, 136].

7.2 The Coulomb gauge with dipole-dipole interactions

The full Hamiltonian, truncation of sums

Consider the Hamiltonian written in the Coulomb gauge, with quantised radiation modes. The operator $\psi_j^\dagger$ creates a photon of wavevector $\mathbf{k}_j$, and polarisation $\hat{\mathbf{e}}_j$. Writing $\mathbf{d}_i = \mathbf{r}_{e,i} - \mathbf{r}_{h,i}$ for the electron-hole separation, and $\mathbf{R}_i$ for the location of site i, this gives:

$$\begin{aligned} H &= \sum_i H_0(i) + \sum_j \hbar\omega_{k_j}\psi_j^\dagger\psi_j \\ &+ \sum_i \left\{ -i\frac{e}{\hbar}\left[H_0(i), \mathbf{d}_i\right] \cdot \right. \\ &\qquad \left. \cdot \sum_j \sqrt{\frac{\hbar}{2\omega_{k_j}\varepsilon_0 V}}\hat{\mathbf{e}}_j \left(\psi_j e^{i\mathbf{k}_j\cdot\mathbf{R}_i} + \psi_j^\dagger e^{-i\mathbf{k}_j\cdot\mathbf{R}_i}\right)\right\} \\ &+ \frac{e^2\hbar}{4m_r\varepsilon_0 V}\sum_i \left\{ \sum_j \left(\frac{\psi_j e^{i\mathbf{k}_j\cdot\mathbf{R}_i} + \psi_j^\dagger e^{-i\mathbf{k}_j\cdot\mathbf{R}_i}}{\sqrt{\omega_{k_j}}} \right) \right\}^2 \\ &- \frac{e^2}{2\varepsilon_0}\sum_{i\neq j} (\mathbf{d}_i)_\alpha \delta^{\parallel}_{\alpha\beta}(\mathbf{R}_i - \mathbf{R}_j)(\mathbf{d}_j)_\beta \end{aligned} \tag{7.2}$$

In this expression, both the coupling to transverse radiation, and the direct Coulomb term (the last term) have been written in the dipole approximation (*i.e.* assuming $d_i \ll |\mathbf{R}_i - \mathbf{R}_j|$). The coupling to transverse radiation, $\mathbf{A}\cdot\mathbf{p}$ has been rewritten using $\mathbf{p}_i = m\dot{\mathbf{r}}_i = im[H_0, \mathbf{r}_i]/\hbar$. H_0 is the bare Hamiltonian for a single TLS, V the quantisation volume, and m_r the reduced mass. $(\mathbf{d}_i)_\alpha$ is the α component of the displacement $\mathbf{d}_i$. The longitudinal delta function in the last term is given by:

$$\begin{aligned}
\delta^{\parallel}_{\alpha\beta}(\mathbf{r}) &= \frac{1}{4\pi r^3}\left(\frac{3r_\alpha r_\beta}{r^2} - \delta_{\alpha\beta}\right) = \frac{\partial^2}{\partial r_\alpha \partial r_\beta}\int \frac{d^3k}{(2\pi)^3}\frac{e^{i\mathbf{k}\cdot\mathbf{r}}}{k^2} \\
&= \frac{1}{V}\sum_k \left[\left(\delta_{\alpha\beta} - \frac{k_\alpha k_\beta}{k^2}\right) - \delta_{\alpha\beta}\right] e^{i\mathbf{k}\cdot\mathbf{r}} \qquad (7.3) \\
&= \left[\frac{1}{V}\sum_j (\hat{\mathbf{e}}_j)_\alpha (\hat{\mathbf{e}}_j)_\beta e^{i\mathbf{k}_j\cdot\mathbf{r}}\right] - \delta_{\alpha\beta}\delta(\mathbf{r}), \qquad (7.4)
\end{aligned}$$

where the last form, eq. (7.4), makes use of the polarisation $\hat{\mathbf{e}}_j$ of the radiation mode with wavevector $\mathbf{k}_j$. The term $\delta(\mathbf{r})$ should not contribute when considering the interaction between dipoles at different sites.

As discussed in section II.C.5 of ref. [137], in the Coulomb gauge there is a non-retarded Coulomb potential between different TLS. This is not physical; when combined with the photon mediated interaction only retarded interactions survive. In order for this to hold, any truncation of the sum over photon modes must apply also to the Coulomb term, via truncation in eq. (7.4).

Projection onto a generalised Dicke model

Performing a truncation to include only the lowest radiation mode, and projecting the matter part into a two-level basis leads to a variant of the Dicke Model:

$$H = \epsilon\sum_i S_i^z + \hbar\omega_0\psi^\dagger\psi + \frac{g}{\sqrt{V}}\sum_i i(S_i^+ - S_i^-)(\psi + \psi^\dagger)$$

$$+ \quad \kappa(\psi+\psi^\dagger)^2 - \eta\sum_{i\neq j}(S_i^+ + S_i^-)(S_j^+ + S_j^-), \tag{7.5}$$

with the parameters,

$$g = \frac{2\epsilon e d_{ab}}{\sqrt{2\hbar\omega_0\varepsilon_0}}, \quad \kappa = \frac{N}{V}\frac{e^2\hbar}{4m_r\varepsilon_0\omega_0}, \quad \eta = \frac{e^2 d_{ab}^2}{2\varepsilon_0 V}. \tag{7.6}$$

Note in eq. (7.5) that the $\mathbf{A}\cdot\mathbf{p}$ term depends on S_j^y, while the dipole-dipole interaction depends on S_j^x. Recalling $\mathbf{p}_i = im[H_0, \mathbf{r}_i]/\hbar$ explains the different spin dependence of these terms.

To look for a phase transition, it is helpful to consider the partition function, written as a coherent state path integral. Introducing a real scalar field ϕ to decouple the dipole interactions, and writing $\psi = \psi' + i\psi''$, gives:

$$\begin{aligned}\mathcal{Z} &= \int d\psi' \int d\psi'' \int d\phi e^{-\beta\left(\hbar\omega_0|\psi|^2 + 4\kappa\psi'^2\right)} \\ &\times \prod_{i=1}^{N}\left(\sum_{\mathbf{S}_i} e^{-\beta\left(\phi S_i^x + 2g\psi' S_i^y/\sqrt{V} + \epsilon S_i^z\right)}\right).\end{aligned} \tag{7.7}$$

Integrating over the TLS gives an effective action

$$\begin{aligned}S_{\text{eff}} &= \hbar\omega_0|\psi|^2 + 4\kappa\psi'^2 + \frac{\phi^2}{4\eta} - \frac{N}{\beta}\ln\left[\cosh\left(\beta E\right)\right], \\ E^2 &= \epsilon^2 + \frac{4g^2\psi'^2}{V} + \phi^2.\end{aligned} \tag{7.8}$$

It can immediately be seen that to minimise this action, $\psi'' = 0$. Minimising w.r.t. ψ', the result of Rzążewski *et al.* still holds, a solution with $\psi' \neq 0$ is possible only if

$$\epsilon\frac{(\hbar\omega_0 + 4\kappa)}{2g^2 N/V} < 1. \tag{7.9}$$

Both κ and the denominator scale linearly with density, and so as $N/V \to \infty$, the ω_0 term may be neglected. However the Thomas-Reiche-Kuhn sum rule (see *e.g.* [138]) implies $2\kappa\epsilon \geq g^2 N/V$, so

eq. (7.9) is never satisfied. For a solution $\phi \neq 0$ to exist requires instead,

$$\epsilon < 2\eta N = \frac{e^2 d_{ab}^2}{\varepsilon_0} \frac{N}{V}. \tag{7.10}$$

A phase transition thus occurs at large densities.

7.3 The electric dipole gauge

This analysis may all be repeated in the electric dipole gauge, by making a unitary transform:

$$\begin{aligned} U &= \exp\left(\sum_j \lambda_j^* \psi_j - \lambda_j \psi_j^\dagger\right) \\ \lambda_j &= \frac{ie}{\sqrt{2\varepsilon_0 \hbar \omega_{k_j} V}} \sum_i \hat{\mathbf{e}}_j \cdot \mathbf{d}_i e^{i\mathbf{k}_j \cdot \mathbf{R}_i} \end{aligned} \tag{7.11}$$

This is a transformation of the full Hamiltonian, eq. (7.2), not the Hamiltonian in the TLS representation. This is important, since the bare TLS Hamiltonian, $H_0(i)$, differs between gauges, so the operations of gauge transformation and projecting onto a two-level basis do not commute. As shown in ref. [137] (Complements $\mathrm{A_{IV}}$ and $\mathrm{C_{IV}}$), such a transformation changes the interaction from $(\mathbf{p} - e\mathbf{A})^2$ to $\mathbf{D} \cdot \mathbf{r}$.

The Coulomb term between different sites also vanishes due to the action of the transform (7.11) on the radiation Hamiltonian:

$$\sum_j \hbar \omega_{k_j} \psi_j^\dagger \psi_j \to \sum_j \hbar \omega_{k_j} \left(\psi_j^\dagger + \lambda_j^*\right)\left(\psi_j + \lambda_j\right). \tag{7.12}$$

From the form of $\delta_{\alpha\beta}^{\parallel}(\mathbf{r})$ in eq. (7.4), it is apparent that $\hbar\omega_{k_j}|\lambda_j|^2$ cancels the direct Coulomb term in eq. (7.2). This cancellation requires that the momentum cutoff agrees between the sums for the radiation modes in eq. (7.2), the delta function (7.3), and in the transformation (7.11). Thus, in the electric dipole gauge eq. (7.2)

becomes:

$$H = \sum_i H_0'(i) + \sum_j \hbar\omega_{k_j}\psi_j^\dagger\psi_j + \sum_i e\mathbf{d}_i\cdot\mathbf{D}_i \qquad (7.13)$$

$$\mathbf{D}_i = \sum_j i\sqrt{\frac{\hbar\omega_{k_j}}{2\varepsilon_0 V}}\hat{\mathbf{e}}_j\left(\psi_j e^{i\mathbf{k}_j\cdot\mathbf{R}_i} - \psi_j^\dagger e^{-i\mathbf{k}_j\cdot\mathbf{R}_i}\right) \qquad (7.14)$$

Note that if, in the Coulomb gauge, dipole interactions had been ignored, there would now be a non-physical interaction in the electric dipole gauge. This non-physical interaction would have the opposite sign to the physical interaction that should exist in the Coulomb gauge. Therefore, such a non-physical interaction can prevent the transition. This latter point was noted by Bialynicki-Birula and Rzążewski [139]. Such a non-physical interaction in the dipole gauge is a result of neglecting the physical interaction in the Coulomb gauge.

Projected onto TLS, this yields the Dicke model:

$$H = \epsilon\sum_i S_i^z + \hbar\omega_0\psi^\dagger\psi + \frac{g'}{\sqrt{V}}\sum_i i(S_i^+ + S_i^-)(\psi - \psi^\dagger) \qquad (7.15)$$

where $g' = (\hbar\omega_0/2\epsilon)g$. Integrating over the TLS in the same way as before gives an effective action:

$$S_{\text{eff}} = \hbar\omega_0|\psi|^2 - \frac{N}{\beta}\ln\left[\cosh\left(\beta E\right)\right],$$
$$E^2 = \epsilon^2 + \frac{4g^2\psi'^2}{V}\left(\frac{\hbar\omega_0}{2\epsilon}\right)^2. \qquad (7.16)$$

Repeating the previous analysis, a phase transition to a state $\psi \neq 0$ occurs under the condition given in eq. (7.9), which with $\kappa = 0$ and the modified value g becomes:

$$\epsilon\frac{\hbar\omega_0}{2g^2N/V}\left(\frac{2\epsilon}{\hbar\omega_0}\right)^2 = \frac{\epsilon\varepsilon_0}{e^2d_{ab}^2}\frac{V}{N} < 1. \qquad (7.17)$$

This is identical to the condition in eq. (7.10), and describes the same transition. Therefore, if the Dicke model is considered as light-matter interaction in the electric dipole gauge, the Hepp and Lieb transition is not an artefact of neglecting terms.

7.4 Conclusion

In conclusion, including the effect of direct Coulomb interactions, a phase transition occurs in a Dicke-like model. This transition leads to a spontaneous polarisation of the two-level systems. Since the system is neutral, $\mathbf{D}_{\parallel} = 0 = \epsilon_0 \mathbf{E}_{\parallel} + \mathbf{P}_{\parallel}$, and so a spontaneous polarisation leads to a longitudinal electric field. Note that although the total polarisation of a two-level system vanishes outside the system, the transverse and longitudinal parts of the polarisation need not vanish.

The phase transition does not however lead to a spontaneous transverse electric field. In the Coulomb gauge, where the bosonic mode represents the transverse electric field there will therefore be no macroscopic occupation of the bosonic mode. In the electric dipole gauge, the system is described by the original Dicke model. The boson field in the electric dipole gauge represents electric displacement, and so the phase transition does lead to an expectation of the bosonic field.

Part IV

Conclusions and appendices

Chapter 8

Conclusions

This chapter provides a brief summary of the conclusions of this dissertation, and suggestions for possible future work related to the projects described here.

8.1 Signatures of exciton condensation

1. Because of the relative strength of interactions between indirect excitons in coupled quantum wells compared to the trap energy scale, Bose condensation of such excitons would not be accompanied by any dramatic change in their spatial profile.

2. When fully condensed, at zero temperature, phase coherence between opposite sides of the exciton cloud causes interference, leading to a strongly peaked angular distribution.

3. At non-zero temperatures, fluctuations reduce the long range phase correlations, leading to a reduction in the angular peak. These phase fluctuations may be considered in a local density approximation.

4. Phase fluctuations lead to a destruction of the angular peak at a temperature, $T_* = T_{\mathrm{B}EC}/\ln(R/\xi_T)$, well below the tran-

sition temperature. This low temperature justifies neglecting the effect of the gapped density fluctuations on the angular profile.

8.2 Thermodynamics of polariton condensation

1. Starting from a model of two-level systems coupled to a continuum of radiation modes, one may consider a mean-field theory and calculate the spectrum of fluctuations about the mean-field solution.

2. In the condensed state, the low energy fluctuations are the Goldstone mode: phase fluctuations with a linear dispersion. Compared to a massive mode, this linear dispersion leads to an increased density of states, and thus a peak in the number of particles at small angles — exactly as discussed for exciton condensation.

3. Thermally populating the spectrum of fluctuations leads to a crossover of the phase boundary from a BEC form, $T_c \propto \rho$, at low densities, through a recovery of the mean field boundary at higher densities, to photon condensation at yet higher densities.

4. The effect of populating fluctuations in two dimensions is more complex than in three dimensions. It requires calculating the fluctuation corrections in the condensed state, in order to describe a Kosterlitz-Thouless transition.

5. The fluctuation contribution to density in the condensed state includes a contribution due to depletion of the order parameter, due to interaction between condensed and uncondensed particles. Inclusion of such a term requires taking total derivatives of free energy.

6. The crossover between BEC and mean-field limits occurs when the transition temperature becomes of the order of the Rabi splitting. Equivalently, it occurs at a density scale set by the wavelength of light.

7. This crossover density scale, resulting from the photon component of excitons, implies that current experiments are in a regime where the phase boundary is best described by the mean field theory.

8.3 Future work

This section discusses a number of possible extensions of this work.

Non-equilibrium problems

One obvious limitation of the work described in this dissertation is that it considers thermal equilibrium properties of the condensate, while current experiments would appear to be far from equilibrium. There are various ways one can study systems out of equilibrium, some of which will be discussed below.

Hamiltonian dynamics — Finding the Heisenberg equations of motion from the Hamiltonian, with possible addition by hand of damping rates and source terms, and studying the evolution from some initial state. See *e.g.* [10, 140] as recent examples.

Keldysh non-equilibrium Green's functions — This method, which will be discussed further below, allows one to find equations of motion for the non-equilibrium Green's function of a system coupled to external baths. There exist formal methods to study the effects of certain types of bath without making the approximations that are implicit in adding damping rates by hand.

(Quantum) Boltzmann equation — Either by making gradient expansions for the Keldysh equations of motion, or by arguing from a phenomenological model, it is possible to construct

equations of motion for the particle distribution function. In general, this should be a distribution in both position and momentum space, and includes scattering of particles taking account of their quantum statistics. See *e.g.* [12, 56].

The Keldysh non-equilibrium Green's function approach is technically challenging, but there are compelling reasons to choose it when studying non-equilibrium but phase coherent systems. In particular, coupling of excitons to a bosonic bath which can create or destroy particles, is in some sense a form of pair-breaking disorder[40, 141, 142]. In the presence of a condensate, the response of the system to such pumping is expected to change, due to the existence of a gap in the spectrum. The study of the Keldysh non-equilibrium problem allows such effects to be correctly treated, demonstrating how condensation modifies pumping and decay processes, and how pumping and decay lead to dynamics of the condensate phase and density.

Experiments on quasiparticle condensates

The experiments proposed in this dissertation are signatures of condensation; *i.e.* they are experiments to test whether a condensate of excitons or polaritons exist. Much of the experimental work to date also concentrates on testing whether a condensate exists; and in trying to compare experimental signatures to those that have been seen in dilute atomic gases. A question that can be asked for the future is *"What experiments could be done on an exciton or polariton condensate that could not be done with other condensed systems?"*. Such experiments would rely on features present in exciton and polariton systems that cannot so easily be realised in other systems. The following list provides some such examples. While some of these features may be seen in other experimental systems, their combination may lead to possible new experiments for exciton and polariton condensates.

Disorder — Excitons and polaritons will directly experience disorder from alloy disorder, well-width fluctuations, phonons, etc. The behaviour of a superfluid flowing through a disordered

medium has been partially studied in the context of Helium in Vycor glass (see *e.g.* [143]).

Finite lifetimes — As discussed above, the finite lifetime of polaritons and excitons can be used to perform experiments which directly study the behaviour of a phase coherent, but non-equilibrium system. For example, it may be possible to experimentally study how the strength of pumping and decay modifies the dynamics of the order parameter phase.

Phase symmetry breaking — The existence of phase symmetry breaking terms in exciton based systems due to interband transitions are expected to modify superfluid properties. Experiments on superfluid flow in coupled quantum well exciton systems, where such interband transitions can to some extent be controlled allows such effects to be investigated experimentally.

Sources of non-classical light — A common motivation for work on polaritons is that the emitted light has non-classical statistics. That there is emitted light is a result of the system being non-equilibrium. The emission of photons whose statistics reflect that of the condensate is a feature not seen in any previous example of condensation.

Appendix A

Green's function in a harmonic profile

This appendix discusses finding the exact Green's function for phase correlations, $G(\mathbf{r}, \mathbf{r}') = \langle \phi(\mathbf{r})\phi(\mathbf{r}') \rangle$, with a density profile given by the Thomas-Fermi distribution for a harmonic trap. By then considering the asymptotic form as $\mathbf{r} \to \mathbf{r}'$, the "local density approximation" used in section 4.4 will be further justified.

The Green's function for phase correlations obeys the equation:

$$-\frac{\beta}{m}\nabla_{\mathbf{r}}\left(\rho(\mathbf{r})\nabla_{\mathbf{r}}G(\mathbf{r},\mathbf{r}')\right) = \delta(\mathbf{r}-\mathbf{r}'), \tag{A.1}$$

where $\rho(r) = \rho_0(1 - r^2/R^2)$. The solution to this can be written as a sum over angular modes. Rescaling $\mathbf{r} = R\mathbf{t}$, and using $\mathbf{t}$ as a new variable, $\rho(t) = \rho_0(1 - t^2)$, the solution is:

$$G(\mathbf{t}, \mathbf{t}') = -\frac{m}{\beta\rho_0}\frac{1}{2\pi}\sum_{l=0}^{\infty} g_l(t, t')e^{il(\theta-\theta')}. \tag{A.2}$$

Substiuting this in eq. (A.1), the equation for mode l has the form:

$$t^2(1-t^2)\frac{d^2g_l}{dt^2} + t(1-3t^2)\frac{dg_l}{dt} - l^2(1-t^2)g = t\delta(t-t').$$

The substitutions $g_l(t) = t^{\pm l} f(t)$ and $y = t^2$ show that this is the hypergeometric equation [120]; *i.e.* the homogeneous equation is:

$$y(1-y)\frac{d^2 f}{d^2 y} + [(1 \pm l) - (1 + (1 \pm l))y]\frac{df}{dy} - \frac{\pm l}{2} f = 0 \qquad \text{(A.3)}$$

The general solution for g_l is thus:

$$g_l(t,t') = t_<^l h_{+l}(t_<)\left[t_>^l h_{+l}(t_>) - t_>^{-l} h_{-l}(t_>)\right], \qquad \text{(A.4)}$$

where h is an hypergeometric function:

$$h_\pm(t) = F(a,b,c;t^2)$$

with

$$a + b = c = 1 \pm l, \qquad ab = \pm l/2,$$

and $t_<(t_>)$ correspond to the smaller(larger) of t, t'.

For the $l = 0$ case, the solution is

$$g_0(t,t') = \ln\left(t_>/(1-t_>^2)^{1/2}\right),$$

which diverges as $t \to 1$.

As $t \to t'$, the value of G is dominated by the large l terms. For these terms, $h_\pm(t)$ tends to $1/\sqrt{2|l|(1-t^2)}$ and so the terms g_l become:

$$g_l(t+\epsilon, t-\epsilon) = \frac{1}{1-t^2}\frac{1}{2l}\left[t^{2l}\left\{1 + \mathcal{O}\left(\epsilon^2\right)\right\} + \left(1 - \frac{2l\epsilon}{t}\right)\right].$$

The second of the terms in brackets gives a divergence as $\epsilon \to 0$, of the form

$$\begin{aligned}\lim_{\epsilon\to 0} G(t+\epsilon, t-\epsilon) &\approx \frac{-m}{\pi\beta\rho_0(1-t^2)}\sum_{l=1}^{\infty}\frac{1}{2l}\left(1-\frac{\epsilon}{t}\right)^{2l} \\ &= \frac{-m}{2\pi\beta\rho(t)}\ln\left(\frac{2\epsilon}{t}\right). \qquad \text{(A.5)}\end{aligned}$$

This takes the form of a local density equation; the divergence is as for the infinite system, but with a local density.

Appendix B

Lehmann representation and broken symmetry

B.1 Analytic properties of thermal and retarded greens functions

The inverse thermal Green's function contains terms proportional to δ_ω. Working from the Lehmann representation, it may be shown that such terms can arise in the thermodynamic Green's function, but not in the dynamic Green's functions.

To see this, consider the standard Lehmann representation (see *e.g.* ref. [144], section 17) for the retarded greens function for Bose fields:

$$G_{\mathrm{R}}(\omega) = \lim_{\delta\to 0^+}\int_{-\infty}^{\infty}\frac{\rho_{\mathrm{L}}(x)dx}{x-(\omega+i\delta)}, \tag{B.1}$$

$$\rho_{\mathrm{L}}(x) = \left(1-e^{-\beta x}\right)\sum_{n,m}\left|\langle n\left|\psi\right|m\rangle\right|^2 e^{\beta(F-E_n)}\delta(x-E_{mn}) \tag{B.2}$$

However, for the thermal Green's function, an extra term may appear,

$$\mathcal{G}(\omega) = \int_0^\beta d\tau e^{i\omega\tau}\mathrm{Tr}\left(e^{\beta(F-H)}e^{H\tau}\psi e^{-H\tau}\psi^\dagger\right) \tag{B.3}$$

$$= \sum_{n,m} |\langle n\,|\psi|\,m\rangle|^2\, e^{\beta(F-E_n)} \int_0^\beta e^{(i\omega - E_{mn})\tau} d\tau \quad \text{(B.4)}$$

$$= \int_{-\infty}^{\infty} \frac{\rho_{\mathrm{L}}(x)dx}{x+i\omega} + \beta\delta_\omega \sum_{n,m} |\langle n\,|\psi|\,m\rangle|^2\, e^{\beta(F-E_n)} \delta(E_{mn}). \quad \text{(B.5)}$$

The last term in (B.5) can be identified as the contribution to the Green's function due to transitions between degenerate states; or due to a macroscopic occupation of the photon in the ground state. Such a term does not occur for the retarded Green's function, and so in calculating the spectral Lehmann density $\rho_L(x)$, one may neglect its effects.

B.2 Matsubara summation with thermal greens functions

The δ_ω terms will contribute to Matsubara sums involving the thermal greens functions, in properties such as the density. In performing the Matsubara summation one must use

$$\sum_{\omega_n} f(\omega_n) = \int_{-\infty}^{\infty} \frac{dz}{2\pi i} A(z) + f(0), \quad \text{(B.6)}$$

$$A(z) = \lim_{\delta\to 0} 2\Im\left[\tilde{f}(z')\frac{\beta}{2}\coth\left(\frac{\beta z'}{2}\right)\right]_{z'=z+i\delta},$$

where although $A(z)$ involves $\tilde{f}$, the analytic continuation of f, $f(0)$ does not involve analytic continuation. If the analytic continuation of f is regular at $z=0$, then

$$\sum_{\omega_n} f(\omega_n) = \sum_{\text{poles of } f} \mathrm{res}\left[\tilde{f}(z)\frac{\beta}{2}\coth\left(\frac{\beta z}{2}\right)\right] + f(0) - \tilde{f}(0), \quad \text{(B.7)}$$

i.e. one must add a term to correct for the difference between f and its analytic continuation at $z=0$.

B.3 Emission and absorption coefficients

Considering the Green's function for photon fluctuations; at zero temperature the function $\rho_L(x)$ would give the density of states, weighted by the photon component of a state. At finite temperatures, one may extract the probability to emit a photon,

$$\begin{aligned} P_{\text{emit}}(x) &= \sum_{n,m} |\langle m\,|\psi|\,n\rangle|^2\, e^{\beta(F-E_n)}\delta(x+E_{mn}) \\ &= n_{\text{B}}(x)\rho_{\text{L}}(x), \end{aligned} \tag{B.8}$$

or to absorb a photon

$$\begin{aligned} P_{\text{absorb}}(x) &= \sum_{n,m} \left|\langle m\left|\psi^\dagger\right|n\rangle\right|^2 e^{\beta(F-E_n)}\delta(x-E_{mn}) \\ &= (1+n_{\text{B}}(x))\rho_{\text{L}}(x), \end{aligned} \tag{B.9}$$

The energy x is measured w.r.t. the chemical potential, so at zero temperature there is only emission of photons at energies below the chemical potential, or absorption of photons above the chemical potential. The Lehmann density itself, $\rho_{\text{L}}(x)$ is the difference of these, and can be interpreted as an absorption coefficient, which when negative represents gain.

Bibliography

[1] J. R. Schrieffer. *Theory of Superconductivity* (Perseus Books, 1983).

[2] P. Kapitza. Viscosity of liquid helium below the λ-point. *Nature*, **141**, 74 (1938).

[3] J. F. Allen and A. D. Misener. Flow of liquid helium II. *Nature*, **141**, 75 (1938).

[4] L. Landau. The theory of superfluidity of helium II. *J. Phys. U.S.S.R.*, **5**, 71 (1941).

[5] W. Ketterle. Nobel lecture: When atoms behave as waves: Bose-Einstein condensation and the atom laser. *Rev. Mod. Phys.*, **74**, 1131 (2002).

[6] E. A. Cornell and C. E. Wieman. Nobel lecture: Bose-Einstein condensation in a dilute gas, the first 70 years and some recent experiments. *Rev. Mod. Phys.*, **74**, 875 (2002).

[7] V. N. Popov. *Functional Integrals in Quantum Field Theory and Statistical Physics* (D. Reidel, 1983).

[8] A. J. Leggett. Bose-Einstein condensation in the alkali gases: Some fundemental concepts. *Rev. Mod. Phys.*, **73**, 307 (2001).

[9] L. P. Pitaevskii and S. Stringari. *Bose-Einstein Condensation* (Clarendon Press, 2003).

[10] F. P. Laussy, G. Malpuech, A. Kavokin and P. Bigenwald. Spontaneous coherence buildup in a polariton laser. *Phys. Rev. Lett.*, **93**, 016402 (2004).

[11] A. Kavokin, G. Malpuech and F. P. Laussy. Polariton laser and polariton superfluidity in microcavities. *Phys. Lett. A*, **306**, 187 (2003).

[12] F. Tassone, C. Piermarocchi, V. Savona, A. Quattropani and P. Schwendimann. Bottleneck effects in the relaxation and photoluminescence of microcavity polaritons. *Phys. Rev. B*, **56**, 7554 (1997).

[13] R. H. Dicke. Coherence in spontaneous radiation processes. *Phys. Rev.*, **93**, 99 (1954).

[14] P. Nozières and S. Schmitt-Rink. Bose condensation in an attractive fermion gas; from weak to strong coupling superconductivity. *J. LTP*, **59**, 195 (1985).

[15] M. Randeria. Crossover from BCS theory to Bose-Einstein condensation. In [145], page 355.

[16] K. Hepp and E. Lieb. Equilibrium statistical mechanics of matter interacting with the quantized radiation field. *Phys. Rev. A*, **8**, 2517 (1973).

[17] K. Hepp and E. Lieb. On the superradiant phase transition for molecules in a quantized radiation field: the Dicke model maser. *Ann. Phys*, **76**, 360 (1973).

[18] J. M. Kosterlitz and D. J. Thouless. Ordering, metastability and phase transitions in two-dimensional systems. *J. Phys. C*, **6**, 1181 (1973).

[19] P. Minnhagen. The two-dimensional Coulomb gas, vortex unbinding, and superfluid-superconducting films. *Rev. Mod. Phys.*, **59**, 1001 (1987).

[20] D. Nelson and J. Kosterlitz. Universal jump in the superfluid density of two-dimensional superfluids. *Phys. Rev. Lett.*, **39**, 1201 (1977).

[21] D. Fisher and P. Hohenberg. Dilute Bose gas in two dimensions. *Phys. Rev. B*, **37**, 4936 (1988).

[22] P. Nozières. Some comments on Bose-Einstein condensation. In [145], page 15.

[23] P. Nozières and D. Saint James. Particle vs. pair condensation in attractive Bose liquids. *J. Physique*, **43**, 1133 (1982).

[24] S. Chu. Nobel lecture: The manipulation of neutral particles. *Rev. Mod. Phys.*, **70**, 685 (1998).

[25] C. N. Cohen-Tannoudji. Nobel lecture: Manipulating atoms with photons. *Rev. Mod. Phys.*, **70**, 707 (1998).

[26] W. D. Phillips. Nobel lecture: Laser cooling and trapping of neutral atoms. *Rev. Mod. Phys.*, **70**, 721 (1998).

[27] D. E. Pritchard. Cooling neutral atoms in a magnetic trap for precision spectroscopy. *Phys. Rev. Lett.*, **51**, 1336 (1983).

[28] M. R. Andrews, C. G. Townsend, H.-J. Miesner, D. S. Durfee, D. M. Kurn and W. Ketterle. Observation of interference between two Bose condensates. *Science*, **275**, 637 (1997).

[29] I. Coddington, P. Engels, V. Schweikhard and E. A. Cornell. Observation of Tkachenko oscillations in rapidly rotating Bose-Einstein condensates. *Phys. Rev. Lett.*, **91**, 100402 (2003).

[30] M. Greiner, O. Mandel, T. Esslinger, T. W. Hänsch and I. Bloch. Quantum phase transition from a superfluid to a Mott insulator in a gas of ultracold atoms. *Nature*, **415**, 39 (2002).

[31] P. R. Eastham and P. B. Littlewood. Bose condensation of cavity polaritons beyond the linear regieme: The thermal equilibrium of a model microcavity. *Phys. Rev. B*, **64**, 235101 (2001).

[32] C. Chin, M. Bartenstein, A. Altmeyer, S. Riedl, S. Jochim, J. H. Denschlag and R. Grimm. Observation of the pairing gap in a strongly interacting Fermi gas. *Science*, **305**, 1128 (2003).

[33] S. Jochim, M. Bartenstein, A. Altmeyer, G. Hendl, S. Riedl, C. Chin, J. H. Denschlag and R. Grimm. Bose-Einstein condensation of molecules. *Science*, **302**, 2101 (2003).

[34] M. Greiner, C. A. Regal and D. S. Jin. Emergence of a molecular Bose-Einstein condensate from a Fermi gas. *Nature*, **426**, 537 (2003).

[35] C. A. Regal, C. Ticknor, J. L. Bohn and D. S. Jin. Creation of ultracold molecules from a Fermi gas of atoms. *Nature*, **424**, 47 (2003).

[36] E. Timmermans, P. Tommasini, M. Hussein and A. K. Kerman. Feshbach resonances in atomic Bose-Einstein condensates. *Phys. Rep.*, **315**, 199 (1999).

[37] M. Holland, S. Kokkelmans, M. Chiofalo and R. Walser. Resonance superfluidity in a quantum degenerate Fermi gas. *Phys. Rev. Lett.*, **87**, 120406 (2001).

[38] A. Perali, P. Pieri and G. C. Strinati. Quantitative comparison between theoretical predictions and experimental results for the BCS-BEC crossover. *Phys. Rev. Lett.*, **93**, 100404 (2004).

[39] S. Simonucci, P. Pieri and G. C. Strinati. Broad vs. narrow Fano-Feshbach resonances in the BCS-BEC crossover with trapped Fermi atoms. *Europhys Lett.*, **69**, 713 (2005).

[40] M. H. Szymanska, P. B. Littlewood and B. D. Simons. Polariton condensation and lasing in optical microcavities: The decoherence-driven crossover. *Phys. Rev. A*, **68**, 013818 (2003).

[41] J. M. Blatt, K. W. Böer and W. Brandt. Bose-Einstein condensation of excitons. *Phys. Rev.*, **126**, 1691 (1962).

[42] S. A. Moskalenko. Reversible optico-hydrodynamic phenomena in a non-ideal exciton gas. *Sov. Phys.–Sol. State*, **4**, 199 (1962).

[43] L. V. Keldysh and Y. V. Kopaev. Possible instability of the semimetallic state toward coulomb interaction. *Sov. Phys.–Sol. State*, **6**, 2219 (1965).

[44] L. V. Keldysh and A. N. Kozlov. Collective properties of excitons in semiconductors. *Sov. Phys.–JETP*, **27**, 521 (1968).

[45] W. Kohn and D. Sherrington. Two kinds of bosons and Bose condensates. *Rev. Mod. Phys.*, **42**, 1 (1970).

[46] R. R. Guseĭnov and L. V. Keldysh. Nature of the phase transition under the conditions of an "excitonic" instability in the electronic spectrum of a crystal. *Sov. Phys.–JETP*, **36**, 1193 (1973).

[47] S. I. Shevchenko. Phase diagram of systems with pairing of spatially separated electrons and holes. *Phys. Rev. Lett.*, **72**, 3242 (1994).

[48] Y. E. Lozovik and V. I. Yudson. Interband transitions and the possibility of current states in systems with electron-hole pairing. *Sov. Phys.–JETP Lett.*, **25**, 14 (1977).

[49] H. A. Fertig. Deconfinement in the two-dimensional XY model. *Phys. Rev. Lett.*, **89**, 035703 (2002).

[50] H. A. Fertig and K. Majumdar. Vortex deconfinement in the XY model with a magnetic field. *Ann. Phys. (NY)*, **305**, 190 (2003).

[51] J. P. Wolfe, J. L. Lin and D. W. Snoke. Bose-Einstein condensation of a nearly ideal gas: Excitons in Cu_2O. In [145], page 281.

[52] J. P. Wolfe and J. I. Jang. New perspective on kinetics of excitons in Cu_2O. *Sol. Stat. Commun.*, **134**, 143 (2005).

[53] Y. E. Lozovik and V. I. Yudson. Feasibility of superfluidity of paired spatially separated electrons and holes; a new superconductivity mechanism. *Sov. Phys.–JETP Lett.*, **22**, 274 (1975).

[54] Y. E. Lozovik and V. I. Yudson. A new mechanism for superconducitivity: paring between spatially separated electrons and holes. *Sov. Phys.–JETP*, **44**, 389 (1976).

[55] S. I. Shevchenko. Theory of superconductivity of systems with pairing of spatially separated electrons and holes. *Sov. J. Low. Temp. Phys.*, **2**, 251 (1976).

[56] A. L. Ivanov, P. B. Littlewood and H. Haug. Bose-Einstein statistics in thermalization and photoluminescence of quantum-well excitons. *Phys. Rev. B*, **59**, 5032 (1999).

[57] X. Zhu, P. B. Littlewood, M. S. Hybertsen and T. M. Rice. Exciton condensate in semiconductor quantum well structures. *Phys. Rev. Lett.*, **74**, 1633 (1995).

[58] L. V. Keldysh. Macroscopic coherent states of excitons in semiconductors. In [145], page 246.

[59] L. V. Butov. Condensation and pattern formation in cold exciton gases in coupled quantum wells. *J. Phys.: Condens. Matter*, **16**, R1577 (2004).

[60] A. V. Larionov, V. B. Timofeev, P. A. Ni, S. V. Dubonos, I. Hvam and K. Soerensen. Bose condensation of interwell excitons in double quantum wells. *Sov. Phys.–JETP Lett.*, **75**, 570 (2002).

[61] J. A. Kash, M. Zachau, E. E. Mendez, J. M. Hong and T. Fukuzawa. Fermi-Dirac distribution of excitons in coupled quantum wells. *Phys. Rev. Lett.*, **66**, 2247 (1991).

[62] T. Fukuzawa, E. E. Mendez and J. M. Hong. Phase transition of an exciton system in GaAs coupled quantum wells. *Phys. Rev. Lett.*, **64**, 3066 (1990).

[63] L. V. Butov, A. Zrenner, G. Abstreiter, G. Bhm and G. Weimann. Condensation of indirect excitons in coupled AlAs/GaAs quantum wells. *Phys. Rev. Lett.*, **73**, 304 (1994).

[64] L. V. Butov, A. L. Ivanov, A. Imamoglu, P. B. Littlewood, A. A. Shashkin, V. T. Dolgopolov, K. L. Campman and A. C. Gossard. Stimulated scattering of indirect excitons in coupled quantum wells: Signature of a degenerate Bose-gas of excitons. *Phys. Rev. Lett.*, **86**, 5608 (2001).

[65] L. V. Butov, A. C. Gossard and D. S. Chemla. Macroscopically ordered state in an exciton system. *Nature*, **418**, 751 (2002).

[66] D. Snoke. Spontaneous Bose coherence of excitons and polaritons. *Science*, **298**, 5597 (2002).

[67] D. Snoke, S. Denev, Y. Liu, L. Pfeiffer and K. West. Long-range transport in excitonic dark states in coupled quantum wells. *Nature*, **418**, 6899 (2002).

[68] L. V. Butov, L. S. Levitov, A. V. Mintsev, B. D. Simons, A. C. Gossard and D. S. Chemla. Formation mechanism and low-temperature instability of exciton rings. *Phys. Rev. Lett.*, **92**, 117404 (2004).

[69] L. S. Levitov, B. D. Simons and L. V. Butov. Pattern formation as a signature of quantum degeneracy in a cold exciton system. **94**, 176404 (2005).

[70] L. S. Levitov, B. D. Simons and L. V. Butov. Pattern formation in exciton system near quantum degeneracy. *Sol. Stat. Commun.*, **134**, 51 (2005).

[71] V. Negoita, D. W. Snoke and K. Eberl. Harmonic-potential traps for indirect excitons in coupled quantum wells. *Phys. Rev. B*, **60**, 2661 (1999).

[72] L. V. Butov, C. W. Lai, A. L. Ivanov, A. C. Gossard and D. S. Chemla. Towards Bose-Einstein condensation of excitons in potential traps. *Nature*, **417**, 47 (2002).

[73] R. Rapaport, G. Chen, S. Simon, O. Mitrofanov, L. Pfeiffer and P. M. Platzman. Electrostatic traps for dipolar excitons (2005). Cond-mat/050417.

[74] A. T. Hammack, N. A. Gippius, G. O. Andreev, L. V. Butov, M. Hanson and A. C. Gossard. Excitons in electrostatic traps (2005). Cond-mat/0504045.

[75] S. I. Pekar. The theory of electromagnetic waves in a crystal in which excitons are produced. *Sov. Phys.–JETP*, **6**, 785 (1958).

[76] J. J. Hopfield. Theory of the contribution of excitons to the complex dielectric constant of crystals. *Phys. Rev.*, **112**, 1555 (1958).

[77] G. Khitrova, H. M. Gibbs, M. K. F. Jahnke and S. W. Koch. Nonlinear optics of normal-mode-coupling semiconductor microcavities. *Rev. Mod. Phys.*, **71**, 1951 (1999).

[78] C. Weisbuch, M. Nishioka, A. Ishikawa and Y. Arakawa. Observation of the coupled exciton-photon mode splitting in a semiconductor quantum microcavity. *Phys. Rev. Lett.*, **69**, 3314 (1992).

[79] J. P. Reithmaler, G. Sęk, A. Löffer, C. Hoffmann, S. Kuhn, S. Reitzenstein, L. Keldysh, V. D. Kulakovskii, T. L. Reinecke and A. Forchel. Strong coupling in a single quantum dot — semiconductor microcavivty system. *Nature*, **432**, 197 (2004).

[80] T. Yoshi, A. Schere, J. Hendrickson, G. Khitrova, H. M. Gibbs, G. Rupper, C. Ell, O. B. Shchekin and D. G. Deppe. Vacuum Rabi splitting with a single quantum dot in a photonic crystal nanocavity. *Nature*, **432**, 200 (2004).

[81] L. S. Dang, D. Heger, R. André, F. Bœuf and R. Romestain. Stimulation of polariton photoluminescence in a semiconductor microcavity. *Phys. Rev. Lett.*, **81**, 3920 (1998).

[82] H. Deng, G. Weihs, C. Santori, J. Bloch and Y. Yamamoto. Condensation of semiconductor microcavity exciton polaritons. *Science*, **298**, 199 (2002).

[83] H. Deng, G. Weihs, D. Snoke, J. Bloch and Y. Yamamoto. Polariton lasing vs. photon lasing in a semiconductor microcavity. *P.N.A.S.*, **100**, 15318 (2003).

[84] G. Weihs, H. Deng, D. Snoke and Y. Yamamoto. Polariton lasing in a microcavity. *Phys. Stat. Sol.*, **201**, 625 (2004).

[85] M. Richard, J. Kasprzak, R. André, L. S. Dang and R. Romenstain. Angle reseolved spectroscopy of polariton stimulation under non-resonant excitation in CdTe II-VI microcavity. *J. Phys.: Condens. Matter*, **16**, S3683 (2004).

[86] L. S. Dang and J. Kasprzak. Private Communication (2005).

[87] F. Tassone and Y. Yamamoto. Exciton-exciton scattering dynamics in a semiconductor microcavity and stimulated scattering into polaritons. *Phys. Rev. B*, **59**, 10830 (1999).

[88] P. G. Savvidis, J. J. Baumberg, R. M. Stevenson, M. S. Skolnick, D. M. Whittaker and J. S. Roberts. Angle-resonant stimulated polariton amplifier. *Phys. Rev. Lett.*, **84**, 1547 (2000).

[89] J. J. Baumberg, P. G. Savvidis, R. M. Stevenson, A. I. Tartakovskii, M. S. Skolnick, D. M. Whittaker and J. S. Roberts. Parametric oscillation in a vertical microcavity: A polariton condensate or a micro-optical parametric oscillation. *Phys. Rev. B*, **62**, R16247 (2000).

[90] J. J. Baumberg, P. G. Savvidis, P. G. Lagoudakis, M. D. Martin, D. Whittaker, R. Butte, M. Skolnick and J. Roberts. Polariton traps in semiconductor microcavities. *Physica E*, **13**, 385 (2002).

[91] A. Baas, J.-P. Karr, M. Romanelli, A. Bramati and E. Giacobino. Quantum degeneracy of microcavity polaritons (2005). Cond-mat/0501260.

[92] S. Savasta, O. D. Stefano, V. Savona and W. Langbein. Quantum complementarity of microcavity polaritons (2004). Cond-mat/0411314.

[93] A. Griffin. *Excitations in a Bose-condensed Liquid* (Cambridge University Press, 1994).

[94] J. C. Ward. An identity in quantum electrodynamics. *Phys. Rev.*, **78**, 182 (1950).

[95] Y. Takahashi. On the generalized Ward identity. *Nuovo Cimento*, **6** (1957).

[96] S. Weinberg. *The Quantum Theory of Fields*, volume I (C.U.P., 2000).

[97] Y. Nambu. Quasi-particles and gauge invariance in the theory of superconductivity. *Phys. Rev.*, **117**, 648 (1960).

[98] E. Talbot and A. Griffin. Symmetry breaking, Ward identities, and the two-fluid model. *Phys. Rev. B*, **29**, 3952 (1984).

[99] A. Griffin. Sum rules and the momentum distribution in Bose-condensed systems. *Phys. Rev. B*, **30**, 5057 (1984).

[100] E. Talbot and A. Griffin. High- and low-frequency behaviour of response functions in a Bose liquid: One-loop approximation. *Ann. Phys*, **151**, 71 (1983).

[101] A. Griffin. Density fluctuation spectrum of superfluid ^{4}He at finite temperatures. *Phys. Rev. B*, **19**, 5946 (1979).

[102] A. Griffin and T. H. Cheung. Excitations in a Bose gas at finite temperatures. II. Relation between single-particle and density fluctuations. *Phys. Rev. A*, **7**, 2086 (1973).

[103] S.-K. Ma and C.-W. Woo. Theory of a charged Bose gas. I. *Phys. Rev.*, **159**, 165 (1967).

[104] V. K. Wong and H. Gould. Long-wavelength excitations in a Bose gas at zero temperature. *Ann. Phys.*, **83**, 252 (1974).

[105] L. C. Andreani, F. Tassone and F. Bassani. Radiative lifetime of free excitons in quantum wells. *Sol. Stat. Commun.*, **77**, 641 (1991).

[106] S. L. Chuang. *Physics of Optoelectronic devices* (Wiley, New York, 1995).

[107] E. Hanamura. Rapid radiative decay and enhanced optical nonlinearity of excitons in a quantum well. *Phys. Rev. B*, **38**, 1228 (1988).

[108] G. Björk, S. Pau, J. Jacobson and Y. Yamamoto. Wannier excition superradiance in a quantum-well microcavity. *Phys. Rev. B*, **50**, 336 (1994).

[109] P. R. Eastham and P. B. Littlewood. Bose condensation in a model microcavity. *Solid State Commun.*, **116**, 357 (2000).

[110] D. G. Lidzey, D. D. C. Bradley, T. Virgili, A. Armitage, M. S. Skolnick and S. Walker. Room temperature polariton emission from strongly coupled organic semiconductor microcavities. *Phys. Rev. Lett.*, **82**, 3316 (1999).

[111] D. G. Lidzey, D. D. C. Bradley, M. S. Skolnick, T. Virgli, S. Walker and D. M. Whittaker. Strong exciton-photon coupling in an organic semiconductor microcavity. *Nature*, **395**, 53 (1998).

[112] U. Woggon, R. Wannemacher, M. V. Artemyev, B. Moller, N. Lethomas, V. Anikeyev and O. Schops. Dot-in-a-dot: electronic and photonic confinement in all three dimensions. *Appl. Phys. B-Lasers Opt.*, **77**, 469 (2003).

[113] H. F. Hess, E. Betzig, T. D. Harris, L. N. Pfeiffer and K. W. West. Near-field spectroscopy of the quantum constituents of a luminescent system. *Science*, **264**, 1740 (1994).

[114] K. Rzążewski, K. Wódkiewicz and W. Żakowicz. Phase transitions, two-level atoms, and the A^2 term. *Phys. Rev. Lett*, **35**, 432 (1975).

[115] V. Popov and S. Fedotov. The functional-integration method and diagram technique for spin systems. *Sov. Phys. JETP*, **67**, 535 (1988).

[116] Y. Ohashi and A. Griffin. Superfluidity and collective modes in a uniform gas of Fermi atoms with a Feshbach resonance. *Phys. Rev. A*, **67**, 063612 (2003). But see cond-mat/0302196 for expanded version.

[117] Y. Ohashi and S. Takada. Goldstone mode in charged superconductivity. *J. Phys. Soc. Jpn.*, **66**, 2437 (1997).

[118] S. T. Beliaev. Energy-spectrum of a non-ideal Bose gas. *Sov. Phys. JETP*, **7**, 299 (1958).

[119] F. M. Marchetti, B. D. Simons and P. B. Littlewood. Condensation of cavity polaritons in a disordered environment. *Phys. Rev. B*, **70**, 155327 (2004).

[120] E. Whittaker and G. Watson. *A course of Modern Analysis* (C.U.P, 1927).

[121] U. A. Khawaja, J. O. Andersen, N. P. Proukakis and H. T. C. Stoof. Low dimensional Bose gases. *Phys. Rev. A*, **66**, 013615 (2002).

[122] P. R. Eastham, M. H. Szymanska and P. B. Littlewood. Phase-locking in quantum and classical oscillators: polariton condensates, lasers, and arrays of Josephson junctions. *Solid State Commun.*, **127**, 117 (2003).

[123] P. B. Littlewood, P. R. Eastham, J. M. J. Keeling, F. M. Marchetti, B. D. Simons and M. H. Szymanska. Models of coherent exciton condensation. *J. Phys.: Condens. Matter*, **16**, S3597 (2004).

[124] F. M. Marchetti, M. H. Szymanska, P. R. Eastham, B. D. Simons and P. B. Littlewood. Condensation and lasing of microcavity polaritons: Comparison between two models. *Solid State Commun.*, **134**, 111 (2004).

[125] H. Haken. Cooperative phenomena in systems far from thermal equilibrium and in nonphysical systems. *Rev. Mod. Phys.*, **47**, 67 (1975).

[126] D. M. Whittaker. Classical treatment of parametric processes in a strong-coupling planar microcavity. *Phys. Rev. B*, **63**, 193305 (2001).

[127] P. R. Eastham and D. M. Whittaker. Steady states of a χ^3 parametric oscillator with coupled polarizations. *Phys. Rev. B.*, **68**, 075324 (2003).

[128] M. H. Szymanska and P. B. Littlewood. The crossover between lasing and polariton condensation in optical microcavities. *Solid State Commun.*, **124**, 103 (2002).

[129] Y. K. Wang and F. T. Hioe. Phase transition in the Dicke model of superradiance. *Phys. Rev. A*, **7**, 831 (1973).

[130] K. Rzążewski, K. Wódkiewicz and W. Żakowicz. Remark on the superradiant phase transition. *Phys. Lett.*, **58A**, 211 (1976).

[131] K. Rzążewski and K. Wódkiewicz. Stability of matter interacting with photons. *Phys. Rev. A*, **43**, 593 (1991).

[132] C. Emary and T. Brandes. Chaos and the quantum phase transition in the Dicke model. *Phys. Rev. E*, **67**, 066203 (2003).

[133] R. A. Barankov and L. S. Levitov. Atom-molecule coexistence and collective dynamics near a Feshbach resonance of cold fermions. *Phys. Rev. Lett.*, **93**, 130403 (2004).

[134] C. F. Lee and N. F. Johnson. First-order superradiant phase transitions in a multiqubit cavity system. *Phys. Rev. Lett.*, **93**, 083001 (2004).

[135] V. I. Emeljanov and Y. L. Klimontovich. Appearance of collective polarisation as a result of phase transition in an ensemble

of two-level atoms, interacting through electromagnetic field. *Phys. Lett. A*, **59**, 366 (1976).

[136] J. M. Knight, Y. Aharonov and G. T. C. Hsieh. Are superradiant phase transitions possible? *Phys. Rev. A*, **17**, 1454 (1978).

[137] C. Cohen-Tannoudji, J. Dupont-Roc and G. Grynberg. *Photons and Atoms* (Wiley, 1989).

[138] E. Merzbacher. *Quantum Mechanics* (Wiley, 1998).

[139] I. Bialynicki-Birula and K. Rzążewski. No-go theorem concerning the superradiant phase transition in atomic systems. *Phys. Rev. A*, **19**, 301 (1979).

[140] D. Sarchi and V. Savona. Dynamical condensation of polaritons (2005). Cond-mat/0411084.

[141] A. A. Abrikosov and L. P. Gor'kov. Theory of superconducting alloys with paramagnetic impurities. *Sov. Phys.–JETP*, **12**, 1243 (1961).

[142] J. Zittartz. Theory of the excitonic insulator in the presence of normal impurities. *Phys. Rev.*, **164**, 575 (1967).

[143] K. Huang. Bose-Einstein condensation and superfluidity. In [145], page 31.

[144] A. Abrikosov, L. Gorkov and I. Dzyaloshinski. *Methods of Quantum Field Theory in Statistical Physics* (Dover, 1975).

[145] A. Griffin, D. Snoke and S. Stringari, editors. *Bose-Einstein Condensation* (C.U.P, 1995).